CIRCULATION IN THE INDIAN OCEAN IN RELATION TO THE MONSOON CIRCULATION OF THE ATMOSPHERE

THESIS

SUBMITTED TO THE UNIVERSITY OF COCHIN

FOR THE DEGREE OF

DOCTOR OF PHILOSOPHY

IN

PHYSICAL OCEANOGRAPHY

IN THE FACULTY OF MARINE SCIENCES

By

R. NARENDRAN NAIR, M. Sc.

DEPARTMENT OF MARINE SCIENCES, UNIVERSITY OF COCHIN

COCHIN - 682 016

FEBRUARY, 1983

CERTIFICATE

This is to certify that this Thesis is an authentic record of research work carried out by Mr. Narendran Nair, R, under my supervision and guidance in the Department of Marine Sciences for Ph.D. degree of the University of Cochin and no part of it has previously formed the basis for the award of any other degree in any University.

Dr. G. S. Sharma
(Supervising Teacher)
Professor and Head
Dept. of Marine Sciences
University of Cochin

Cochin 682016
February, 1983.

.....

ACKNOWLEDGEMENT

I welcome this opportunity to acknowledge my deep sense of gratitude and indebtness to Professor Dr. G.S. Sharma, Head of the Department of Marine Sciences, for suggesting the problem and for his valuable guidance, keen interest, constant encouragement and critical scrutiny of the manuscript.

My thanks are also due to the authorities of University of Cochin for providing me with necessary facilities and for awarding a Junior Research Fellowship during the tenure of the present study.

I am grateful to Mr. P.M. John, Officer-in-Charge, Computer Centre, University of Kerala, for the assistance rendered in the computer programming and its execution.

I am also thankful to my colleagues, Mr. Basil Mathew (Dept. of Marine Sciences) and Mr. Sreedhara, V. (IIT Bombay) for their persistent encouragement, courtesy and kindness.

Finally, my thanks are due to Mr. Chandran, K.V. (Dept. of Marine Sciences) and Mr. Rajappan Nair V.P.(IIT Bombay) for typing the thesis.

CONTENTS

PREFACE

The atmospheric and oceanic processes are so intimately coupled that one derives energy from the other and vice-versa particularly at the interface of the two. A knowledge of the state of the upper ocean and its interaction with the atmosphere is of vital importance not only to the physical oceanographers but also to meteorologists for an effective weather forcasting.

Indian Ocean is the only one of the three major oceans that is land locked in its northern boundary while the rest are connected to both the poles. This peculiar situation of the Indian Ocean gives rise to a unique interplay of oceanic and continental climate called the monsoons in its northern region. Because of these monsoons the surface circulation in the North Indian Ocean and its interaction with the atmosphere has an anomalous nature compared to the other oceans. As such a study of the surface circulation of the Indian Ocean in relation to the atmospheric circulation over it is all the more important to have a clear understanding of the interplay of these two systems. Hence it is proposed to study the dependence of oceanic circulation on the atmosphere in the region north of $20^{\circ}S$ which is termed as the North Indian Ocean in the present investigation using the available oceanographic and meteorological data.

The Thesis has been divided into six chapters with further subdivisions.

Chapter one consists of two parts. Part one presents the general introduction while part two describes the material and method of the present investigation.

The distribution of the zonal and meridional components of the windstress in the North Indian Ocean is presented in chapter two.

Chapter three deals with the distribution of the curl of the windstress over the North Indian Ocean.

The general features of the surface circulation in the North Indian Ocean is dealt in chapter four.

Chapter five has three subdivisions. First part relates the windstress components and its vorticity with the surface circulation pattern. Second part makes a comparison of the present results of the windstress components and its vorticity with earlier works. Third part discusses the anomalous features in the surface circulation of the North Indian Ocean.

The last chapter presents summary of the investigation and conclusion arrived at.

CHAPTER 1

PART 1. INTRODUCTION

The Ocean currents follow the pattern of mean winds in the atmosphere. The Ocean over which there is strongest seasonal variation in the prevailing winds is the northern Indian Ocean. This regular variation in the prevailing winds causes seasonal reversal of surface currents between summer and winter in the Indian Ocean north of 10^{0}S. This peculiar feature is observed by mariners for over 1000 years (Warren, 1966) and is depicted in all good atlases.

1.1.1 Early Explorations

The Indian Ocean occupies about $74.118 \times 10^{6} km^{2}$ and covers 14 percent of the earth's surface. Exploration of this ocean began at a much earlier date than that of the Atlantic and Pacific oceans. The Arab and Persian ships frequently visited the coasts of India, Malaya and China well before the year 846 A.D. due to the flourishing trade with these countries. The Arabs acquired knowledge about

the reversing currents in the North Indian Ocean associated with the seasonal reversal of winds from the beginning of the 9th century (Aleem,1967). During the early voyages of India, Arab and Chinoese sailors, the southern part of the Indian Ocean was believed to be enclosed by land and the southern part of Africa appeared as an extension of Australia. This concept was dispelled by the voyage of Bartholomew Diaz who went around the southern tip of Africa into the Indian Ocean in 1487. Later in 1497, Vasco da Gama sailed around the southern part of Africa and visited 'Kozhikode' a port in Kerala in 1498; thus,confirmed the connection between the Atlantic and Indian oceans. Similarly, the voyage of Tasman, a Dutch navigator, around Australia to south in 1642 proved that the Indian ocean was also connected to the Pacific ocean. Captain Cook by his historical voyage in 1772-1775 established the southern extent of the Indian Ocean. The Challenger expedition (1872-1876) marked a new phase in oceanographic research in the Indian Ocean. This expedition had been organised specifically to collect complex oceanographic data like temperature, specific gravity and amount of chemical elements of sea water. Following the Challenger expedition, a large number of oceanographic expeditions had been taken place in the Indian Ocean, such as Investigator (1884-1925), Vityaz (1886-1906), Egeria (1894), Valdivia (1890-1899), Siloega (1899-1900), Gauss (1901-1903), Sea Lark (1905), Planet (1906), Dana (1920-1922), Carnegia (1928-1929),

Swallies (1929), Discovery II (1929-1931) and Mabahiss (1933-1934). In addition to these expeditions the survey ships of the British Admiralty supplemented a good amount of data. The above expeditions had studied oceanographic features of parts of the Indian Ocean. Later, British John Murray expedition (1933-1934) made extensive observations in the Arabian Sea and H.M.I.S. Investigator collected many valuable information about the Bay of Bengal and the Arabian Sea (Sewell, 1927, 1928, 1929, 1932). Mollar (1929) formulated the broad circulation pattern and water masses in the Indian Ocean using all the data available through 1929. Clowes and Deacon (1935) critically studied the investigations of the earlier workers and compared with the results of the expedition Discovery II (1929 - 1931). Barlow (1934, 1935) studied the circulation pattern of the Arabian Sea and Bay of Bengal in detail. Some of the other prominent studies were those of Ballmon (1922), Michaelis (1923) and Galle (1924, 1928, 1930). In 1939 the ocean research was interrupted by the II World War. The next period of oceanographical research (1946-1956) began after the war and continued until the beginning of the International Geophysical year. Swedish cruises of the Albatross III (1947-1948) collected much data about the Equatorial Counter-current during the winter and found that it occurred between 6°S and 8°S in February with maximum velocity of 22 cm/sec. During 1955-1956 Norsel I and II studied the structure of

currents of the North Equatorial Section (Tchernea et al., 1958).

1.1.2 Recent Explorations

The most important event in the field of oceanographical investigations was the organisation of the International Indian Ocean Expedition (1960-1965) under the combined auspicious of the International Council of Scientific Unions (ICSU) and UNESCO in which 25 countries participated. The IIOE made extensive surveys on vast spaces of the Indian Ocean, previously, almost unknown to science and collected large amount of physical, chemical, geological and biological oceanographic data. A number of research papers pertaining to all the above fields were published in the form of collected reprints of the International Indian Ocean Expedition. Particularly, mention may be made to the Oceanographic Atlas of the IIOE by Wyrtki (1971). Such an attempt to explore the Indian Ocean in large scale was carried out because the Indian Ocean projects many fascinating problems, especially its seasonal reversal of currents which affects the monsoon and the biological productivity of the area. Another important event in the field of oceanographical and meteorological research is the GARP (Global Atmospheric Research Programme) Monsoon Sub-Programme. This programme includes the Indosoviet Monsoon Experiment (1973) or (ISMEX-73), the Monsoon-77 Experiment (1977) and the Monsoon Experiment (1979)

or (MONEX). The GARP-Monsoon Sub-programme has been proposed by the countries of the region affected by the monsoon and endorsed by the Joint Oceanography Committee(JOC) as an important component of GARP. Under this Sub-programme ISMEX-73 was conducted during the period 15 May to 10 July by USSR and India. The results of ISMEX-73 have provided useful data and experience for developing a similar experiment in 1977 which is called the Monsoon-77 experiment. Both the Monsoon-77 experiment and ISMEX-73 served as the background for a major experiment known as MONEX. The main objective of MONEX is to find out the dynamic and thermodynamic structures of the Asian Monsoon of the northern hemisphere. Intensive and time dependent surveys were carried out in the Indian Ocean, especially in the Arabian Sea and Bay of Bengal during the phases of the above experiments. A major part of the results of the above experiments has already been published.

World charts of the ocean surface currents are the result of the observations collected by navigators.

Schott (1898), Witte (1879) presented the first comprehensive charts of ocean currents. Later, modern current charts were presented by Schumacher (1940, 1943), Schott (1942), the British Admiralty, the United States Hydrographic Office (1944), Koninklijk Netherlands Meteorologisch Institut (1952) and the Dutch Hydrographisches

Institut (1960). The results obtained from continuous general oceanographic research activities nourished and improved the information of the ocean currents represented by the above charts.

1.1.3 The Forcing Function of Ocean Circulation

The surface circulation of all the oceans are mainly induced by the prevailing winds superimposed by the thermohaline effects. The action of the wind against the ocean surface supplies momentum and kinetic energy to the surface to drive the ocean currents. The nonuniformity of the wind field characterized by the curl of the frictional stress produces set up and set down of the surface waters. The wind-driven currents are produced by the corresponding horizontal pressure gradients. Thus, the origin and pattern of the surface circulation is due to the averaged wind field over the ocean surface.

Many theories have been put forward to explain the origin of ocean currents. Hough (1897), assuming the absence of friction and meridional boundaries of the ocean, concludes that a zonal distribution of precipitation and evaporation would produce a uniformly accelerated system of purely east-west geostrophic currents. Goldbrough (1933) discusses a model with meridional boundaries and concludes

that if the integral of precipitation-evaporation function vanishes along each paralle of latitude between the two boundaries, then steady stationary current fields containing main dynamical features will arise. Ekman (1905) notes that the direct stress of the wind is confined to a thin surface boundary layer and that viscous shearing stresses are unimportant dynamically in the deeper body of the ocean. Later, Ekman (1923) has deduced some important laws concerning the curl of the deep current for the case of steady motion and derived a remarkable differential equation for horizontal wind-driven ocean currents. This equation describes the effects of a variable wind stress, a variable Coriolis parameter with latitude, a variable friction and a variable ocean depth. Defant (1926) and Rossby (1936) have pointed out that lateral shearing stresses associated with horizontal exchange in eddies may play an important role in the general circulation of both the atmosphere and ocean. Similarly, Montgomery (1939) and Montgomery and Palmen (1940) indicate the importance of lateral stresses in the dynamic balance of ocean currents.

Earlier investigations of wind-driven ocean circulation are mostly concerned with the general features of the horizontal current systems and their relationship to the distribution of the mean wind field over the oceans. Later, much progress towards a better understanding of the average large-scale wind-driven oceanic circulation has been

made since about 1946. Sverdrup (1947) studied the wind-driven circulation in a baroclinic ocean and concluded that the distribution of density and mass transport by the equatorial currents of all the oceans depend entirely upon the average stress on the surface by the prevailing winds. Stommel (1948), in his study of the wind-driven circulation in a homogeneous ocean under the influence of surface wind stress, points out that the westward concentration of stream-lines is a result of the variation of the Coriolis parameter with latitude. The results of Sverdrup (1947) and Stommel (1948), inspired a number of scientists and a series of theoretical studies on the general wind-driven circulation followed, like Hidaka (1949) and Munk (1950). In 1950 Munk stated that permanent ocean currents are related to the rotating components of the wind stress field over the ocean and these currents would vanish where the wind stress field is irrotational. The vorticity tendency equation derived by Munk (1950) illustrates that the zonal wind system divides the general circulation into a number of gyres separated at latitudes by lines of zero vorticity of the wind stress. The maximum width of the gyre is found at latitudes where the vorticity of the wind stress reaches a maximum. He also investigated theoretically the effect of the meridional stress components on the general wind-driven circulation. Munk's theoretical studies are in good agreement with the actual observations. Munk and Carrier (1950) applied the same

vorticity tendency equation to a triangular ocean basin of constant depth and represented the horizontal mass transport by streamlines. Reid (1948a) formulated a model of ocean covered everywhere by a thin homogeneous layer of uniform density but of variable depth and is underlain by a region in which the density increases to a fixed bottom density by an exponential law. This model exhibits much similarity with reality, especially, in the eastern equatorial Pacific Ocean. Reid (1948 b) also explained the importance of the stress of the wind in maintaining the equatorial currents of the Pacific Ocean. In 1948, the Scripps Institute of Oceanography published the field of mean monthly wind stress over the North Pacific. In 1958, Hidaka computed the wind stress of the South Pacific, Indian and Atlantic oceans for four seasons and their annual mean values using the pilot charts of wind roses for 5° squares of the U.S. Navy Hydrographic Office adopting a method of Reid (1948b)

Fofonoff (1954) formulated a mathematical model to study the frictionless steady horizontal flow in a homogeneous ocean of constant depth and concluded that intensified currents were present along the eastern and western coasts. Sarkisian (1954) derived a numerical solution for the wind-driven circulation for a model approximated to the North Atlantic

and explained the formation and dynamical character of the western boundary currents. At the same time Charney (1955) and Morgan (1956) put forward theoretical models including non-linear field acceleration instead of frictional terms and concluded that the action of acceleration terms can initiate western boundary currents like the Gulf Stream. In 1955, Hidaka, theoretically, studied the general circulation of the Pacific Ocean and the results coincide with the actual observations. Fofnoff and Montgomery (1956) considers the Equatorial Undercurrent as a permanent feature of the oceanic circulation and finds that it is consistent with the observation of absolute cyclonic vorticity in the equatorial flow. Stommel (1957) clearly illustrates the physical meaning of the simple Sverdrup type solution in a homogeneous ocean of constant depth, bounded by an eastern coast acted upon by a zonal wind stress. Hasson (1958) formulated a model of wind-driven ocean circulation and indicated a strong countercurrent under the intense western currents. Wealander (1959) computed the transport in the three oceans from the Sverdrup's equation using the actual slope of ocean boundaries and the wind stress data published by the Scripps Institution of Oceanography (1948) and Hidaka (1958). He could not explain the western concentration of streamlines but discussed in detail the importance of the lateral friction, incomplete compensation at the variable lower boundary of the currents, the effects of evaporation and precipitation and the local time variations

which are neglected in the Sverdrup's equation. Charney (1960) made a non-linear theoretical study on the equatorial motion produced by a uniform east wind blowing over a homogeneous ocean of constant depth. The results clearly reveal an undercurrent whose intensity increases with the decreasing values of the eddy viscosity.

Eversince modern dynamic oceanography developed so much from the study of basic linear theories to non-linear theories, attempts have been made to combine the wind-driven and thermohaline components in one model of the general ocean circulation (Bryan and Cox, 1967). They formulated a mathematical model of the combined wind-driven and thermohaline circulation for the three major oceans, the results of which coincide with the observed features of the oceanic circulation and associated temperature stratification. Other theoretical studies to be mentioned about the response of the wind forcing to the oceans are Durst (1924), Francés (1954), Lineikin (1955), Neumann (1955), Carrier and Robinson (1962), Veronis (1963, 1966 a,b), Moore (1963), Ilyin and Kamenkowich (1963), Bryan (1963, 1969), Stewart (1964), Baiyac (1967), Krauss (1968), Krauss and Harrison (1966), Gates (1968), Mantel (1969), Bryan and Cox (1968), and Woolander (1968).

Later, a number of investigations have been carried out to interrelate the wind stress and curl of the wind stress

with general oceanic circulation. Hellerman's (1967) computation of the wind stress values for 5° squares of the world oceans remains as a comprehensive study of this type. He also computed the annual mean of the wind stress for four seasons based on the frequency distribution of the surface wind. Holopainen (1967) calculated the annual mean of the wind stress curl for the northern hemisphere north of 10°N by vertically integrating the atmospheric vorticity equation between the upper (100 mb) and lower (1000 mb) boundaries of the atmosphere, based on the charts of Crutcher (1959). His observations coincide with the results of Stommel (1965), especially, in the North Atlantic and Indian oceans. According to Stommel (1965), cyclonic values of the curl of the wind stress prevail on the tropics and anticyclonic values in the middle and subtropical latitudes. A similar conclusion would be derived from the wind vorticity charts of Mintz and Deem (1952). Using data from the Koninklejek Netherlands Meteorologisch Institut (1952), Hantel (1970) computed the monthly surface wind stress curl for the whole Indian Ocean for 2° squares. This remains as the most comprehensive study of the distribution of the surface wind stress curl in the Indian Ocean in which more importance is given to the time variation of the parameter. In continuation to the above study Hantel (1971) formulated a barotropic model of an ocean and found that the curl of the surface wind stress

would be independent of forcing function of models describing wind-driven currents. He used the wind stress values computed by Hellerman (1967). According to Hantel (1972), the monsoon currents in the Indian Ocean reverse due to the periodical reversing of the curl field. But an extensive comparison of the distribution of the curl of the wind stress with the pattern of the general wind-driven ocean circulation is not carried out so far, eventhough the importance of the curl of the wind stress as the forcing function of oceanic movements is revealed by the above studies.

Evenson and Veronis (1975) computed the wind stress and curl of the wind stress for the world oceans and found that unlike the other oceans, Indian Ocean would possess greater stresses during northern summer. Leetma and Bunker Stommel (1979) computed the geostrophic transports, the oceanic total transport and the Ekman transport in the North Atlantic using the wind stress values of Bunker (1976). The results are in good agreement with the dynamic computations of the circulation in the upper ocean. Cane (1977 a,b) also studied the response of an equatorial ocean to simple wind stress patterns by formulating a model and presented the numerical results. Cane (1980) found an excellent correlation of local winds with both surface and subsurface currents. According to him, the Equatorial Undercurrent is driven by meridional

advection of vorticity and eastward pressure gradient produced by the easterly winds. At the same time a linear stratified ocean model of the Equatorial Undercurrent by McCreary (1980) generates many of the features of the Equatorial Current System. So a detailed comparative study of the distribution of the wind stress and curl of the wind stress of the Indian Ocean with that of the other oceans will give rise many interesting features.

Further theoretical studies of special interest are Charney and Spiegal (1971) Kiehl and Dubbleday (1970), Veronis (1973), McKee (1973), Hurt et al. (1974), Hill (1975), Cane and Sarachek (1976), Rye et al. (1975), Creigan and Johnson (1978), Hellerman (1978/80), Anderson et al. (1979), Busalachi and O'Brien (1980), Dengay and Henin (1980), Brown et al. (1980), Furnes (1980), Hughes (1980), Bishop (1979, 1980), deszmeke (1980), Masahero (1980), Mohnson (1979) Gordon et al. (1981) and Philander and Pacinowski (1981).

Various mathematical models are formulated for the Indian Ocean from time to time in which the ocean's response to the atmospheric forcing are predicted. These predictions, when compared with the actual observations show good agreement. For example, Lighthill (1969) applied a sudden negative curl of the wind stress along a zonal strip near the equator and

worked out analytically the response of the ocean. In such a situation, transient current patterns are set up propagating a northward flux westwards and concentrating it into a western boundary current. The results of this model agree with the actual observations of the Somali Current. A three dimensional numerical model with seven layers and a minimum grid size of 1° square covering the Indian Ocean north of 20°S was formulated by Cox (1970). The monsoon is stimulated by a periodic wind stress. The main features of the Somali Current are qualitatively well produced in the model. Duing (1970) formulated another model using a periodic wind stress stimulating the monsoon. The results are compared with the dynamic topography of the ocean surface. The complex patterns of vortices can be observed in the model. The observed transport and width of the Somali Current and the general pattern of circulation are reproduced in the model. Colen (1964), Duing and Saikiella (1971), Hurlburt and Thompson (1976), Anderson and Rowlands (1976) and Ghosh et al. (1978) also studied the response of the ocean to monsoon in detail in their theoretical and observational investigations.

1.1.4 General Wind-Driven Circulation in the Indian Ocean

From the above discussion it is clear that the prime forcing of the general oceanic circulation is the wind field.

It is very much applicable to the Indian Ocean where the surface currents are induced by the monsoon winds which reverse their direction seasonally. During the southwest monsoon the currents in the North Indian Ocean are set easterly and flow in a clockwise direction while during the northeast monsoon the currents set in a westerly and counter-clockwise direction. Wyrtki (1973) divides the general circulation pattern of the Indian Ocean into three systems such as the seasonally changing monsoon gyre, the southern hemisphere anticyclonic gyre and the Antarctic waters with the Circumpolar Current. The reversing monsoon gyre is a unique feature of the Indian Ocean while the other two systems are similar to the corresponding systems of the other two major oceans. The monsoon gyre is separated from the subtropical gyre by a very pronounced front in the hydrochemical structure at about 10°S (Wyrtki, 1973). By February itself the current flows north along Somali coast along north of the equator. (Varadachari and Sharma, 1967). By May everywhere north of the equator, current flows towards east. During this period, the Equatorial Countercurrent which is present in the Atlantic and Pacific throughout the year, appears to merge with the eastward flowing Monsoon Current in the Indian Ocean. The South Equatorial Current is steady during the entire year and flows towards west. It becomes stronger during the south-west monsoon and supplies most of its water to the Somali Current

which flows towards north along the Somali coast. The monsoon winds are much stronger in July and corresponding currents attain their maximum speed in July. The southwest monsoon lasts longer than the northeast monsoon and the wind velocities are generally higher during the former than the latter in the Arabian Sea. Thus, the wind-driven gyre in the Equatorial Indian Ocean during the southwest monsoon comprises of the eastward flowing Monsoon Current, the South Equatorial Current and the Somali Current.

The circulation pattern induced by the southwest monsoon is maintained upto September. Only in October does it start to breakdown and is slowly replaced by the northeast monsoon circulation (Varadachari and Sharma, 1967). During this season the North Equatorial Current flows towards west and the current along the Somali Coast reverses its direction and flows towards south. The Equatorial Countercurrent is well developed along the doldrum belt and extends upto 8°S. Off the coast of Somali most of the water of the North Equatorial Current crosses the equator and forms the Equatorial Countercurrent. A study of Sharma et al (1982) reveals that the currents start to reverse in the Bay of Bengal as early as in February. The time of reversal of currents which precedes the monsoon circulation of the atmosphere is a crucial problem to be dealt with.

The South Equatorial Current is a part of the subtropical gyre of the southern Indian Ocean. A long high pressure ridge extends from the Agulhas Current system across the entire ocean into the Timor Sea, divides the westward flow to the north of the ridge from the eastward flow south of it. The South Equatorial Current forms near south of Java and is fed by the Monsoon Current or the countercurrent. Near the Malagasy Island the South Equatorial Current splits into two; one flowing northward and the other southward along the east coast of the island. Sharma et al. (1978) computed the zonal geostrophic currents along 84°E between 2°S and 28°S and found that the mean zonal component of the South Equatorial Current on this section is about 30 cm/sec. It also agrees with that of the zonal component of the South Equatorial Current at 65°E (Sharma 1976 a). During the northeast monsoon the South Equatorial Current lies between 6°S and 20°S (Sharma et al.,1982). Eventhough the wind conditions in the southern hemsphere is similar to that in the other oceans throughout the year, the width and strength of the South Equatorial Current varies with seasons. One of the aims of the present study is to investigate into the time variations of this current and its response to the atmospheric forcing.

An important current in the Indian Ocean is the Somali current. It is evident from Schott's Chart (1935) that it is a western boundary current like the Gulf Stream

and Kuroshio with differences that it crosses the equator and appears during the southwest monsoon and is absent during the rest of the year. During the northeast monsoon the wind regime over the Indian Ocean is similar to that over the Pacific and Atlantic Oceans. During the southwest monsoon the wind regime over the Indian Ocean is completely dissimilar to that over the other oceans. In this particular context, the presence of the Somali Current during the southwest monsoon and its absence during the northeast monsoon is of special significance. Several theoretical and observational studies have been carried out to get a comprehensive picture of the Somali Current and its response to the monsoonal circulation of the atmosphere. According to Warren et al.(1966), Somali Current appears as a banded zone of 100-150 miles wide flowing northward along the African Coast. Most of the high speed flow is concentrated in the surface layer and intense upwelling along the coast occurs between 5°N to 11°N, where the entire warm surface layer is replaced by the subsurface water with temperature well below 20°C. Velocity and transport of the Somali Current increases toward northeast paralleling the coast from the equator to 7° - 9°N, where it appeared to reach maximum strength. At this point, the flow turns offshore toward the coast at 9°N (Swallow and Bruce 1966). The direct current measurements off the Somali Coast during the southwest monsoon in 1964 show that the flow is mainly geostrophic which can be

related to local winds and in some cases estimates of maximum velocities exceed 300 cm/sec. and transport range between 90 x 10^6 m^3/sec and 65 x 10^6 m^3/sec (Swallow and Bruce, 1966). Computations of Bruce (1969) show that the transport of the Somali current during the southwest monsoon between 7°N and 9°N is 48 x 10^6 m^3/sec for 0-200 m and 74 x 10^6 m^3/sec for 0 - 1000 m. Bruce and Volkmann (1969) prove that strong anti-cyclonic eddy exists offshore from the Somali current during the southwest monsoon which persists below the surface during the northeast monsoon. This subsurface eddy would have an effect on the regrowth of the Somali current. Large parts of the Somali current are recirculated in an intense eddy, the centre of which is about 300 km offshore. This elongated eliptical eddy stretches for about 100 km parallel to the coast. Duing (1970) explains that the system of eddies in the Arabian Sea is intimately connected with the dynamics of the monsoon gyre. Leetma (1972) from direct current measurements showed that the commencement of the Somali current is in phase with the local winds. But growth in the next few weeks is due to the strengthening of the South Equatorial Current. The temperature gradients of the Somali current during the early formation stage in all years are also directly proportional to the wind speed with an average phase lag of 12 days (Duing and Saukielda 1971). Bruce (1973) carried out a hydrographic survey of the Somali Current between the equator and 12°N during August and September 1970. Cellular structure was observed

in the current pattern and the velocity of the flow was found to exceed 200 cm/sec during the peak of monsoon. Further detailed studies of the response of Somali current to the onset of southwest monsoon are due to Duing (1980), Luyten and Cenilla (1980) and Findlater (1974). Eventhough a number of extensive investigations on the Somali current are carried out, no attempt has been made so far to study the time variation of the wind stress and curl of the wind stress and the associated variation of circulation pattern in the region of Somali Current.

The Agulhas Current is also a part of the subtropical gyre which is considered as a strong western boundary current. The Agulhas Current extends from the south of the Madagascar island along the South African Coast and is fed by the South Equatorial Current (Darbyshire, 1964). A speed near about 200 cm/sec is recorded at the core of the current. Due to the joint action of the southeast trades south of the equator and southwesterly winds north of the equator, the Equatorial Currents are largely deflected north of the equator during the northern summer. Hence, the portion of the South Equatorial Current flowing south of the equator is small which results in the weakening of the Agulhas Current during the southwest monsoon. During the northern winter

the northeast monsoon winds blowing north of the equator strengthen the South Equatorial Current south of the equator which results in the strengthening of the Agulhas Current System (Darbyshire, 1964). In a study, Pearce (1977) notes that like the Florida Current, the Agulhas Current meanders over many tens of kms off Durban, possibly, in response to the atmospheric forcing. Other noteworthy studies about the Agulhas Current are due to Darbyshire (1963), Nemis (1972), Duncan (1970, 1976) and Lutjeharms (1976).

The Equatorial Undercurrent is present in the Atlantic and Pacific oceans throughout the year. But in the Indian Ocean, it is generally present only during the northeast monsoon. Difference of opinions exist about the period of occurrence of the Equatorial Undercurrent in the Indian Ocean. Taft and Knauss (1967) carried out the first detailed study of the Undercurrent in the Indian Ocean in 1962-63. From direct current measurements they confirmed the existence of an eastward subsurface flow at 61°E in March and at 92°E in April. Swallow (1964, 1967) established the presence of the Undercurrent in the Western Indian Ocean from the latter half of the northeast monsoon to the beginning of the southwest monsoon. Sharma (1968) from the physical properties of sea water inferred the presence of the undercurrent in the Indian ocean from November to the end of May. A recent study of the undercurrent in the Indian Ocean during February-June, 1975

and 1976 clearly reveals the presence of a strong (80 cm/sec) Equatorial Undercurrent throughout the period of observation (Leetma and Stommel,1980). From the hydrographic characteristics, Muraleedharan et al (1980) finds the undercurrent to be present in the Indian Ocean from January to June with a shifting of its core from north of the equator to south. Robinson (1966) in a theoretical study concludes that an undercurrent can be formed if the zonal components of wind stress irrespective of its direction, are large relative to the meridional components. Such conditions are found in the Indian Ocean during the end of the northeast monsoon. All the earlier mentioned studies confirm the presence of the Undercurrent in the Indian Ocean during the latter part of the northeast monsoon, thus supporting the theory of Robinson. More importance should be given to investigate into further details of this theory and to find out whether it is truly applicable to the Indian Ocean.

Another principal current in the Indian Ocean is the Equatorial Jet detected by Wyrtki (1973) which appeared due to strong westerly winds during the transition months. The Jet is well depicted in the monthly maps of surface currents published by the hydrographic offices of several countries. It is also well depicted by Sharma (1971) in the current charts eventhough it has not been reported as a

separate current from the Equatorial Current System until 1973. The Jet appears in April and May and again in October and November. The width of the Jet is about 500 km and is placed along the equator. The Jet is strongest between 60°E and 90°E where the average surface flow speeds often exceed 64 cm/sec. Maximum values of 215 cm/sec have also been reported. The direct current measurements of Taft and Knauss (1967) in May 1963 along 53°E show that the surface flow at the equator often exceeds 50 cm/sec which decreases rapidly to a depth of 80 m and reverses direction below 120 m. O'Brien and Hurlburt (1974) gave a theoretical explanation of the Equatorial Jet in the Indian ocean. Current measurements over nearly two years at Gan near the Maladive Islands confirm the appearance of the Jet in the thermocline as well as at the surface with speed exceeding 100 cm/sec (Knox, 1976). During the course of a hydrographic survey made from 50°30'E to 95°E between 1°N and 1°S in December 1976 and January 1977, a large volume of anomolously saline water is found along the equator, east of the Maladive Islands which is brought by the Equatorial Jet (Eriksen, 1979).

The South Equatorial Countercurrent was first discovered by Reid in 1959. Yoshida and Kidokoro (1967 a,b) theoretically predicted the presence of the eastward flowing Subtropical Countercurrent in the North Pacific. The Tropical

Countercurrent in the Indian Ocean is similar to the Sub-tropical Countercurrent in the North Pacific. Uda and Hasunuma (1969) identified it in the North Pacific between 20° and 25°N. In both the oceans the pressure gradient force initiated by the thermal front associated with the tropical convergence zone drives the current. Sharma (1976) traced the presence of the South Equatorial Countercurrent and the Tropical Countercurrent along 65°E during the southwest monsoon. Sharma et al(1982) traced the eastward flowing South Equatorial Countercurrent on both the 300 and 400-cl/t surfaces from 77°E to 97°E between 12°S and 15°S. The meridional salinity gradient appears to be responsible for the formation of the South Equatorial Countercurrent in spite of the fact that the prevailing winds are easterly. Sharma et al.(1982) also found the Tropical Countercurrent between 20° and 26°S on the 300-cl/t surface over the width of the ocean. Yoshida (1970) reports alternate easterly and westerly bands associated with the Subtropical Countercurrent. A similar band structure of the Tropical Countercurrent in the Indian Ocean has been reported by Basil Mathew et al.(1982).

1.1.5 Description of the area

The western and eastern boundaries of the Indian Ocean are 20°E and 147°E respectively. In the southeastern,

the boundary is usually placed across Torres Strait and then from New Guinea along the Lesser Sunda Islands across Sunda Strait and Singapore Strait. The surface area with these boundaries is 74.118×10^6 km^2 or about 21% of the surface of all oceans. The volume of the Indian ocean is about 283,000,000 km^3 and the average depth is about 3850m. The Indian ocean differs from the Pacific and Atlantic oceans in two important aspects. Firstly, it is land locked in the north and does not extend into the cold climatic regions of the northern hemisphere and consequently is assymetrical with regard to its circulation. Secondly, the wind systems over its equatorial and northern portions change twice in an year causing an almost complete reversal of its circulation semiannually.

During summer in the northern hemisphere from June through August, a low pressure system is developed over Asia with the centre around Rajasthan desert. The sub-tropical high pressure ridge of the southern hemisphere shifts slightly northward and continues into a high pressure system over Australia. During this season the southeast trades of the southern hemisphere cross the equator and turn to southwesterlies due to the action of Coriolis force. Various workers estimated that a large mass of air crosses the equator, particularly over the extreme western regions of the North

Indian Ocean and the adjoining Somali during this season (Rao,1964; Findlater,1969 and Saha,1970). This is the season of Indian southwest monsoon.

During winter in the northern hemisphere from December through February, the equatorial low pressure though lies at about 10°S. A strong high pressure system is situated over Asia. This situation causes the northeasterlies to blow everywhere north of the equator. This is the northeast monsoon season of the Indian Subcontinent.

The direction and strength of the monsoons vary from one locality to the other. The southwest monsoon is not fully developed over the Bay of Bengal until the middle of June while in the equatorial region it sets in by the middle of May and over the Arabian Sea by the end of May. The northeasterly and easterly winds of the northeast monsoon actually begin to blow in the northern part of the Bay of Bengal in October but they are not fully established over the area until November and in the southern part of the Bay until middle of the month. The northeast monsoon predominates over the eastern regions of the North Indian Ocean while the southwest monsoon plays a major role over the western region of the ocean. The winds are very weak and variable during the transition periods between the two monsoons (March-April and September-October).

The pattern of sea-surface temperature changes considerably with seasons. During February when the ITCZ is near 10°S, the thermal equator is also in the southern hemisphere and most of the area between the equator and 20°S records temperatures near 28°C. The water in the northern parts of the Bay of Bengal and Arabian Sea is much cooler and temperature below 20°C can be found in the northern portions of the Persian Gulf and Red Sea. In the southern hemisphere temperature decreases gradually from the tropics to the polar regions. Surface circulation affects the distribution of temperature and warm water spreads along the coast of Africa and cold water off the west coast of Australia. In August high temperatures are found in the northern hemisphere and in the equatorial region. The Somali Current advects cold upwelled water along the east coast of Africa to the north.

The distribution of surface salinity is controlled by evaporation and precipitation and by run off from the continents. High surface salinities higher than 36‰ are found in the subtropical belt of the southern hemisphere where evaporation exceeds precipitation. An area of low salinity stretches from the Indonesian waters along 10°S to Malagasy. It is caused by the heavy rainfall in the tropics and also by the incursion of the Pacific Ocean water

into the western Indian Ocean along the South Equatorial Current. The Bay of Bengal has very low salinities less than 30‰ as a result of the large river discharge. Because of high evaporation, the Arabian Sea has salinities as high as 36.5‰. High salinities are also found in the Persian Gulf (>38‰) and in the Red Sea (>41‰) representing the arid character of the land masses surrounding them. The annual variation of salinity distribution is not very much pronounced except in the Bay of Bengal where the salinity in the upper layers varies from as low as 5‰ to 34‰.

During the southwest monsoon very strong upwelling takes place along the Somalia Coast and Arabia Coast. The major coastal upwelling regions are located along the eastern boundaries of the oceans with the notable exception of the northwestern Indian Ocean. Upwelling off the southwest coast of India commences in the deep layers of about 90 m in March and the upwelled water reaches the surface by May (Sharma, 1978). Upwelling ceases to be present by July/August when the onshore winds of the southwest monsoon have maximum strength and sinking sets in by September (Sharma, 1978). Upwelling in the Arabian Sea occurs not only over the continental shelf but also over the deep ocean. This is a result of the strong and steady winds nearly parallel to the coast that increase in intensity with distance offshore, resulting

in divergence in the Ekman layer over an area-some 1000 km long and atleast 400 km wide. According to Varadachari (1961), upwelling occurs off the east coast of India from January to July. In a study, LaFond (1968) concludes that upwelling commences off the east coast by March and continues till May and again in August.

The effect of the southwest monsoon prevails in the Indian Ocean upto 10°S. The present investigation is limited from 36°E to 116°E and between 20°S and the northern boundary of the ocean excluding the Red Sea and Persian Gulf.

1.1.6 Objectives of Study

The main objectives of the present investigation are

i. to compute the zonal and meridional components of the wind stress in the Indian Ocean and to study their spatial and time variation

ii. to compute the curl of the wind stress in the Indian ocean and to study its spatial and time variation

iii. to derive the circulation pattern of the Indian Ocean and to study its spatial and time variation

iv. to correlate the distribution of the wind stress and curl of the wind stress with the circulation pattern and

v. to compare and contrast the distribution of the wind stress and curl of the wind stress and the associated circulation with that of the other oceans.

PART 2. MATERIALS AND METHODS

From the various models of wind-driven ocean circulation earlier discussed, the general vorticity equation can be written as

$$\frac{\partial \nabla^2 \psi}{\partial t} + \frac{1}{\rho H} J(\psi, \nabla^2 \psi) + \beta \frac{\partial \psi}{\partial x} - F(\psi) = \text{Curl}_z \tau \quad , \text{ where } \psi (\psi, x, y, t)$$

is the stream function for the horizontal mass transport, H is the depth of the ocean which is considered as constant, Z is the ocean's free surface, J is the Jacobian operator, β the meridional derivative of the Coriolis parameter f, ρ is the density of water and τ is the horizontal wind stress vector at sea level. The function F indicates friction which varies with different models.

The horizontal mass transport components Mx and My are

$$Mx = \int_{-H}^{Z} \rho u \, dz = -\frac{\partial \psi}{\partial y} \text{ and}$$

$$My = \int_{-H}^{Z} \rho v \, dz = \frac{\partial \psi}{\partial x}$$

Combining the above equations we get the famous Sverdrup transport equation (Sverdrup 1947), as

$$M = \frac{\text{Curl}_z \tau}{\beta}$$

If β is assumed to be constant then M will be directly proportional to the curl of the wind stress components.

The general vorticity equation expresses a balance between the effects of time dependence, non-linearity, the β effect, friction and wind stress. The left-hand side of the equation depends on ψ whereas the right-hand side is the forcing function. This proves clearly that the curl of the surface wind stress over the ocean is a fundamental quantity in discussing the wind-driven ocean circulation. From the distribution of the curl of the wind stress, cyclonic and anticyclonic vortices can be found since the zero contour indicates the boundary between them.

The data used for the present study have come from the monthly charts of the surface currents and winds of the Atlas entitled 'Indian Ocean Oceanographic and Meteorological Charts' published by the Royal Netherlands Meteorological Institute in 1952. These data are based on observations of the ship's drift made during different months of the year for more than a centuary.

On these charts, the direction of the winds are indicated by arrows and force in Beaufort scale over 2° latitude-longitude quadrangle. Similarly, the direction and magnitude of the currents are represented by means of an arrow and a number of nautical miles per day respectively in each 2° latitude-longitude quadrangle along with the number of observations.

The Atlas also contains additional fields of surface air pressure, temperature and storm tracks. There are certain limitations in the data of the surface currents obtained from observations of ship's drift and the wind data. The effect of wind on the ship and the errors in position fixing of the ships reduce the accuracy of drift data. The observations represent averages over a period of 12 to 24 hours. A uniform distribution of data is scarce, since the observations are mostly concentrated on the shipping routes. Very weak currents and the effect of tidal currents cannot be represented in the Atlas.

In spite of these limitations, these are the most detailed and best compiled of the various climatological summaries published by various countries (Swallow and Bruce, 1966; Wooster et al, 1967). The observations of Taft and Knauss (1967), Swallow and Bruce (1966) and Leetma and Stommel (1980) closely agree with the data presented in this Atlas,

especially for the monsoon months with some slight deviations during the transition months.

1.2.1 Computation of the Wind Stress

The zonal and meridional components of the wind stress have been computed using the bulk aerodynamic formula,

$$\tau = \rho C_D W^2$$

where τ is the wind stress (dynes cm^{-2}), ρ is the density of air (gm cm^{-3}), C_D the drag coefficient and W the wind speed (cm sec^{-1}).

The winds are always measured from the north and hence the zonal component of the wind stress $\tau_x = \rho C_D W^2 \sin\theta$ and meridional component of the wind stress $\tau_y = \rho C_D W^2 \cos\theta$ where θ is the angle of the wind vector from north.

The value of ρ is taken as 1.2259×10^{-3} gm cm^{-3}. The selection of the drag coefficient which is a dimensionless quantity is a problem. Various studies have been carried out to discuss the selection of the drag coefficient and its variation. Munk (1947) assumes a jump in the drag coefficient at Beaufort 4. Hidaka (1958) uses a value 0.8×10^{-3} for winds having speed below 6.6 m sec^{-1} and 2.6×10^{-3} for winds having speed above 6.6 m sec^{-1}. Hillerman (1968) in his updated estimate of wind stress over the world ocean, adopts a value with 40 percent jump at Beaufort 4. Many

investigators use constant drag coefficient. Duing (1970) uses a value 2.6×10^{-3} for the Indian Ocean. Weiler and Burling (1967) finds no systematic decrease or increase of the drag coefficient in the range of wind speed 1.5 to 10.5 m sec^{-1}. Hasse (1968), from his own measurements as well as a comparison of the results of several earlier authors, comes to the conclusion that in the wind speed range 2 to 12 m sec^{-1}, there is no variation of the drag coefficient. He also summarized the values of C_D and found that they are in the range of 1.0 to 1.3×10^{-3} with individual errors of 17 to 28 percent. Hantel (1970) uses a value 1.2×10^{-3} for his computation of the curl of the windstress in the whole Indian Ocean. Badgley et al. (1972) choose the value of the drag coefficient as 1.4×10^{-3}. Brooks and Krugermeyer (1972) on the basis of numerous profile measurements in the North Sea and the Baltic Sea as well as in the Atlantic Ocean, concludes that at wind speeds between 4 and 12 m sec^{-1}, the drag coefficient only slightly depends on the wind velocity. They give a value $1.3 \times 10^{-3} \pm 16\%$ which has also been confirmed by the results of direct measurements in various regions of the oceans. A constant value for the drag coefficient (1.3×10^{-3}) is assumed according to wind stress measurements taken simultaneously with the STD profiles (Denman and Miyake, 1973) where no significant dependence of drag coefficient on wind speed is observed.

Similarly, determinations of the wind stress or momentum flux with fairly direct estimates show that C_D = (1.3 to 1.5) x 10^{-3} on an average with a considerable amount of scatter and an uncertainity of the mean of 20 to 30% (Pond et al., 1974; Stewart, 1974). The above experimental studies prove that C_D does not increase appreciably with increasing wind speed for mean wind speeds upto 17 m sec^{-1}. The maximum average wind speed observed in the Indian Ocean is lower than 17 m sec^{-1}. So, for the present investigation the value of the drag coefficient is chosen as 1.3 x 10^{-3} which is a reasonable value for the Indian Ocean, evident from the mean speed of the surface winds.

The computation of the wind stress has been carried out over 2^0 squares for each month using a computer programme.

1.2.2 Computation of the curl of the Wind Stress

The curl of the wind stress has been computed by finite differences method using the formula

$$\text{Curl}_z \bar{\tau} = \frac{\partial \tau_y}{\partial x} - \frac{\partial \tau_x}{\partial y}$$

$$= \frac{1}{4}\left[\frac{\{(\tau_{y_1} + \tau_{y_4}) - (\tau_{y_2} + \tau_{y_3})\}}{2\Delta x} - \frac{\{(\tau_{x_1} + \tau_{x_2}) - (\tau_{x_3} + \tau_{x_4})\}}{2\Delta y}\right]$$

where τ_x and τ_y are the zonal and meridional components of the wind stress respectively. Δx is 1^0 longitude ($\approx$100 km)

and Δy is 1° latitude (≈ 111 km).

Since the area under investigation lies in the lower latitudes, the effect of curvature due to the converging of longitudes is negligible and hence not considered.

The computation of the curl of the wind stress has been carried out over 4° latitude-longitude quadrangle for each month using a computer programme.

For computing the wind stress and curl of the wind stress, the x and y directions are taken positive to the east and north respectively.

Contours have been drawn for the wind stress and curl of the wind stress for each month. While contouring both the fields whenever any of the values are noticed to be very much of a deviation from the general pattern and if they are based on very few observations, such values are ignored. The contouring has been done to get a spatial and time variation of both the fields of wind stress and curl of the wind stress and to correlate it with the pattern of general circulation.

1.2.3 Method to derive the circulation pattern

The circulation pattern for all the months has been

derived using free-hand method in order to study the singularities in the streamline pattern in relation to the curl of the wind stress field.

In the free-hand method, the data are plotted on a map in the form of arrows pointing in the direction of the flow at all stations. Streamlines are drawn free-hand, keeping the line always parallel to the velocity vector at all points through which it passes. The maps thus constructed represent the direction of flow at every place. Since the direction of current vector is given in each 2° square, such a representation of streamlines will give a reliable and detailed pattern of circulation.

The magnitude of each current vector is plotted on a separate sheet at the centre of each 2° square and isovels, indicating equal speeds are drawn. These isovels are superimposed on the streamline-pattern in order to get the direction and speed of currents at the same time.

1.2.4 Three representative longitudes (65°E, 77°E and 89°E) are selected and zonal components of wind stress and current velocity have been drawn along them. The purpose of such a representation is to study the latitudinal and longitudinal variations of the above parameters and to find

out the relationship between them.

Since the data used have been collected in different years at different places on different days of the month, the pattern of the curl field and circulation for any month cannot be considered as synoptic but climatological. These patterns are a reliable and comprehensive representation, especially away from the coast with few limitations arising from the type of data and methods of analysis.

CHAPTER 2

DISTRIBUTION OF THE ZONAL AND MERIDIONAL COMPONENTS OF THE WINDSTRESS

The atmosphere can be considered as a thermodynamic engine which is mainly driven by the temperature differences between low and high latitudes. But in the oceans, the temperature or salinity differences between the equator and poles play only a minor role in initiating ocean surface circulation. The prime factor that instigate the ocean surface circulation is the wind stress. Therefore, the knowledge of the wind stress distribution is essential to draw the general features of the surface circulation of the oceans.

The distribution of the zonal and meridional components of the wind stress for all the months are presented in figures 1 to 12. The shaded zones represent areas of negative components. The positive zonal and meridional components represent eastward and northward wind stress, while the negative zonal and meridional components represent westward and southward wind stress respectively. It is

clear from the distribution of the windstress that the southwest monsoon exist from May to August and the north-east monsoon from November to February. March and April are the transition months from the northeast monsoon to the southwest monsoon while September and October are the transition months from the northeast monsoon to the south west monsoon. It is not possible to divide the seasons strictly on monthly basis because the transition from one season to another varies from place to place. For example the southwest monsoon lasts longer in the Arabian Sea while the northeast monsoon predominates in the Bay of Bengal.

Before discussing the monthly distribution of the windstresses the salient features are given. The zero contour along 2°S separates the eastward windstress in the north and westward wind stress in the south from May to September. Highest value of the eastward wind-stress is noticed in July in the Arabian Sea. Lowest value of the eastward windstress is observed in May and September. Northward windstress prevails in the entire Indian Ocean throughout the southwest monsoon except in the eastern parts of the Arabian Sea. Maximum value of the northward windstress is noticed in July in the Somali Current region. The monthly variation of the eastward and northward wind stresses south of 2°S is not much pronounced and the contours

almost run parallel to the latitudes indicating steady winds blowing over this region.

Conditions of the northeast monsoon exist from November through February. A belt of eastward wind stress is observed in between the westward wind stress in the northern and southern parts of the ocean. The Somali Current region experiences westward wind stress throughout the season with the maximum value in January. The values of the southward windstress are generally higher in December and January. The monthly variation of the wind stress south of $10^{\circ}S$ is not conspicuous. In general, the zonal and meridional components of the windstress are considerably higher during the southwest monsoon than the northeast monsoon.

Winds start to reverse in the northern parts of the Bay of Bengal and northeastern parts of the Arabian Sea by March. The intensity of the wind stress is markedly weakened during the transition period. A relatively higher belt of eastward stress is observed in the central equatorial region in April-May and October-November.

The distribution of the zonal and meridional components of the wind stress in each month is discussed in the following paragraphs in detail.

JANUARY

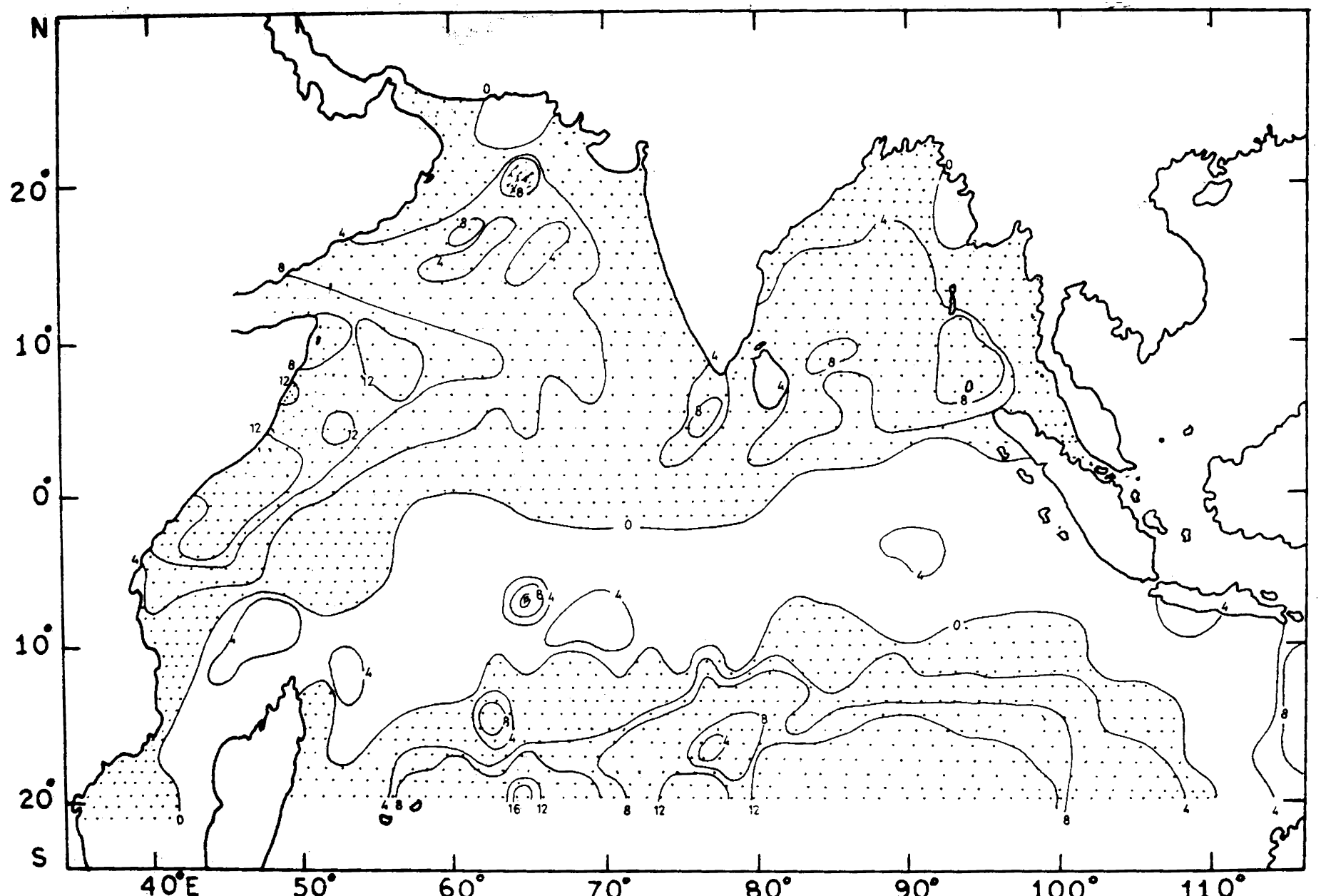

FIG. 1a. ZONAL COMPONENT OF THE WIND STRESS (10^{-1} dynes cm^{-2}) IN JANUARY.

January (Fig.1a) are negative (westward) north of the equator and south of 12°S. Between the equator and 12°S they are positive (eastward). The region of the wind reversal can be traced by the zero contour of the windstress. The zero contour extends into the southern hemisphere west of 60°E and into the northern hemisphere east of 80°E. The westward stress north of the equator drives the westward flowing North Equatorial Current. From the distribution of the windstress it is clear that the North Equatorial Current extends into the southern hemisphere west of 60°E and supplies water to the Equatorial Countercurrent and the Mozambique Current. The westward stress which generally acts between the equator and 12°S drives the Equatorial Countercurrent. When it reaches the coast of Sumatra, the Equatorial Countercurrent flows into the southern hemisphere and supplies water to the South Equatorial Current. Westward stress predominates south of 12°S and drives the South Equatorial Current. The distribution of the zonal components of the wind stress in the Bay of Bengal shows no difference from that in the Arabian Sea. Generally, the intensity of the zonal components of the wind stress is comparactively low in January eventhough higher values are found near the Somali Coast. The maximum value recorded over the entire ocean is only about 17.3×10^{-1} dynes cm^{-2} in the Somali region. Lower values are observed in the equatorial region

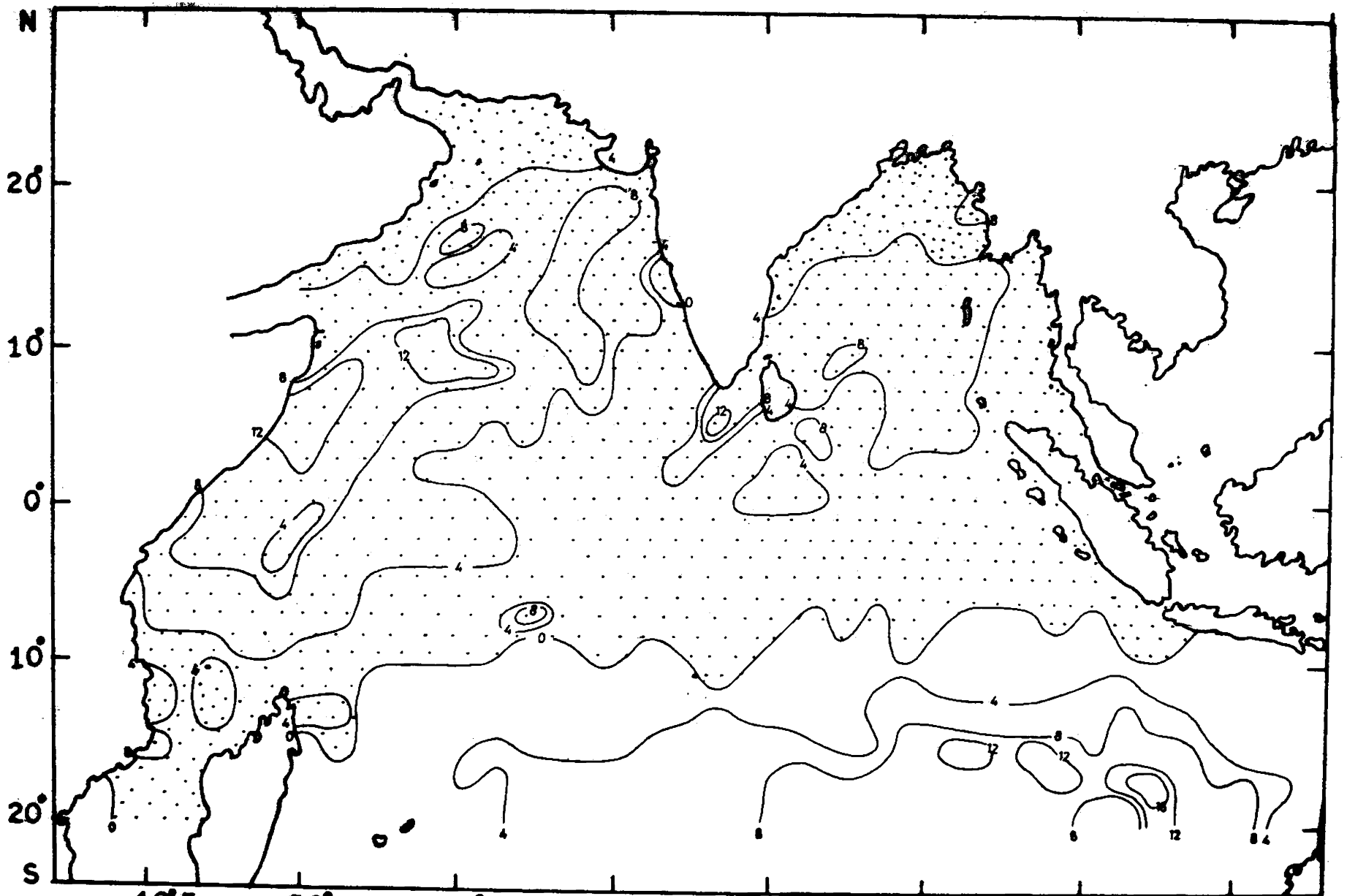

FIG: 1b MERIDIONAL COMPONENT OF THE WIND STRESS (10^{-1} dynes cm^{-2}) IN JANUARY.

east of 60°E and also near the coasts of Arabia, India, Burma and Sumatra.

The meridional components of the windstress in January (Fig.1b) are negative (southward) north of 10°S and positive (northward) south of 10°S. The region near the Somali Coast experiences higher southward stress. From the distribution of the windstress, it is clear that the current off the Somali Coast flows towards southwest and is fed by the North Equatorial Current.

In the western and eastern parts of the equatorial region, the westward windstress exceeds the southward windstress. While southward wind stress exceeds the westward wind stress in the central equatorial region , the zonal components of the wind stress exceeds the meridional components of the wind stress south of the equator.

FEBRUARY

The zonal components of the wind stress in February (Fig.2a) are negative except in a belt between 2°S and 12°S and in the northern parts of the Bay of Bengal and Arabian Sea. The westward stress in the Bay of Bengal is higher than that in the Arabian Sea. The region near the east coast, south of 16°S records westward stress 10 times greater than that near the west coast of India. The Somali

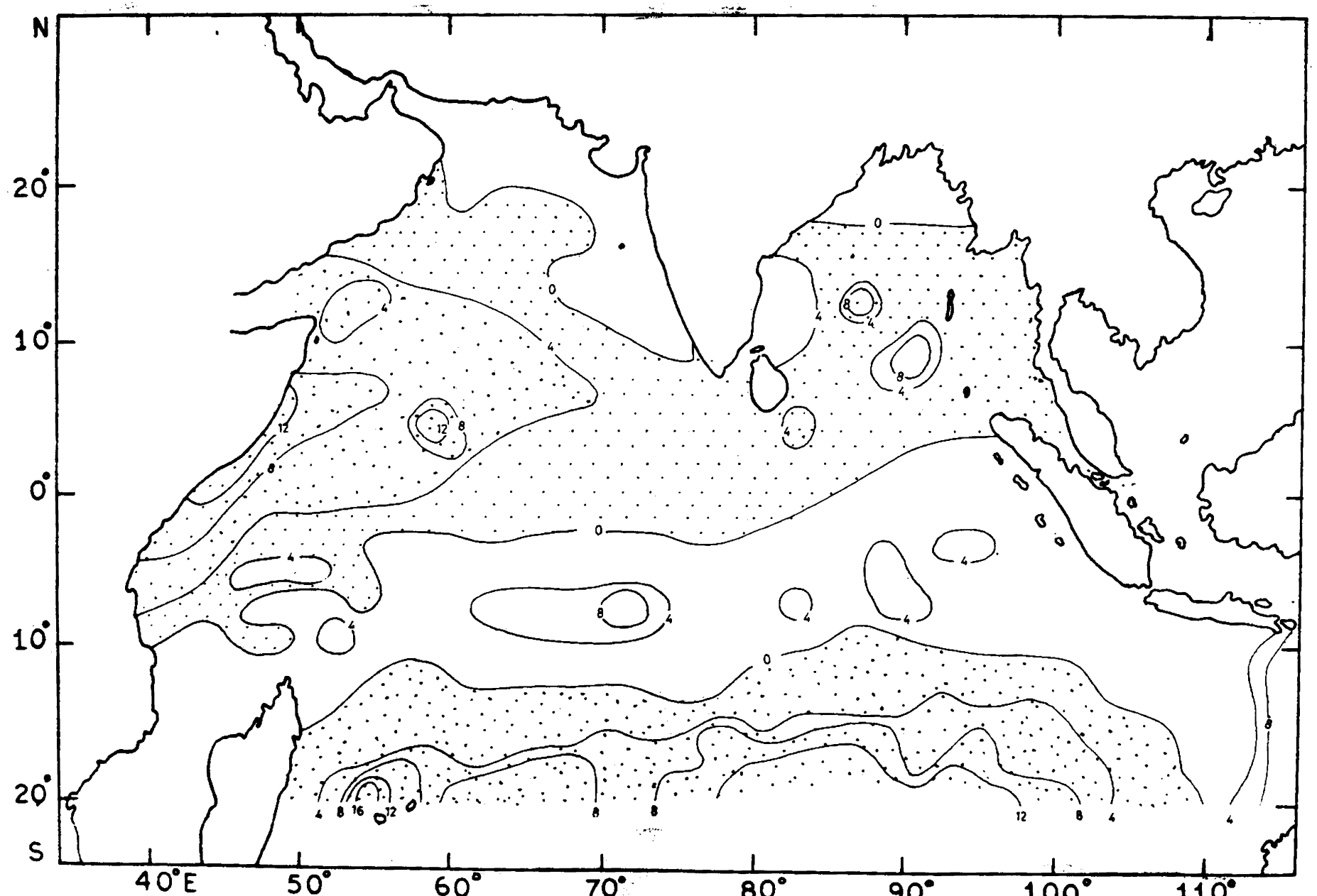

FIG. 2a. ZONAL COMPONENT OF THE WIND STRESS (10^{-1} dynes cm^{-2}) IN FEBRUARY.

region also shows higher values which decrease northward and southward. The westward stress increases south of 12°S. The values of eastward stress between 2°S and 12°S are higher than that in January. This belt of eastward stress extends south of the equator, east of 100°E.

The westward stress north of 2°S and south of 12°S drives the westward flowing North Equatorial Current and South Equatorial Current respectively. The eastward stress in between them drives the eastward flowing Equatorial Counter-current which lies completely in the southern hemisphere. The eastward stress in the northern parts of the Bay of Bengal and Arabian Sea shows that the winds start to reverse by February itself. Lower values of the zonal components are recorded in the northern parts of the Arabian Sea and Bay of Bengal and just south of 3°S. The higher values are noted near the Somali Coast and south of 16°S.

The meridional components are negative (southward) in February (Fig.2b) except south of 10°S. The values of southward stress are higher in the Arabian Sea than those in the Bay of Bengal. The east and west coasts of India record lower values. The values of the southward stress are higher near the Somali Coast and in the eastern parts of the South Indian Ocean. The values of the northward stress south of 10°S are slightly lower than those in January.

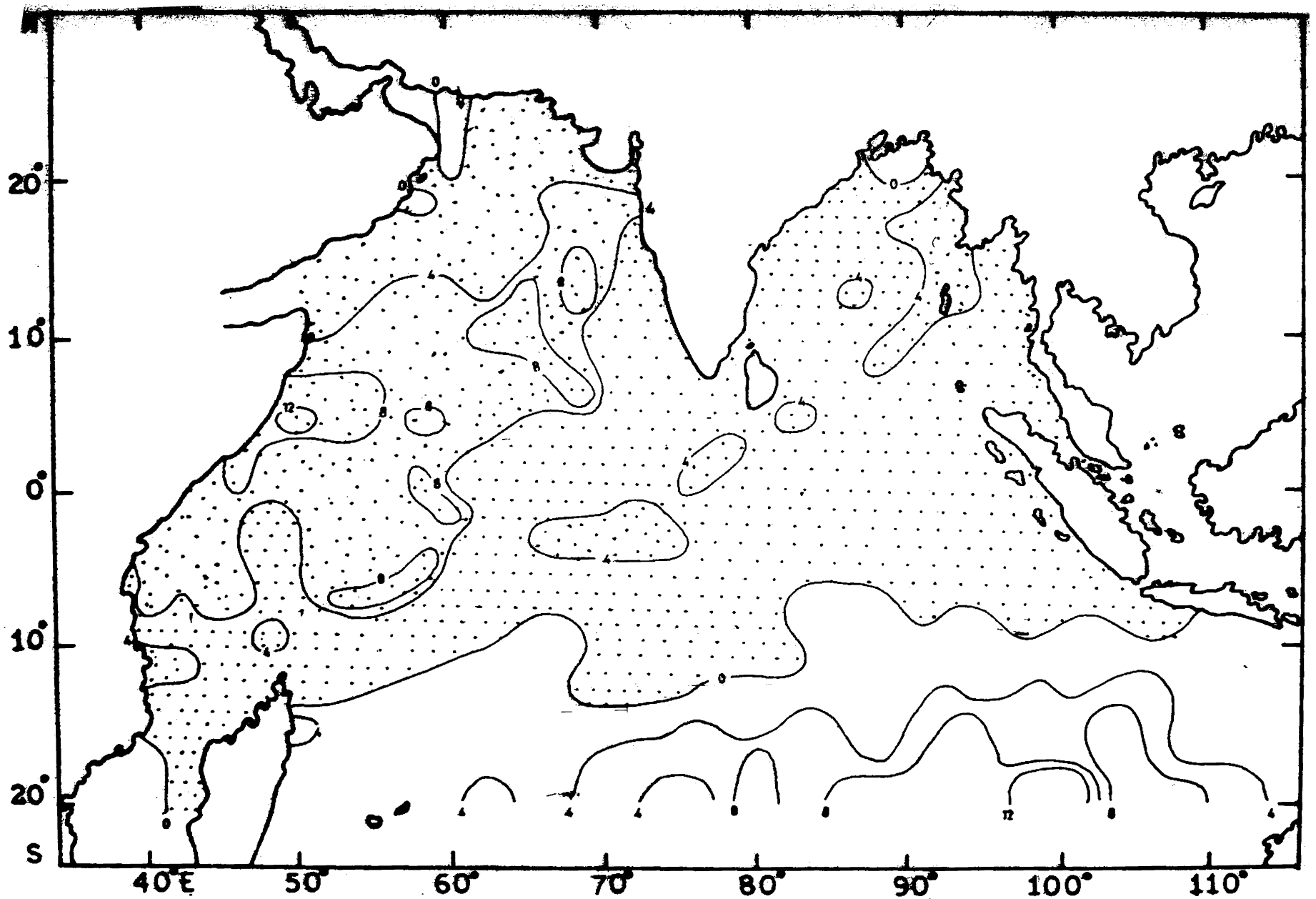

FIG: 2b. MERIDIONAL COMPONENT (τ) OF THE WIND STRESS (10^{-1} dynes cm^{-2}) IN FEBRUARY.

The zonal components of the wind stress are higher than the meridional components in the Somali region and Bay of Bengal but lower in the Arabian Sea, irrespective of their direction. The meridional components of the wind stress exceed the zonal components east of 58°E in the equatorial region. South of the equator, the zonal components of the wind stress generally exceed the meridional components.

MARCH

The zonal components of the windstress are negative in March (Fig.3a) except east of 50°E between the equator and 10°S in the northeastern parts of the Arabian Sea and in the northern parts of the Bay of Bengal. The Arabian Sea and Bay of Bengal record lower values of westward wind stress but higher values are observed in the Somali region and in the southern parts of the Indian Ocean. The values of the eastward wind stress are lower than those in February.

The meridional components of the wind stress in March (Fig.3b) are negative except south of 8°S and near the east coasts of India and Arabia. The southward stress in the Bay of Bengal is lower than that in February, but no conspicuous difference is observed in the Bay of Bengal by March from the previous months. Somewhat higher values are

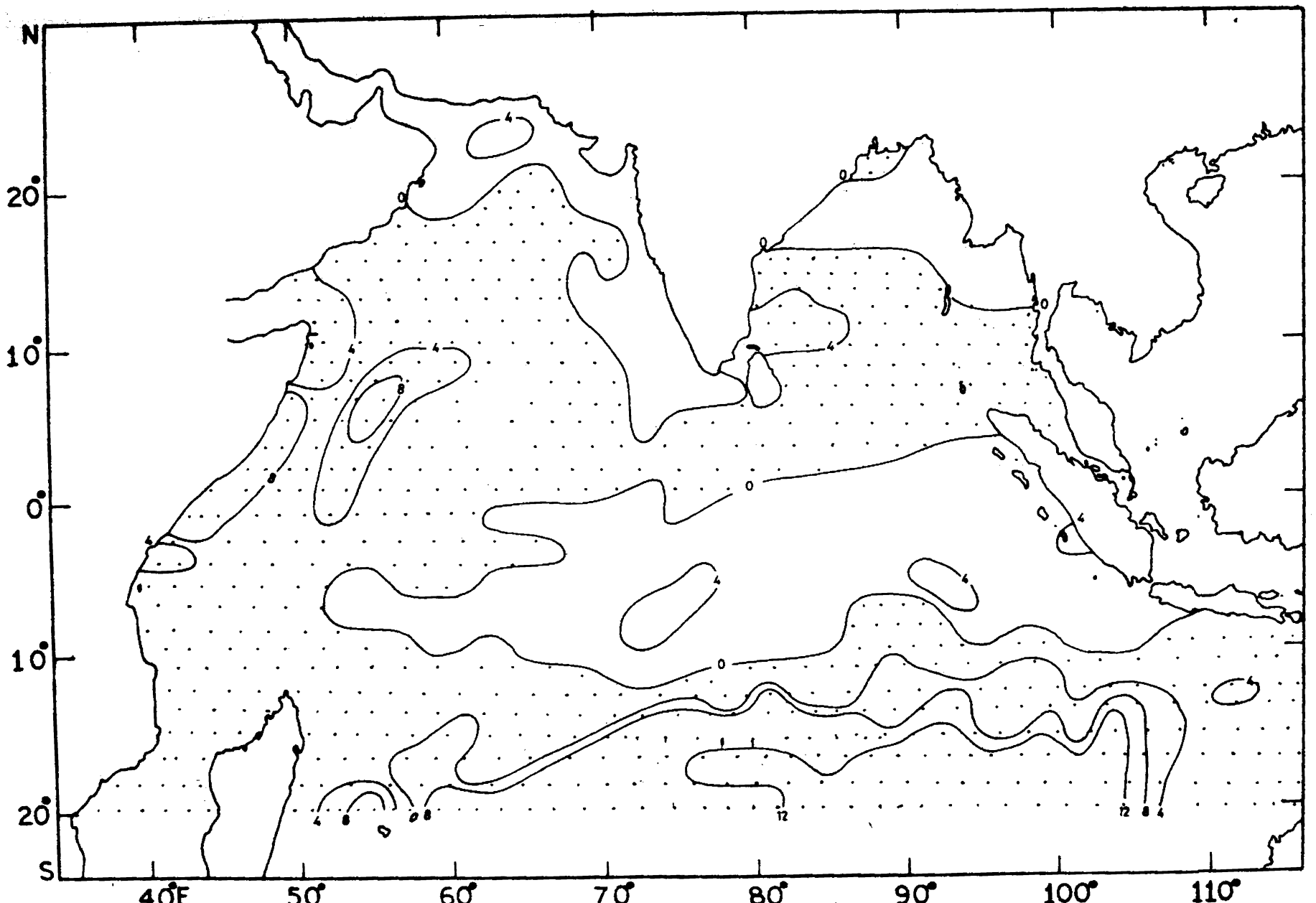

FIG:3a. ZONAL COMPONENT OF THE WIND STRESS (10^{-1} dynes cm^{-2}) IN MARCH

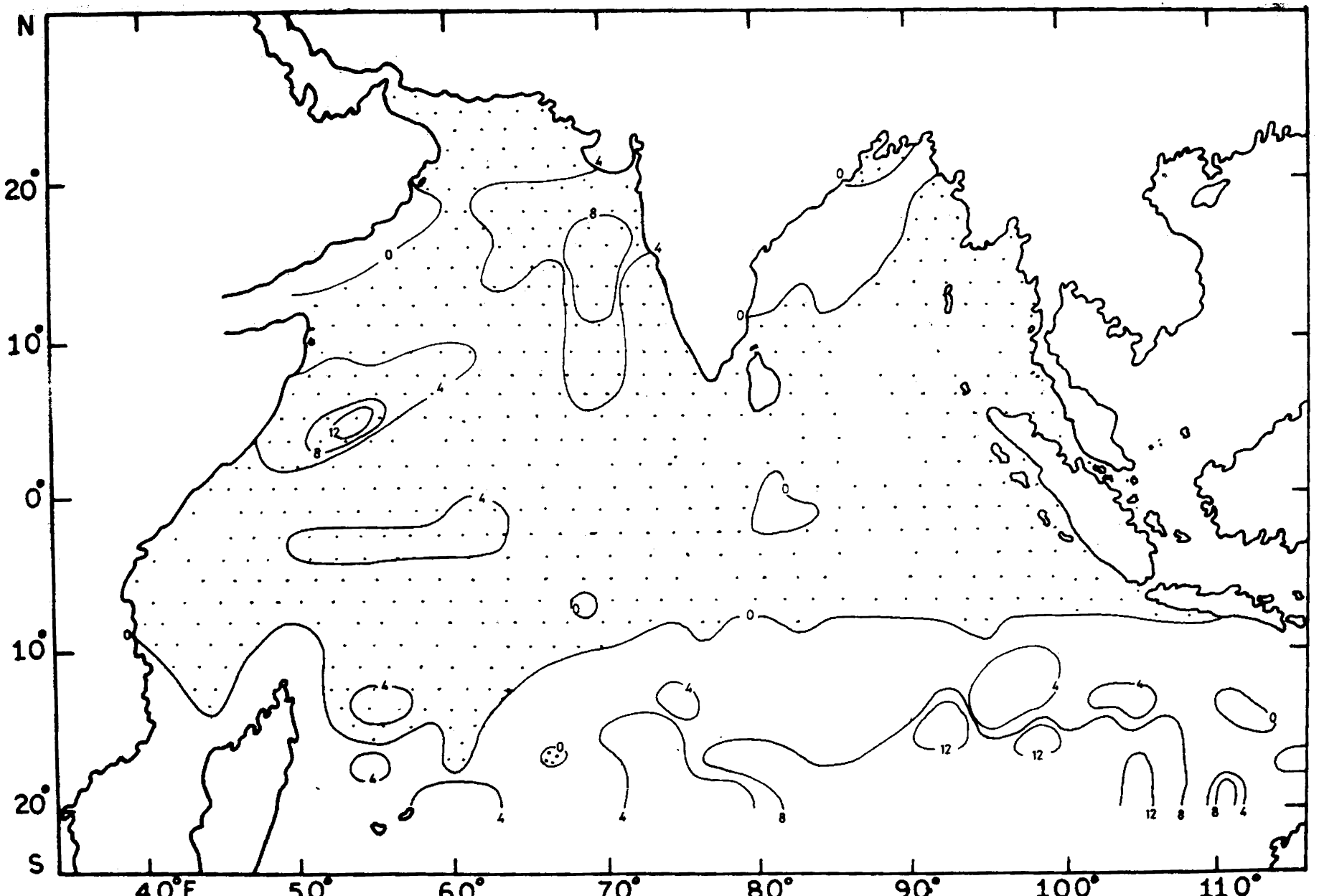

FIG: 3b. MERIDIONAL COMPONENT OF THE WIND STRESS (10^{-1} dynes cm^{-2}) IN MARCH

recorded in the Somali region compared to those in the adjacent areas. Lower values of southward stress are observed near the equatorial region. Northward stress prevails south of 8°S and increases southward. The area of the northward stress considerably decreases compared to that in the other months. The northward stresses found near the east coast of India indicate the reversal of the northeasterlies to the southwesterlies. Similarly, the distribution of the zonal and meridional components of the wind stress clearly reveals that the winds are blowing from a northwest direction near the northeastern parts of the Arabian Sea.

The values of the zonal components exceed the meridional components in the Arabian Sea, Bay of Bengal and Somali region irrespective of their direction. The meridional components are higher than the zonal components in the equatorial region between 60° and 90°E. The zonal components of the wind stress exceed the meridional components west of 60°E and east of 90°E, in the equatorial region. The zonal components are higher than the meridional components in the southern parts of the Indian Ocean.

APRIL

This is the month of transition from the northeast monsoon to the southwest monsoon. The transition character is evident from the nonuniformity of the distribution of the zonal and meridional components of the wind stress (Fig.4a). The southeasterlies of the southern hemisphere start to reverse

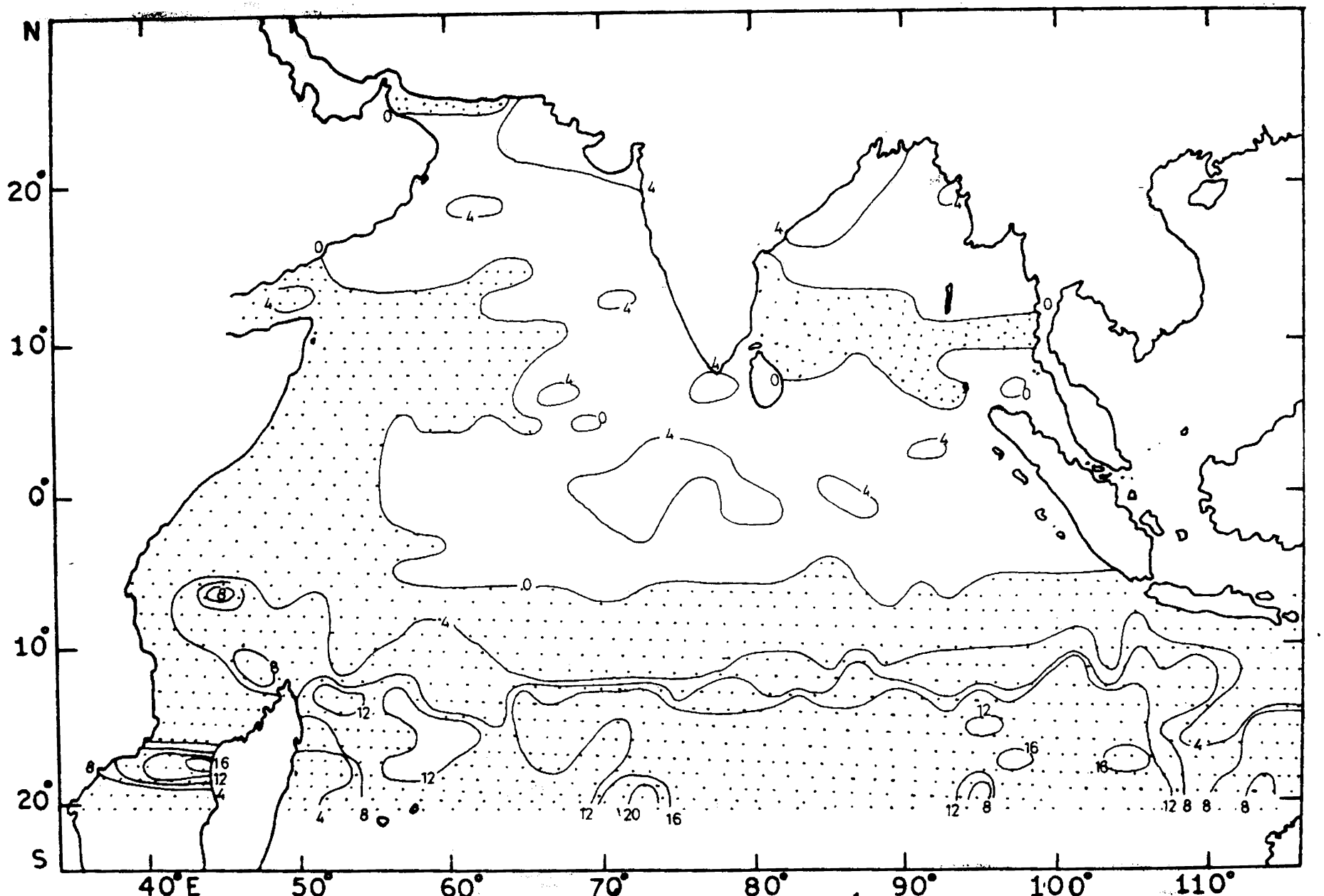

FIG: 4a. ZONAL COMPONENT OF THE WIND STRESS (10^{-1} dynes cm^{-2}) IN APRIL

into southwesterlies at about 6°S, east of 60°E. West of 60°E, the southeasterlies exist upto 14°N. A belt of westward stress is found in the Bay of Bengal between 6°N and 12°N. Westward wind stress prevails south of 6°S. Unlike in the previous months, higher values of eastward stress are found in the equatorial region between 68° and 92°E, almost symmetrical about the equator. This higher eastward stress is responsible for the eastward flowing Equatorial Jet which starts to flow by April. The values of the eastward stress in other parts of the ocean are lower than those in the previous months. The maximum value of the eastward stress is only a little greater than 4×10^{-1} dynes cm^{-2} observed in the equatorial region, central Arabian Sea and the northwestern parts of the Bay of Bengal. The westward stress south of 6°S is, generally, higher than that in the previous months and increases to south. A latitudinal steadiness of westward windstress is found south of the equator. Lower values of the westward wind stress are also found in the western parts of the Arabian Sea.

The meridional components of the wind stress in April (Fig.4b) are positive almost over the entire ocean. Southward stress prevails in the Arabian Sea from 20° N to 8°S between 50° and 80°E. The maximum value observed is a little greater than 8×10^{-1} dynes cm^{-2} in the western parts of the Bay of Bengal. A secondary maximum is observed in the Arabian Sea

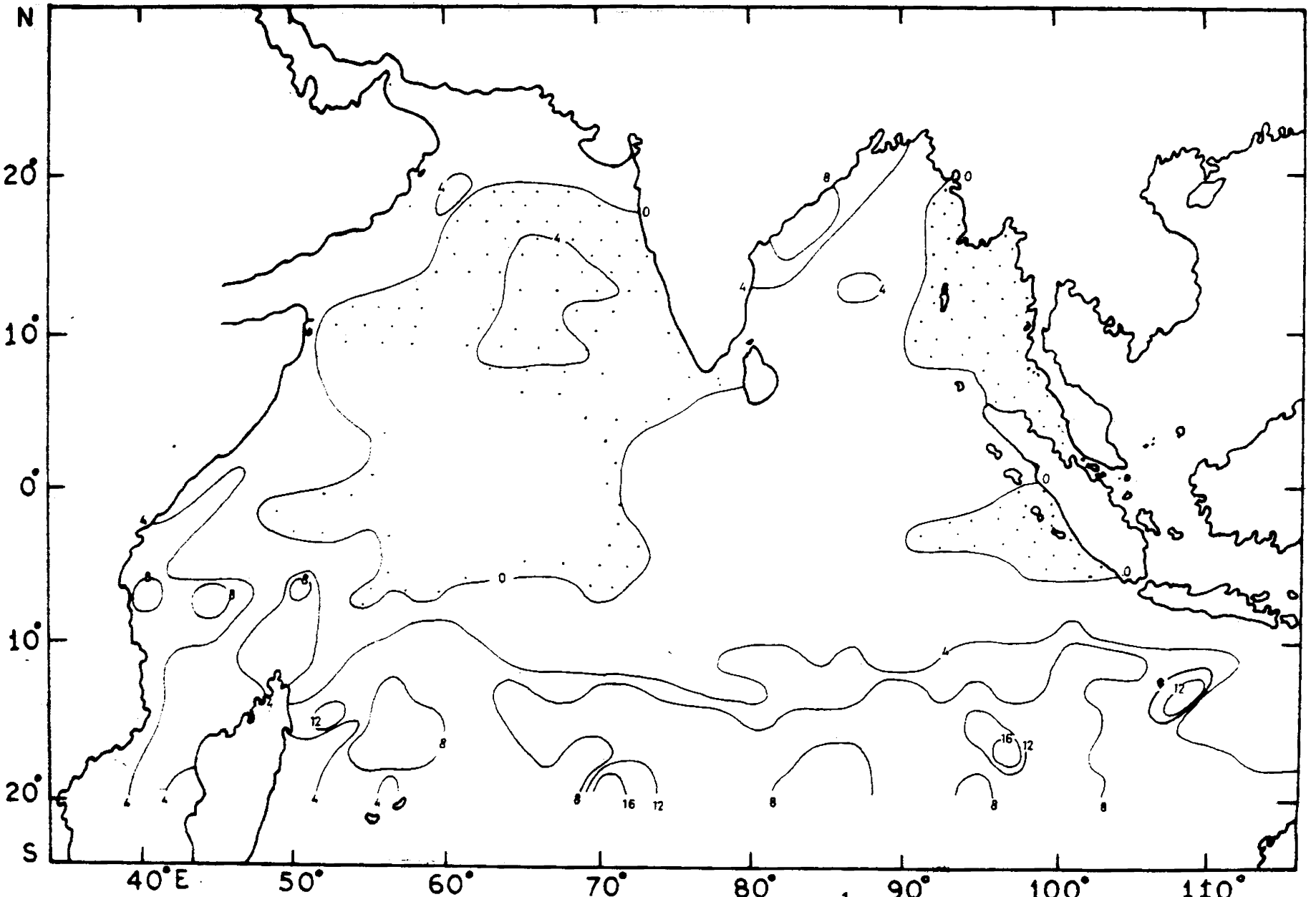

FIG: 4b. MERIDIONAL COMPONENT OF THE WIND STRESS (10^{-1} dynes cm^{-2}) IN APRIL

which is less than 7 x 10^{-1} dynes cm^{-2}. The meridional components of the wind stress north of 10°S are, generally, lower than those in the previous months. The values of the northward stress south of 10°S with maximum of about 16 x 10^{-1} dynes cm^{-2} are, generally, higher in extent than those in March. The presence of the northward wind stress in the Somali region indicates the set up of the Somali Current by April itself. But the lower values of the northward wind stress clearly reveal that the Somali Current is very weak during April.

The magnitude of the zonal components of the wind stress in the equatorial region is higher than the magnitude of the meridional components irrespective of their direction. Higher values of westward stress are observed between the African Coast and the Malagasy Coast. The zonal components of the wind stress generally, exceed the meridional components of the wind stress south of the equator.

MAY

The conditions of the southwest monsoon have fully attained during this month Figs (5a & 5b). Strong eastward stress is observed north of 2°S. The maximum value of the eastward stress (20.5 x 10^{-1} dynes cm^{-2}) is observed in the Somali region. A secondary maximum of 12x10^{-1} dynes cm^{-2} is observed south of Sri Lanka. The Bay of Bengal exhibits lower

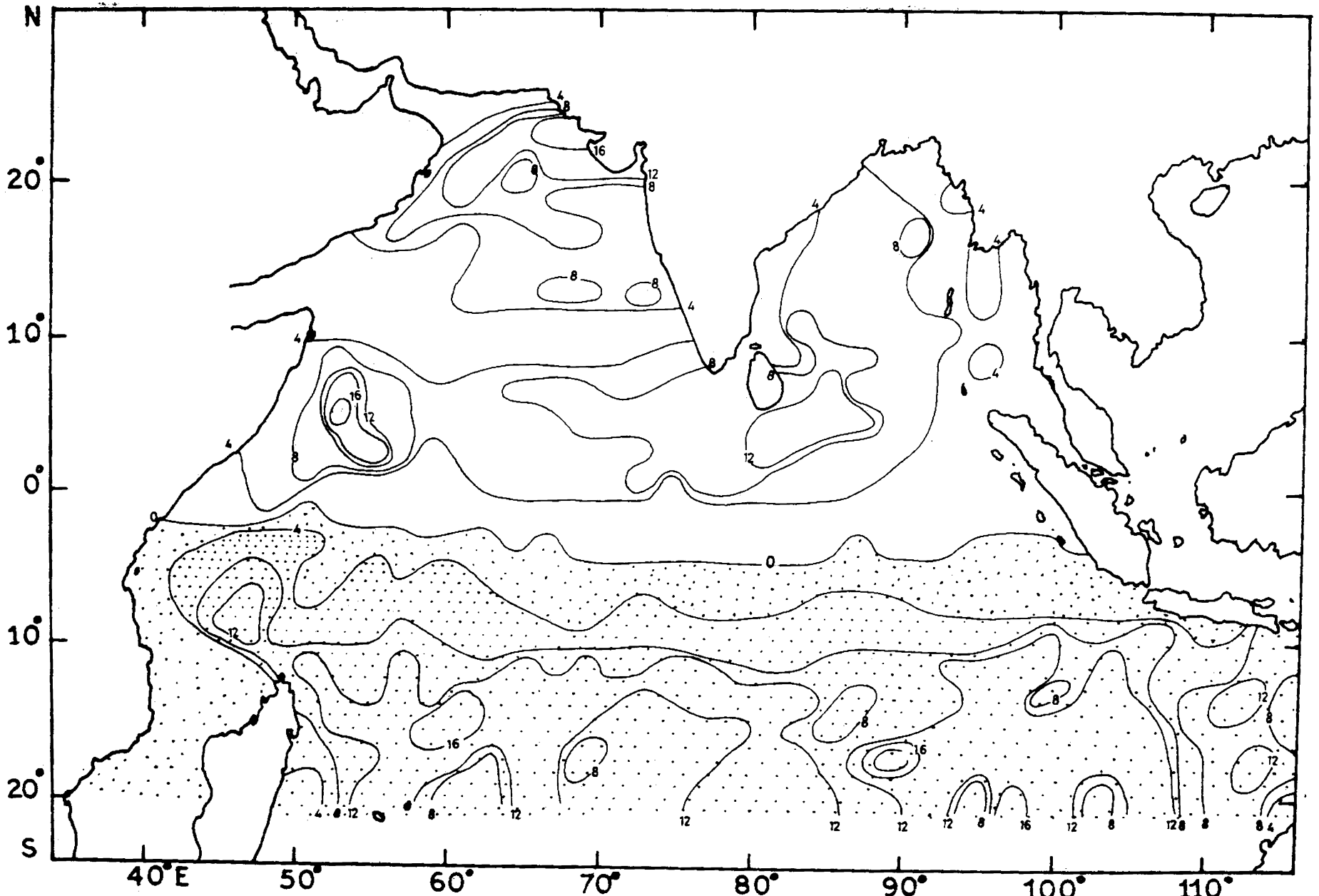

FIG: 5a. ZONAL COMPONENT OF THE WIND STRESS (10^{-1} dynes cm^{-2}) IN MAY.

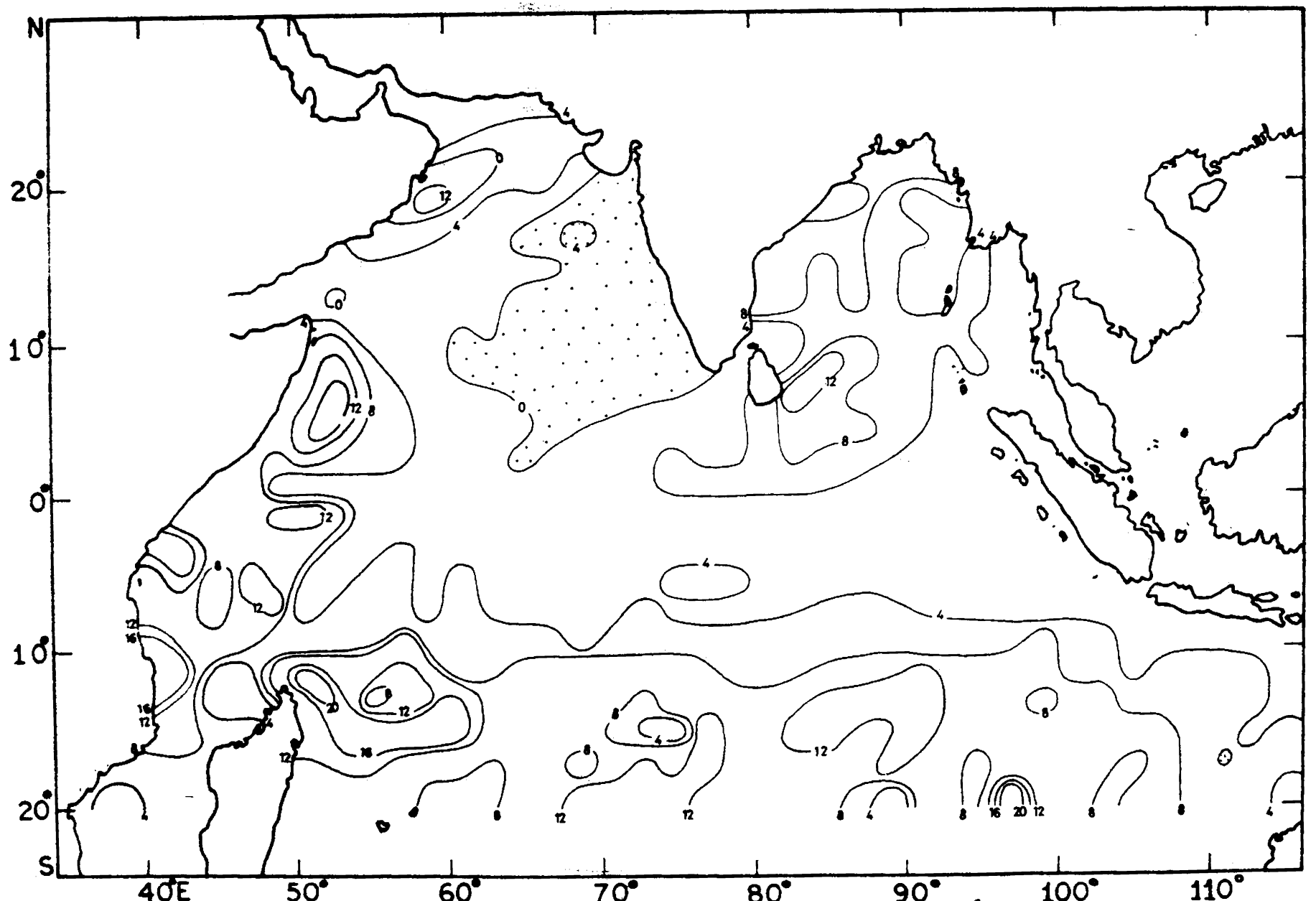

FIG:5b. MERIDIONAL COMPONENT OF THE WIND STRESS(10^{-1} dynes cm^{-2}) IN MAY.

values than those in the Arabian Sea. Weak and variable stress is observed near 2°S which represents the doldrum area. Higher values of eastward stress are found along the equator from 45° to 90°E. This belt of higher eastward stress drives the Equatorial Jet. The values of the eastward stress increase at least 4 times by May. Generally, lower values are encountered near the coasts compared to other regions. The higher eastward stress south of 2°S drives the eastward flowing Southwest Monsoon Current.

Westward stress predominates in the southern Indian Ocean south of 2°S. A latitudinal steady distribution of the westward wind stress is found and the values are, generally, higher than those in April, especially, in the western region of the ocean. The values of the westward wind stress are lower in the eastern parts of the ocean, compared to those in the previous months. The maximum which is found west of Malagassy in April, is not present in May. The values of the westward stress generally, increases towards south. This westward stress drives the westward flowing South Equatorial Current.

Northward wind stress predominates in the entire Indian Ocean, except in the eastern parts of the Arabian Sea. The maximum value of the northward wind stress (21.6×10^{-1} dynes cm^{-2}) is found just north of Malagasy. Higher values

of northward wind stress are also predominant near the African Coast, especially, in the Somali region. The values of the meridional components of the wind stress are higher in the Bay of Bengal than those in the Arabian Sea.

The zonal components of the wind stress exceed the meridional components in the equatorial region and in the Arabian Sea. The meridional components are higher than the zonal components in the Bay of Bengal and south of the equator especially, between the African Coast and the Malagasy Island.

JUNE

The zonal components of the wind stress are positive (Fig 6a) north of 4°S upto 70°E . The values of the eastward stress considerably increases from May to June. The eastward wind stress in the Bay of Bengal is only about half of that in the Arabian Sea. The maximum value of about 37×10^{-1} dynes cm^{-2} is recorded in the Arabian Sea. The Somali region also experiences higher values of eastward wind stress. Lower values are observed just south of the equator and near the Sumatra coast. There is not much difference in the distribution of the eastward wind stress in the central equatorial region in June from that in May, eventhough a slight decrease is experienced south of the equator. The higher eastward wind

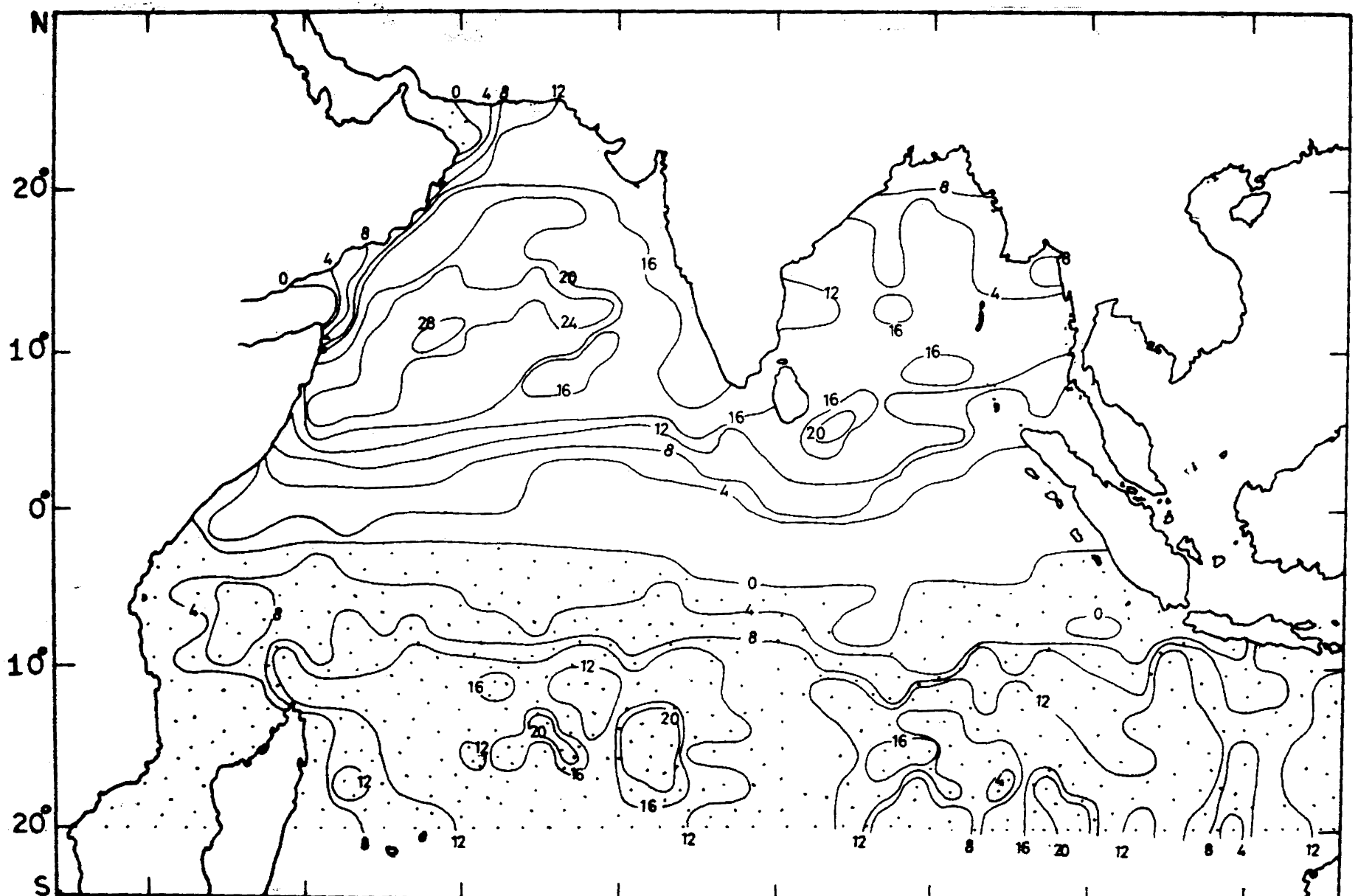

FIG: 6(a) ZONAL COMPONENT OF THE WIND STRESS (10^{-1} dynes cm^{-2}) IN JUNE

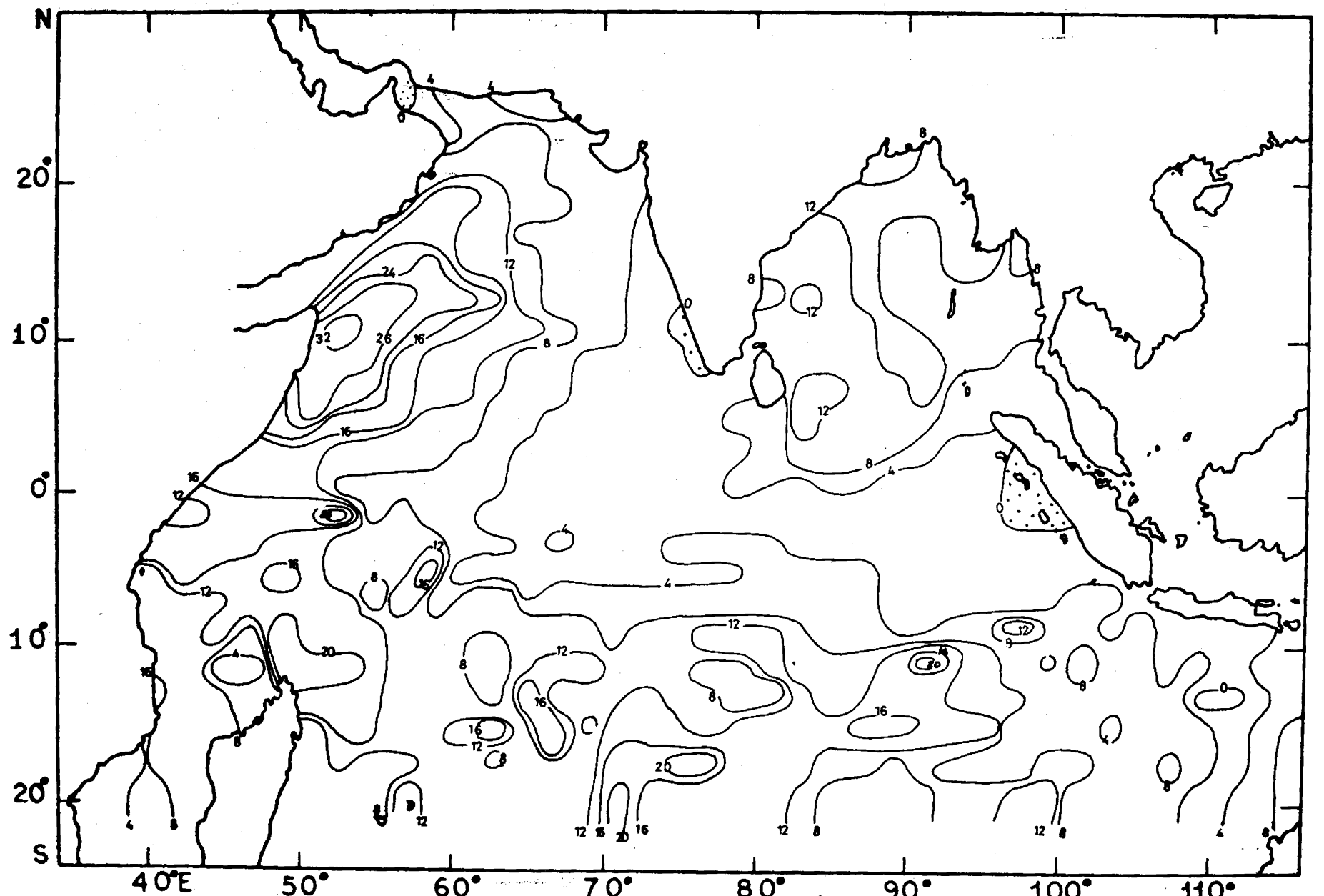

FIG: 6(b) MERIDIONAL COMPONENT OF THE WIND STRESS (10^{-1} dynes cm^{-2}) IN JUNE

stress north of 2°S drives the Monsoon Current.

Westward wind stress predominates in the South Indian Ocean. The maximum value of the westward wind stress (23.5 x 10^{-1} dynes cm^{-2}) is observed from 70° to 74°E between 12° and 16°S. The latitudinal steadiness of the westward wind stress is slightly distrubed in June, especially in the eastern parts of the ocean. The coastal regions of Sumatra and Africa experience lower values of westward wind stress.

The meridional components of the wind stress are positive in June (Fig.6 b) in the entire ocean, north of 20°S except in a narrow belt near the southeast coast of India. Maximum value is found in the Somali region (> 34 x 10^{-1} dynes cm^{-2}). Lower values are observed off the southern tip of India while higher values are observed in the central parts of the South Indian Ocean.

The zonal components of the wind stress exceed the meridional components in the Arabian Sea and the Bay of Bengal. In the equatorial region the meridional components of the wind stress are higher than the zonal components west of 64°E while the zonal components exceed the meridional components east of 64°E.

JULY

The southeasterlies of the southern hemisphere reverse into southwesterlies at about 2°S except in the central region where the reversal takes place at about 6°S. Eastward wind stress occurs north of 2°S (Fig.7a) with higher values in the Arabian Sea and the Somali Current region while the Bay of Bengal records weak and variable stress. Lower values are observed in the equatorial region where the reversal of winds take place. The maximum value of the eastward wind stress (45×10^{-1} dynes cm^{-2}) is observed in the Arabian Sea. In general, the values of the eastward wind stress increase considerably by July.

Westward wind stress predominates south of 2°S and increases southward with some highs and lows in between. However, the values are higher compared to those in June, even-though the rate of increase is not much conspicuous as that of the eastward stress. Unlike the contours of the eastward stress, the contours of the westward stress run almost parallel to the latitudes. This character indicates the steadiness of the southeasterlies and the associated steadiness of the South Equatorial Current. Higher values of the westward stress are observed near 10°S between 46° and 50°E, and between 60° and 64°E. The region between Africa and Malagasy experiences very

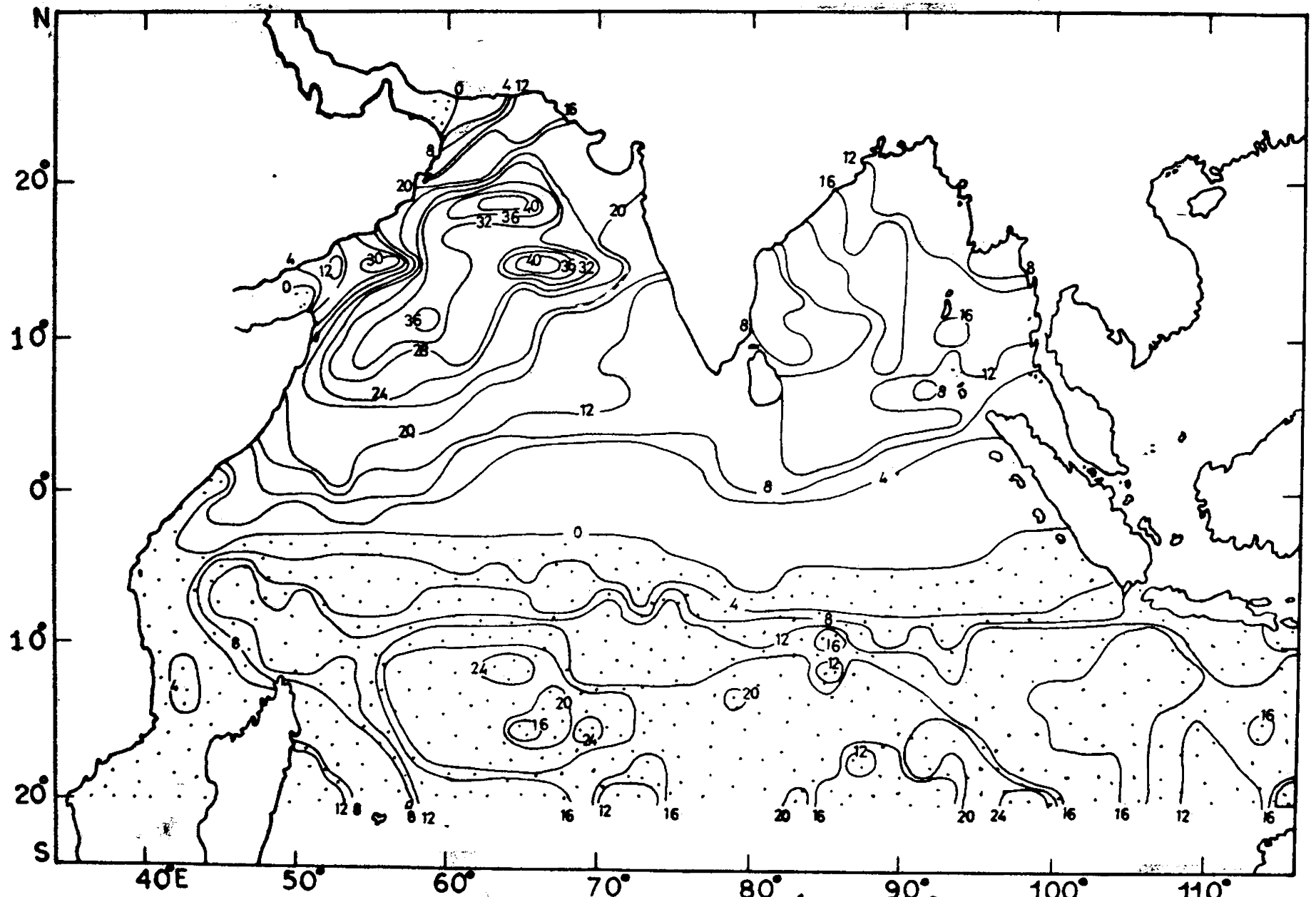

FIG: 7(a) ZONAL COMPONENT OF THE WIND STRESS (10^{1} dynes cm^{-2}) IN JULY

low westward wind stress while it reaches a maximum of 25 x 10^{-1} dynes cm^{-2} just north of Malagasy.

The meridional components of the wind stress are positive in July (Fig.7b) in the entire region, except near the southwest coast of India. A maximum value exceeding 46 x 10^{-1} dynes cm^{-2} is observed near the Somali coast. This is the highest value noted out of all the months. At the same time, the northward stress is very low in the Bay of Bengal compared to that in the Arabian Sea. Higher values are also found in the southern parts of the ocean. A maximum exceeding 34 x 10^{-1} dynes cm^{-2} is observed just north of the Malagasy Island. The equatorial region, east of 62°E experiences lower values of the northward stress. It is of interest to note that both the higher values of the zonal and meridional components of the wind stress are observed away from the Somali coast. The area covered by the negative meridional components near the southwest coast of India increases considerably by July.

The meridional components of the wind stress are higher than the zonal components in the equatorial region, west of 60°E, irrespective of their direction. Between 60° and 90°E the zonal components exceed the meridional components. In the Somali Current region, the meridional components of the wind stress exceed considerably the zonal components. The

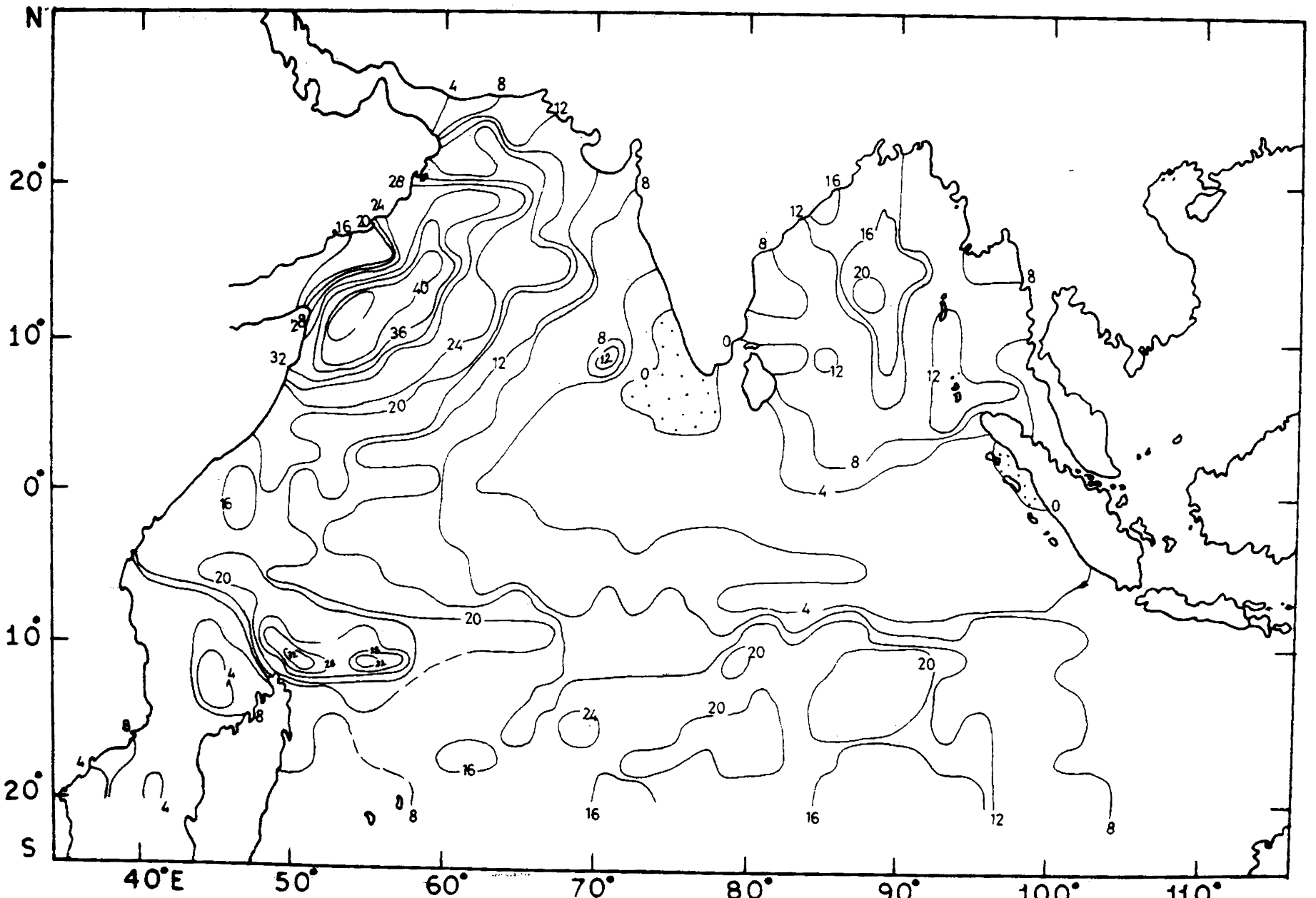

FIG: 7(b) MERIDIONAL COMPONENT OF THE WIND STRESS (10^{-1} dynes cm^{-2}) IN JULY

zonal components of the wind stress are higher than the meridional components, north of the equator and east of the Somali Current. This indicates that the Monsoon Current is very strong in this region. The predominance of the meridional components of the wind stress over the zonal components in the western parts of the ocean reveals that as the South Equatorial Current approaches the western region, its northward transport increases and feeds the Somali Current.

AUGUST

Eastward stress predominates the entire region north of the equator, except at the mouth of the Persian Gulf (Fig.8a). The reversal of winds occur earlier in the western and eastern parts of the Indian Ocean. The maximum value of the eastward wind stress ($>32 \times 10^{-1}$ dynes cm^{-2}) is observed in the central part of the Arabian Sea. Higher values are also found in the Somali Current region. The eastward wind stress in the Bay of Bengal is found to be nearly half of that in the Arabian Sea. However, the eastward stress increases towards the central parts of the Arabian Sea and the Bay of Bengal from north and south. Along the equatorial region, especially, between 60° and $72^{\circ}E$, the eastward wind stress is much smaller compared to that in the other regions. Lower values are again encountered in the equatorial region, east of $90^{\circ}E$, while

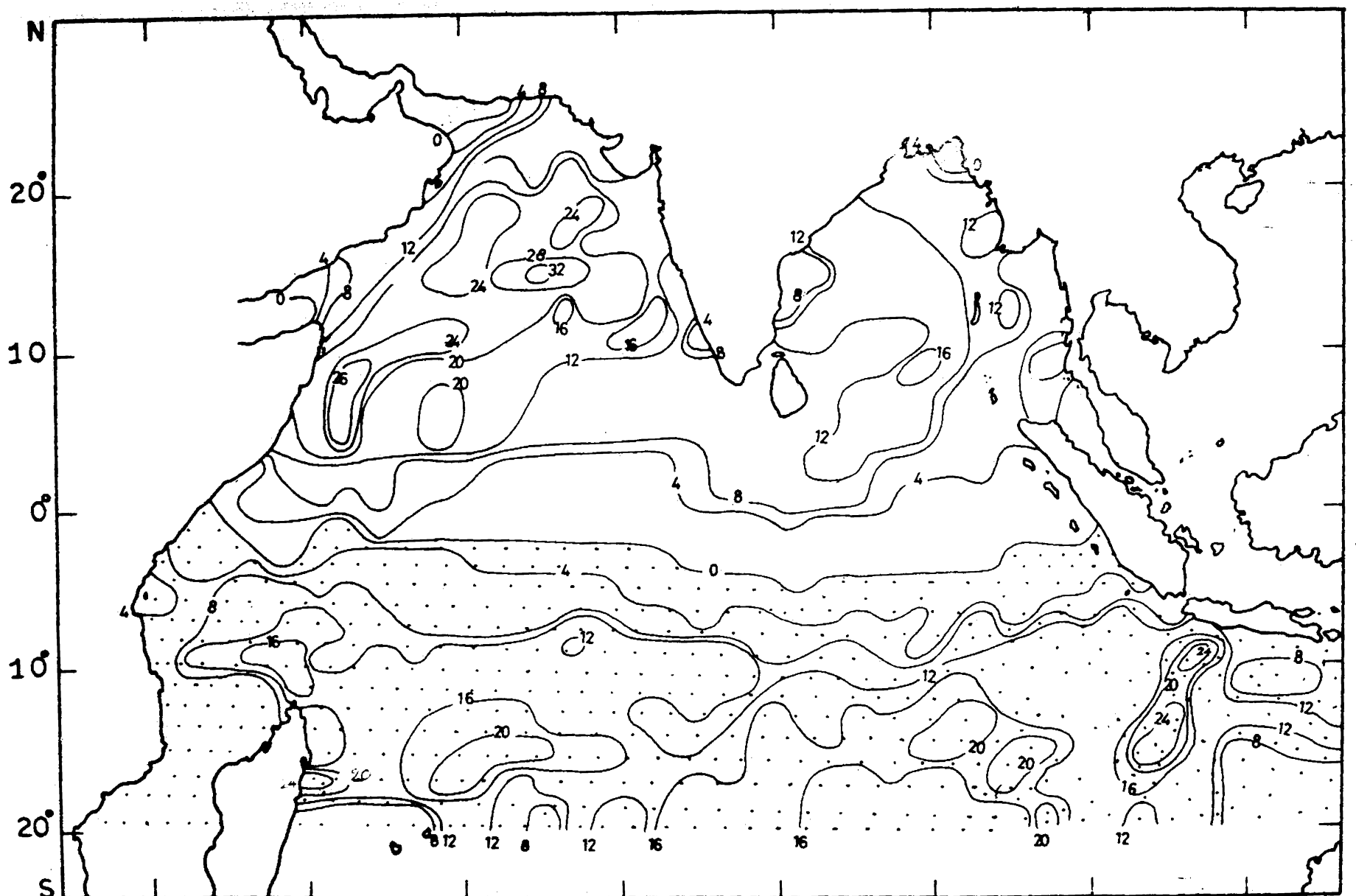

FIG: 8a. ZONAL COMPONENT OF THE WIND STRESS (10^{-1}dynes cm^{-2}) IN [redacted]GUST

higher values exceeding 9 x 10^{-1} dynes cm^{-2} are found between 72° and 90°E. Similarly, a maximum value of about 14 x 10^{-1} dynes cm^{-2} is found in the equatorial region, west of 72°E. Smaller values are, generally, found along the southwest coast of India.

The zonal components of the wind stress are negative south of the equator. The higher value of the westward wind stress (24 x 10^{-1} dynes cm^{-2}) is found in the southern Indian Ocean east of 100°E. Another higher value of about 20 x 10^{-1} dynes cm^{-2} is found between 86° and 94°E, and between 60° and 66°E, south of 10°S. The contours of the westward wind stress, generally, run parallel to the latitudes in the South Indian Ocean, indicating steady and strong southeasterly winds.

The meridional components of the wind stress are positive in August (Fig.8b) in the entire Indian Ocean north of 20°S, except near the southwest coast of India. The southward stress, near the southwest coast of India indicates that the winds are coming from the west with a slight southerly components. The Somali Current region records the maximum northward stress having a value greater than 36 x 10^{-1} dynes cm^{-2}. A secondary maximum of 24 x 10^{-1} dynes cm^{-2} is found between 76°E and 86°E, south of 10°S. The Bay of Bengal experiences lower values of northward stress than those in the Arabian Sea. The equatorial region shows lower values,

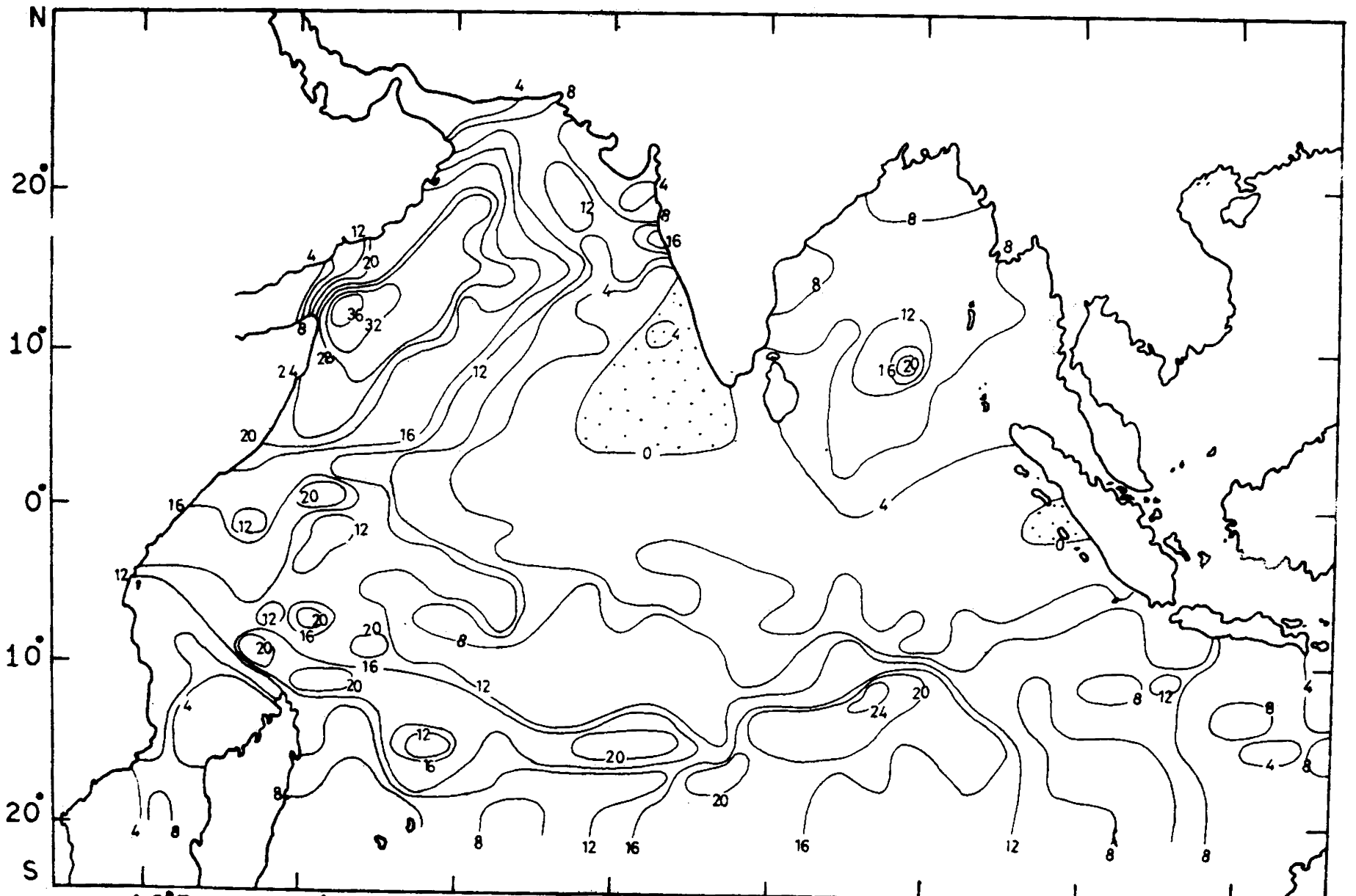

FIG: 8 (b) MERIDIONAL COMPONENT OF THE WIND STRESS (10^{-1} dynes cm^{-2}) IN AUGUST

especially, between 64° and 78°E, and east of 90°E.

The meridional components of the wind stress are generally, higher than the zonal components in the Somali Current region . Along the equator, the zonal components of the wind stress exceed the meridional components east of 76°E. Similarly, the zonal components are generally, higher than the meridional components in the Arabian Sea and the Bay of Bengal, and in the southern parts of the Indian Ocean. However, the region between Africa and Malagasy experience higher meridional wind stress than the zonal wind stress.

SEPTEMBER

Eastward wind stress is observed in the entire Indian Ocean except at the mouth of the Persian Gulf and at the head of the Bay of Bengal (Fig.9a). The southeasterlies of the southern hemisphere reverse into the southwesterlies, first in the central part of the ocean at about 8°S. The zonal components of the wind stress are very much lower compared to those in August which are due to the weakening of the south-west monsoon. The Arabian Sea records higher values than those in the Bay of Bengal. The maximum eastward stress is observed near the Somali coast, with values nearly half of that in August. The northern parts of the Bay of Bengal show very low values, indicating the preceeding wind reversal during

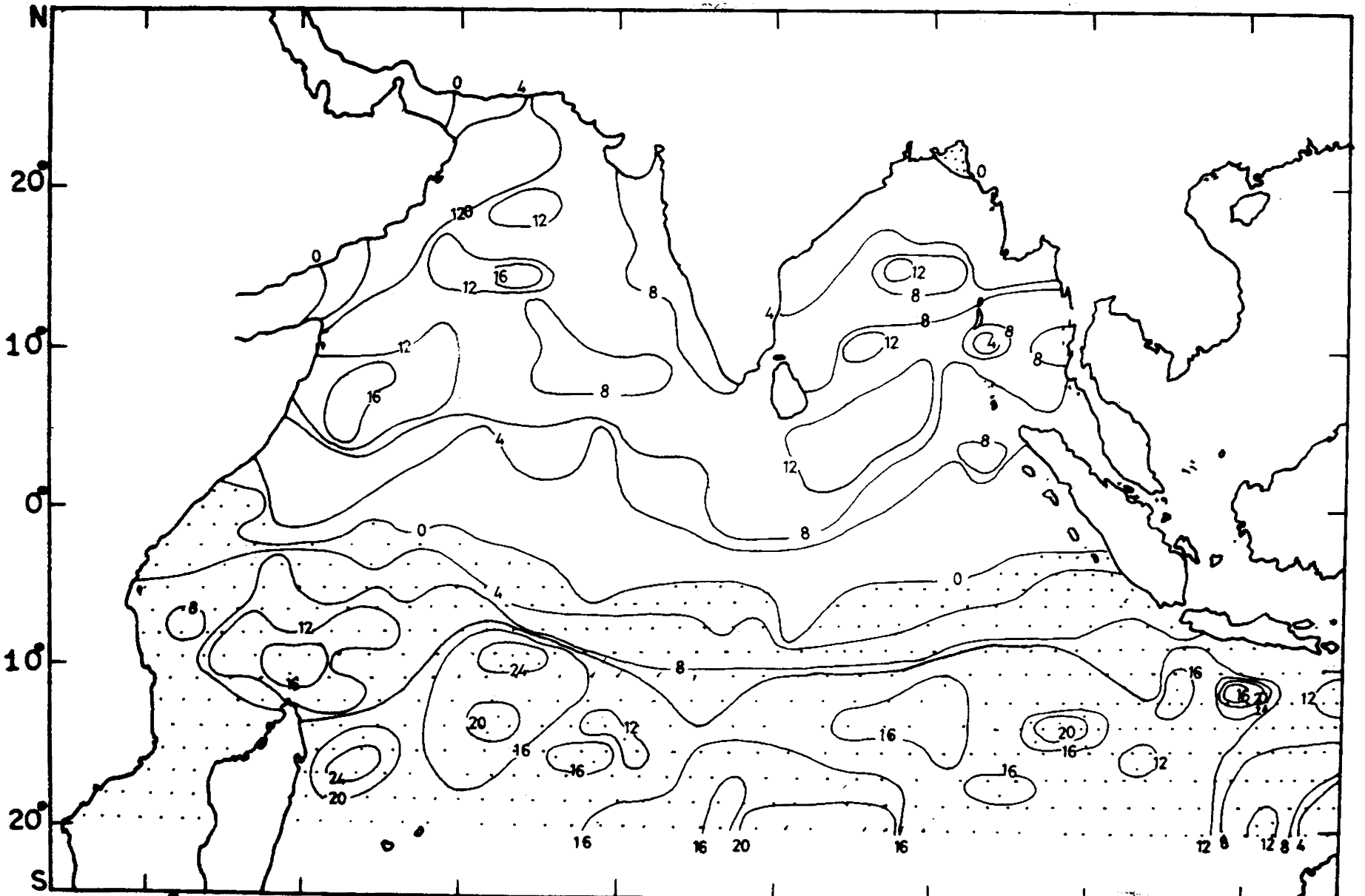

FIG: 9(a) ZONAL COMPONENT OF THE WIND STRESS (10^{-1} dynes cm^{-2}) IN SEPTEMBER

October. Similar to the case of August, very much lower values of the eastward wind stress are observed in the equatorial region between 60° and 70°E, and east of 92°E.

Westward wind stress is observed in the Indian Ocean, generally south of 4°S. Southern parts of the Indian Ocean record higher values of the zonal components of the wind stress. The contours of the westward wind a stress south of the equator run almost parallel to the latitudes. However, the values are lower than those in August. The west coast of Sumatra and the region between Africa and Malagasy also record lower values of the westward wind stress.

The meridional components of the wind stress are positive in September (Fig.9b) in the entire Indian Ocean under study except in the eastern parts of the Arabian Sea. The area covered by the southward wind stress increases considerably from August to September which extends from 20°N to the equator between 64° and 76°E. The Somali Current region records the higher values of northward wind stress of about 22.2×10^{-1} dynes cm^{-2}. The magnitude of the northward wind stress in the Bay of Bengal is relatively weaker than that in the western parts of the Arabian Sea. The equatorial region and the northern parts of the ocean record the lower values of the northward wind stress with higher values in

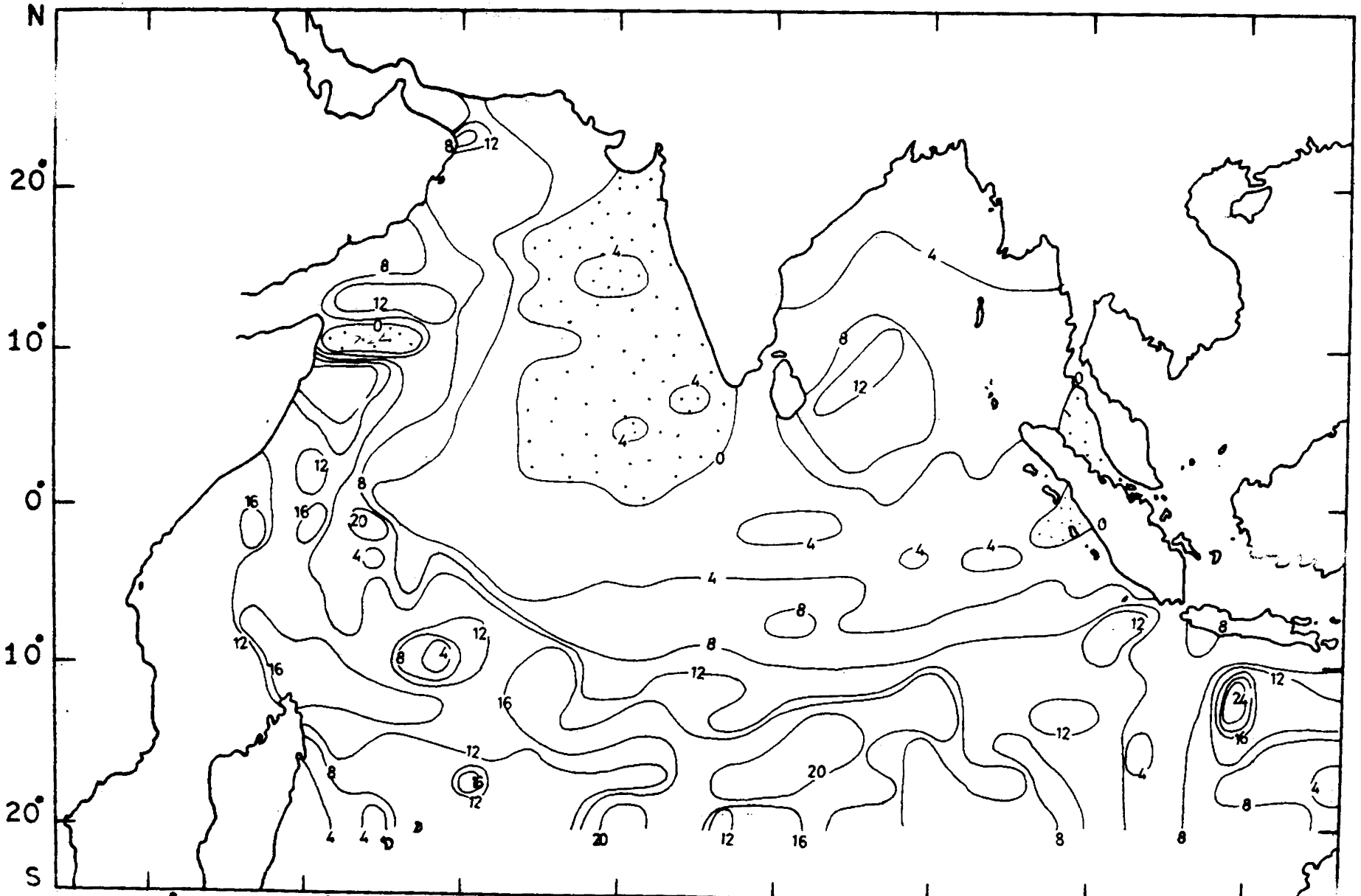

FIG. 9(b) MERIDIONAL COMPONENT OF THE WIND STRESS (10^{-1} dynes cm^{-2}) IN SEPTEMBER

between. A steady southward increase can also be observed south of the equator. A higher value of the northward wind stress of about $2\frac{1}{2} \times 10^{-1}$ dynes cm^{-2} is observed east of 106°E between 10°S and 14°S.

The meridional components of the wind stress exceed the zonal components in the equatorial region west of 60°E. The zonal components of the wind stress exceed the meridional components in the Arabian Sea and in the equatorial region east of 60°E. The zonal components are higher than the meridional components in the Bay of Bengal and in the southern parts of the ocean. Particular mention may be made about the predominance of the zonal components of the wind stress over the meridional components from 70° to 90°E between 2°N and 2°S.

OCTOBER

The non-uniform distribution of the zonal components of the wind stress clearly indicates the transitional character of the month from the southwest monsoon to the northeast monsoon (Fig.10a). Eastward stress prevails north of 4°S except in the northern parts of the Bay of Bengal and in a narrow belt along the Somali and Arabia coasts. A conspicuous feature to be noted is the belt of high eastward stress in the equatorial region south of the southern tip of India. This higher belt of eastward stress drives the Equatorial Jet. The

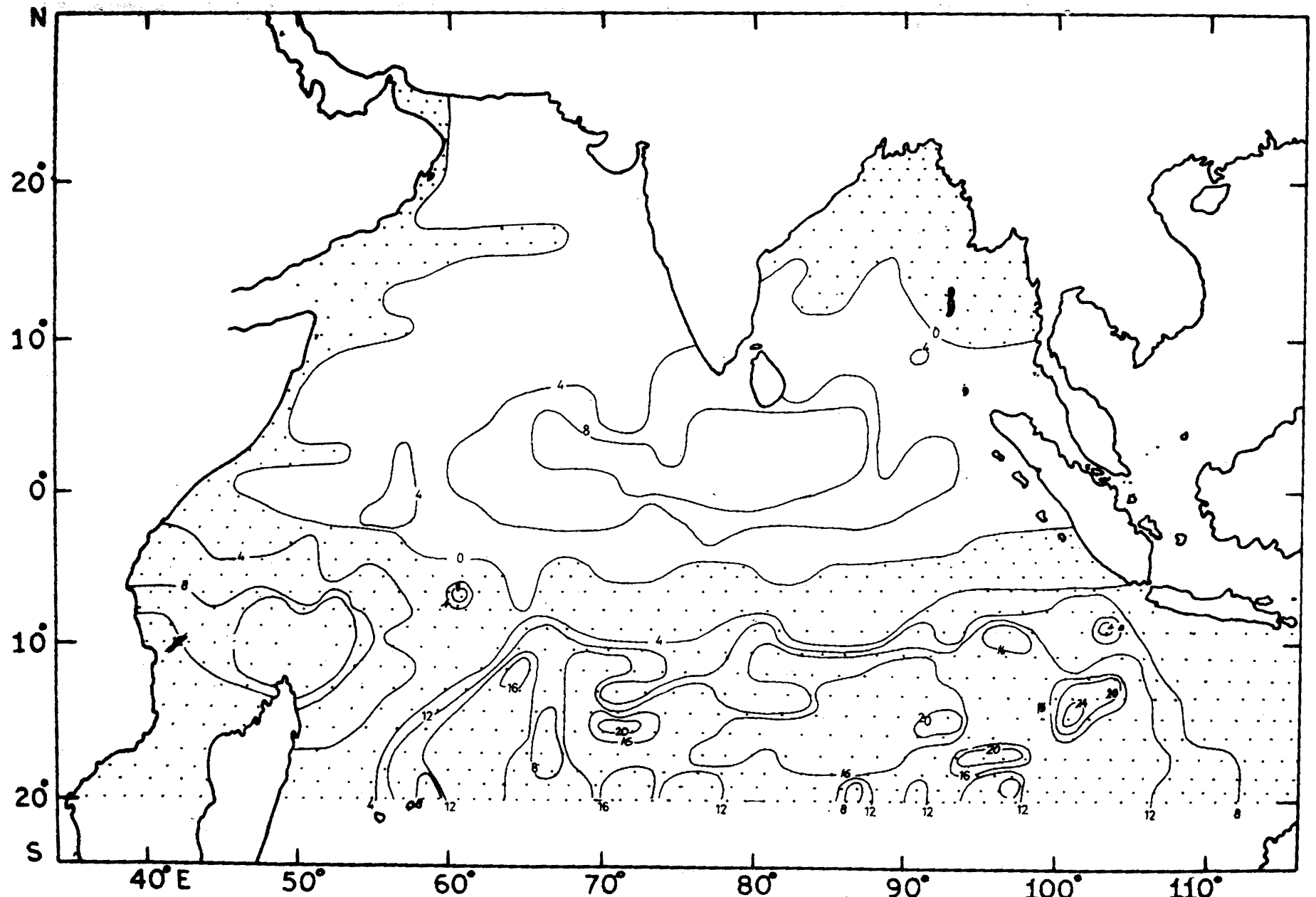

FIG: 10a. ZONAL COMPONENT OF THE WIND STRESS (10^{-1} dynes cm^{-2}) IN OCTOBER.

The maximum value is found north of the equator. In general, the values of the wind stress considerably decrease by October. The minimum value is found in the doldrum area which is represented by the zero contour.

Westward wind stress predominates south of 4°S and increases southward. The maximum value is found in the eastern parts of the ocean between 12°S and 16°S from 100° to 104°E. There is no conspicuous difference in the distribution of the westward wind stress in October from that in September.

The distribution of the meridional components of the wind stress is also nonuniform (Fig.10 b). Northward wind stress prevails in the entire ocean, except in the Arabian Sea and near the coast of Sumatra. The winds over the Arabian Sea are coming from a northwest direction. Southwesterly winds predominate near the Somali Coast and over the northern parts of the Bay of Bengal. Higher values of the northward wind stress are found south of the Somali Current region. The maximum value of the northward stress is observed between 12°S and 16°S, and 88° and 94°E.

The zonal components of the wind stress considerably exceed the meridional components in the equatorial region, east of 60°E. The meridional components of the wind stress are higher than the zonal components in the Arabian Sea and Bay of Bengal.

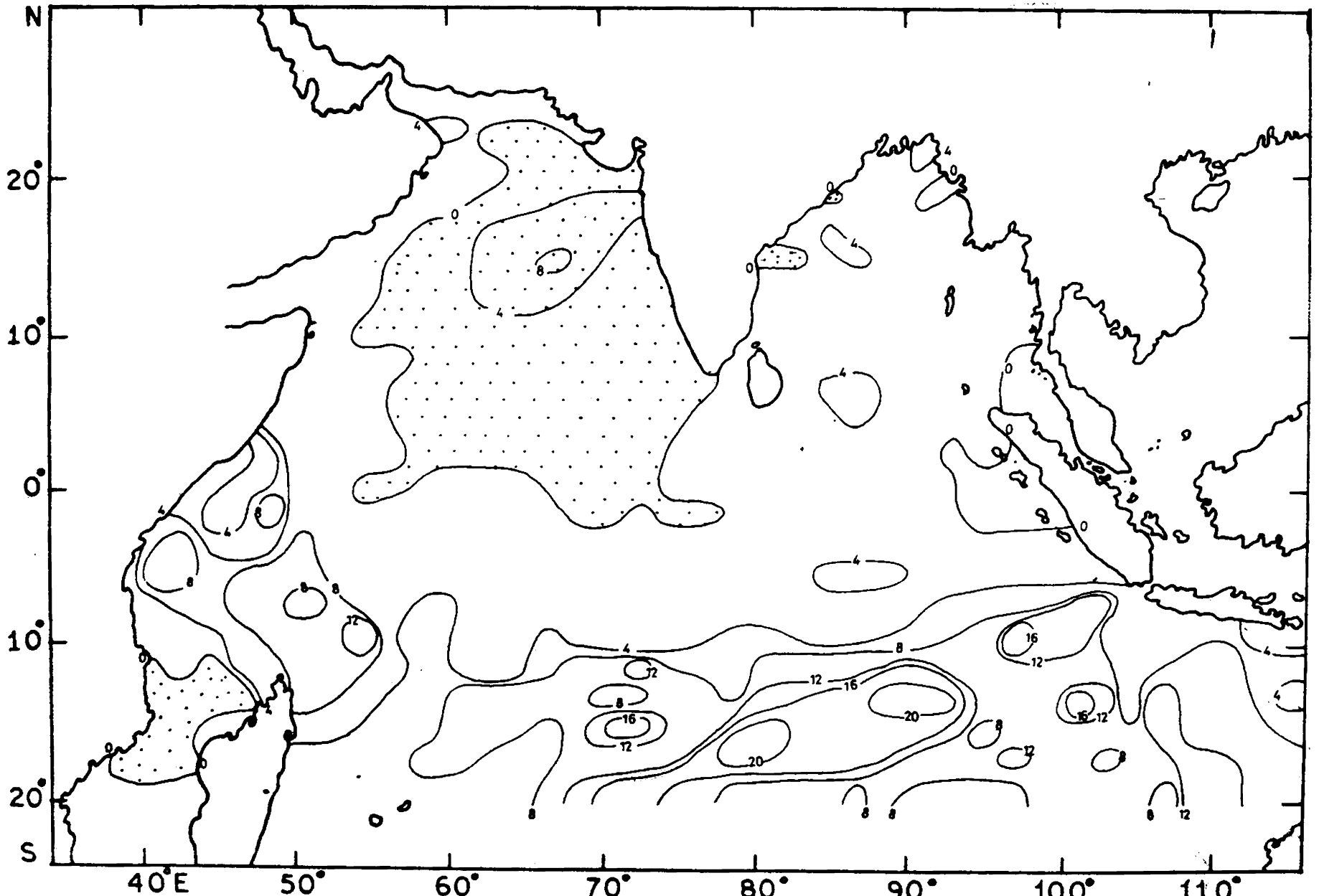

FIG. 10b. MERIDIONAL COMPONENT OF THE WIND STRESS (10^{-1} dynes cm^{-2}) IN OCTOBER.

NOVEMBER

The northeast monsoon is established in the Bay of Bengal and Arabian Sea by November. The zonal components of the wind stress are negative (Fig.11 a) in these regions. There is a considerable increase in the values of the wind stress in November compared to those in October. The Arabian Sea records higher values of the westward wind stress than those in the Bay of Bengal. A belt of eastward wind stress is found to extend from 50°E to the eastern boundary of the eastern ocean between 14°N and 6°S. A narrow belt of higher eastward wind stress is found in the middle of the above belt symmetrical to the equator where the Equatorial Jet is found to exist in the streamline pattern. Very low values are found near the west coast of India, Sumatra and Burma. The lower values of the wind stress are observed in the doldrum area. The zonal components of the wind stress are again negative, south of 6°S and increase to south. But the values are little lower than those in October.

The westward flowing North Equatorial Current and South Equatorial Current are driven by the westward wind stress north of 8°N and south of 6°S. The eastward wind stress in between them drives the eastward flowing Equatorial Countercurrent. The complete reversal of the current off the

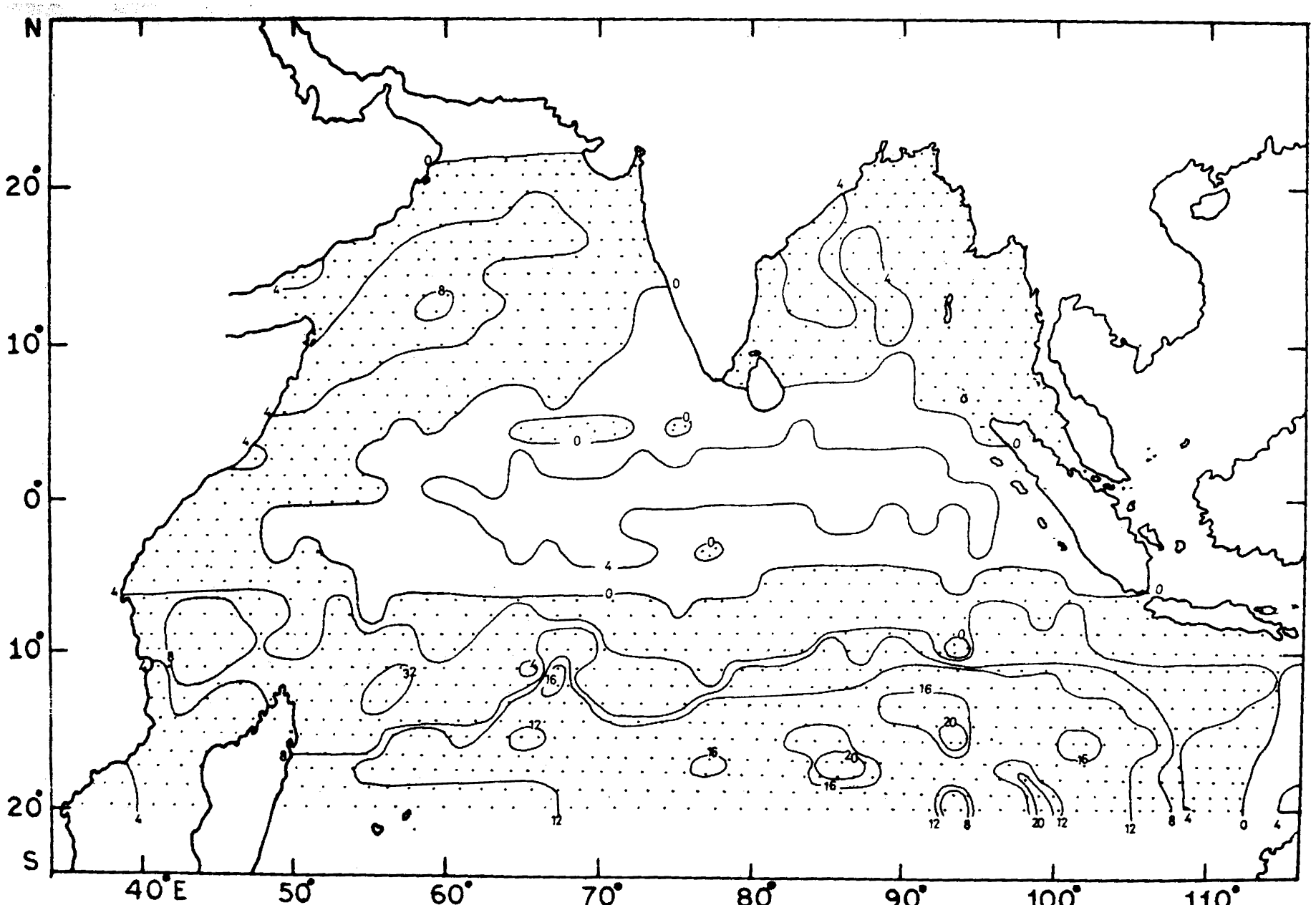

FIG:11a. ZONAL COMPONENT OF THE WIND STRESS (10^{-1} dyens cm^{-2}) IN NOVEMBER.

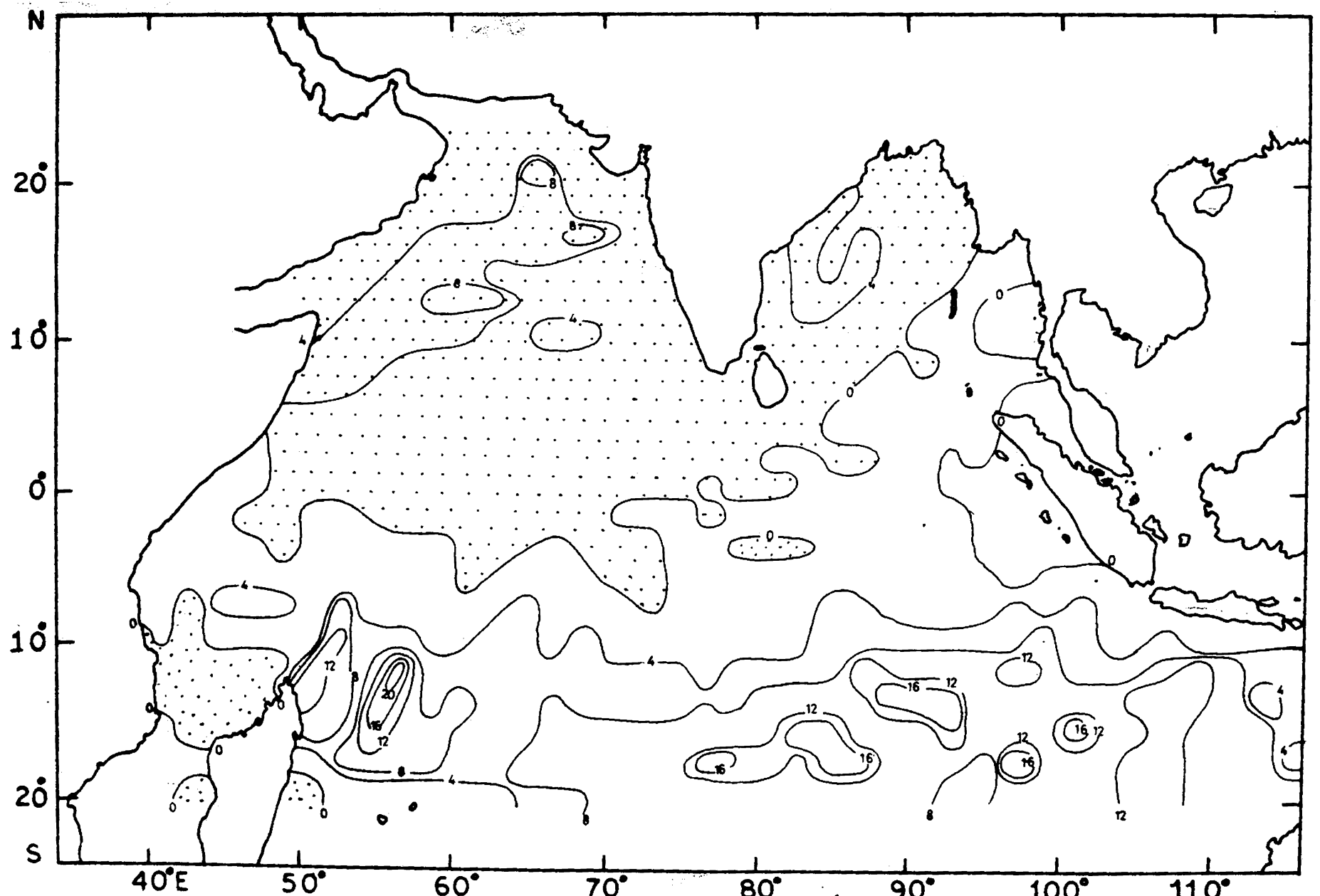

FIG: 11 b MERIDIONAL COMPONENT OF THE WIND STRESS (10^{-1} dynes cm^{-2}) IN NOVEMBER.

Somali Coast is evident from the distribution of the wind stress.

The meridional components of the wind stress are negative west of 70°E and north of 4°S (Fig.11 b). The western half of the Bay of Bengal and the southern parts of Sri Lanka also record negative meridional components of the wind stress. All other parts of the Indian Ocean exhibit positive meridional components. The maximum value of the northward stress is found east of Malagasy. The values north of the equator are slightly higher than those in October. The Equatorial region records lower values of the meridional components of the wind stress.

The zonal components of the wind stress markedly exceed the meridional components in the equatorial region. A relatively slight predominance of the zonal components over the meridional components is also noticed in the northern parts of the Bay of Bengal and southern parts of the Indian Ocean.

DECEMBER

The zonal components of the wind stress are negative (Fig.12 a) north of the equator. Values of the westward stress are higher in the Bay of Bengal than those in the Arabian Sea

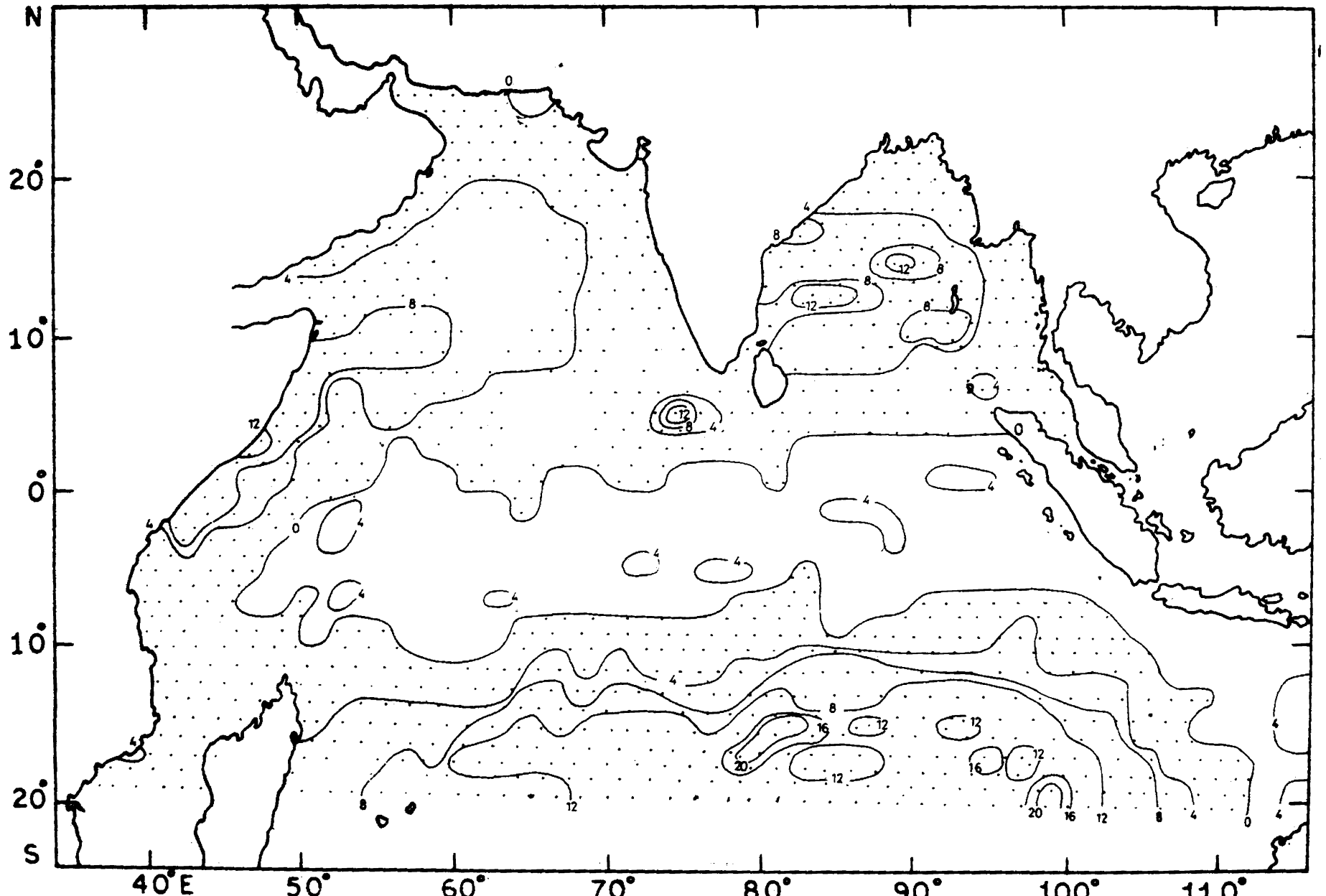

FIG. 12a ZONAL COMPONENT OF THE WIND STRESS (10^{-1} dynes cm^{-2}) IN DECEMBER.

with a maximum of 12 x 10^{-1} dynes cm^{-2}. A belt of lower values of the eastward stress is found east of 50°E between 4°N and 8°S. Higher values of the westward stress are also found near the Somali Coast. The zonal components of the wind stress are positive, generally, between the equator and 8°S. Westward wind stress prevails south of 8°S and increases southward. Very lower values of the westward wind stress are found near the west coast of India while higher values predominate near the east coast. Values of the westward wind stress are higher in the Arabian Sea and Bay of Bengal than those in November. The westward wind stress south of the equator is slightly lower than that in November.

The meridional components of the wind stress are negative (Fig.12 b) north of 9°S in the western parts west of 70°E and north of 4°S and east of 70°E. The maximum southward stress is found in the central Arabian Sea. The regions near the Somali also record higher values of southward wind stress. The values in the Bay of Bengal are slightly lower compared to those in the Arabian Sea. The south west coast of India records very low values of the meridional components of the wind stress. The minimum value is recorded just south of the equator. The maximum value of the northward wind stress is found in the eastern parts of the southern Indian Ocean. There is no conspicuous variation of the northward wind stress south of the equator

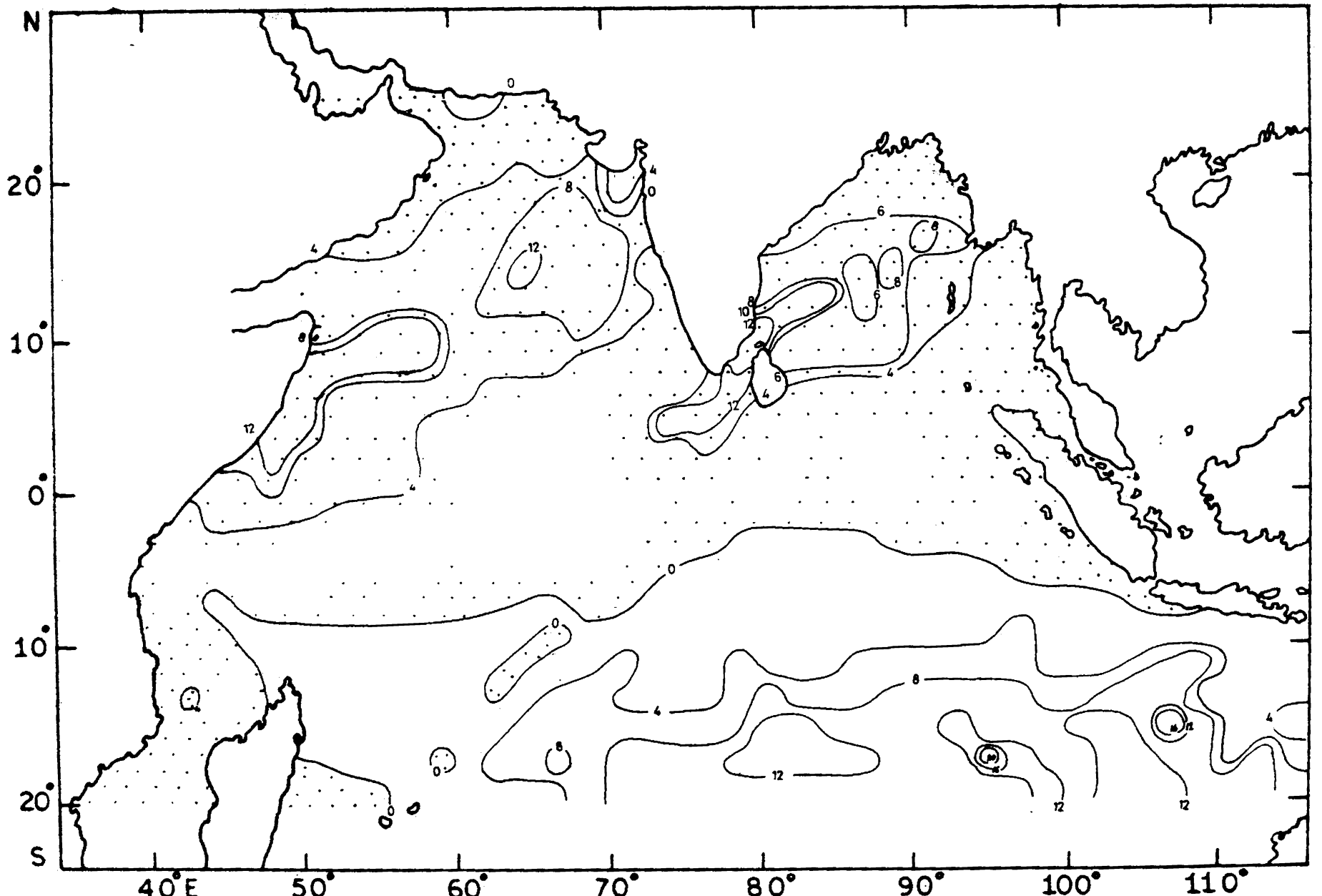

FIG. 12b. MERIDIONAL COMPONENT OF THE WIND STRESS (10^{-1} dynes cm^{-2}) IN DECEMBER.

in December from that in November. But an increase is observed in the northern parts compared to that in the previous month.

The meridional components of the wind stress are higher than the zonal components of the wind stress in the Arabian Sea. But the zonal components exceed the meridional components in the Bay of Bengal except in the northern most parts. Along the equator, the meridional components exceed the zonal components from 46° to 86°E. The zonal components are higher than the meridional components south of the equator.

CHAPTER 3

DISTRIBUTION OF THE CURL OF THE WIND STRESS OVER THE INDIAN OCEAN

Curl of the wind stress (vorticity) is the forcing function in the equations of vertically integrated transport of wind driven ocean currents. Hence, it has become a basic quantity in theoretical oceanography.

The curl field of surface wind stress for different months of the year is mapped and shown in figures 13 to 24. Areas of negative curl are dotted while the areas of positive curl are left blank. The isolines of curl of the wind stress are drawn at an interval of 2×10^{-8} dynes cm^{-3}. As stated earlier, the analysis extends from $20^{\circ}S$ to the border of Asia, along the width of the ocean.

The convention of the sign of the curl field is such that positive values indicate cyclonic (anticlockwise) circulation while negative values represent anticyclonic (clockwise) circulation.

The pattern obtained is not claimed as a very accurate picture of curl field, as there are some limitations in the basic data as well as in the method employed as already explained in chapter 1. Further, it is to be stressed that the pattern does not deal with the small scale process but only the monthly average on a large scale basis.

The curl field shows regular seasonal and space variations due to systematic changes in the wind field both in direction and magnitude in its annual cycle and from place to place. Compared to other oceans, the central and the northern parts of the Indian Ocean exhibit the most pronounced seasonal change of surface conditions. As a result, the vorticity in the Indian Ocean during the northern hemisphere summer shows considerable deviations from the normal pattern. Areas of strong negative curl cover almost the entire Indian Ocean during the southwest monsoon and display an impressive anomaly of the vorticity distribution.

The details of the distribution of the curl of the wind stress for each month are discussed in the following paragraphs.

JANUARY

In January (Fig.13), a large area of positive curl is observed north of 2°S along the width of the ocean.

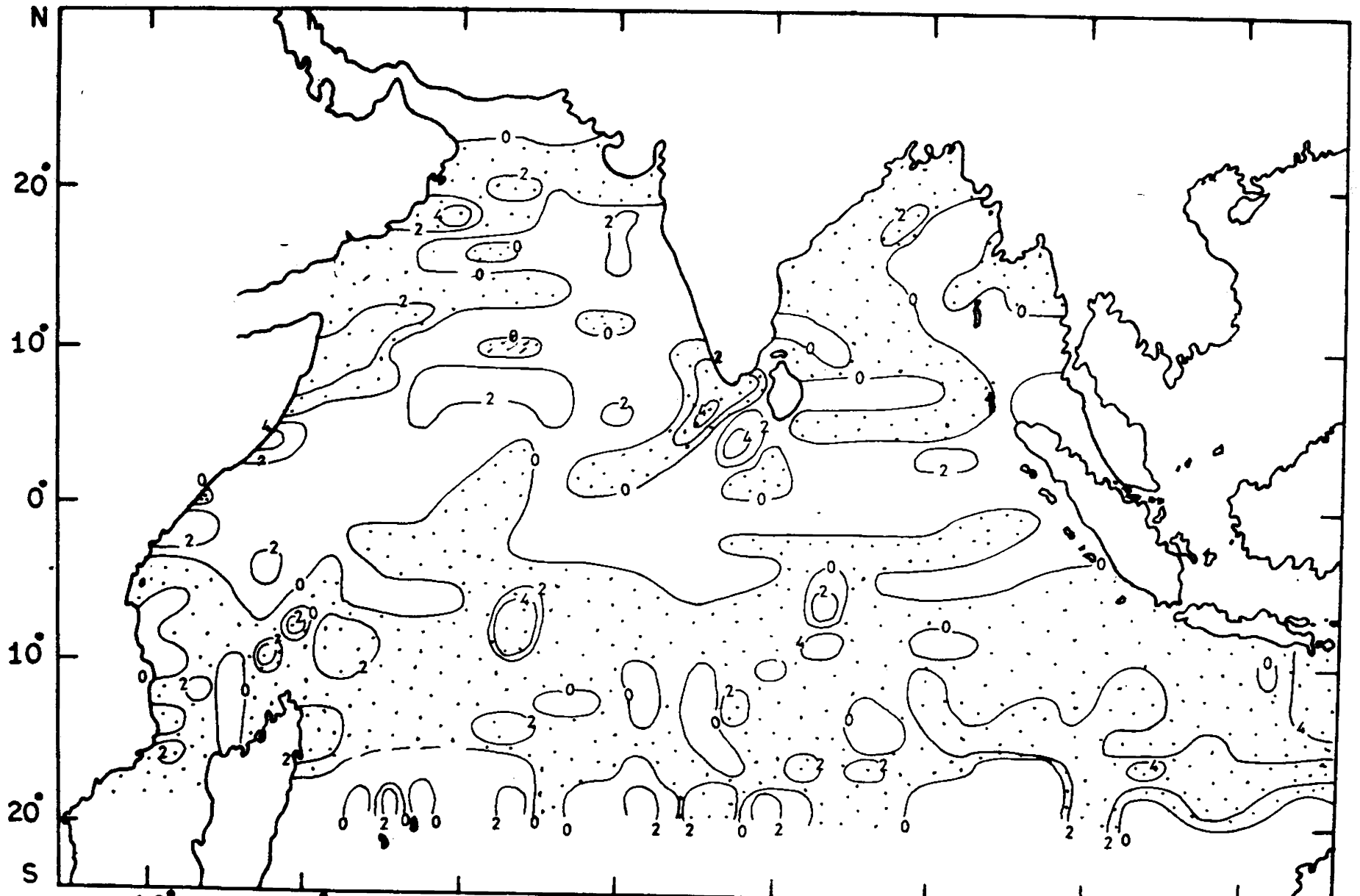

FIG: 13 CURL OF THE WIND STRESS(10^{-8} dynes cm^{-3}) IN JANUARY.

This area is extended upto 6°S, west of 60°E and completely occupies the eastern parts of the Arabian Sea. The eastern parts of the Bay of Bengal is also covered by positive curl. The maximum value observed is of the order of + 4 near the Somali Coast. The values are, generally, higher in the western region than those in the eastern region. A narrow belt of positive curl is observed in the northern most part of the Arabian Sea with most predominating value of the order of + 1.

Negative curl field is, generally, observed south of 2°S along the width of the ocean. However, cells of positive curl are occured here and there in this elongated belt of negative curl. The values are, generally, higher in the western half of the ocean where the maximum value is of the order of - 5.

There are, relatively, large areas negative vorticity in the north-western Arabian Sea and in the northwestern Bay of Bengal. The highest anticyclonic vorticity observed in the northwestern Arabian Sea is of the order of -5 while in the northwestern Bay of Bengal it is of the order of -2 only. A small band of negative curl extends from the south-west coast of India upto 2°N and 68°E with higher values of the order of -5. The northern most part of the Arabian sea is covered by positive curl with most predominating value

of the order of +1. At the same time, the head of the Bay of Bengal is covered by negative curl.

FEBRUARY

A zone of positive curl exists just north of 2°S along the width of the ocean (Fig.14). This zone is extended upto 14°N in the Arabian Sea. The southern boundary of this zone generally, lies along 4°S, east of 60°E and it shifts further north, west of 60°E. In the eastern parts, it extends further south as a narrow curved strip. Positive values are also observed in the eastern half of the Bay of Bengal as a continuation of this belt of positive curl. Low values are predominant in this region and the maximum value is of the order of +4 at 2°N and 48°E.

The area of the negative curl in the northwestern Arabian Sea is slightly increased with highest value of the order of -2. There is no conspicuous change in the area of the negative curl in the western parts of the Bay of Bengal. A narrow belt of negative curl connects the areas of the negative curl in the Arabian Sea and Bay of Bengal. This belt runs between 12°N and 16°N through the central Arabian Sea upto 72°E and follows the southwest coast of India with values as high as the order of -2. However, a narrower

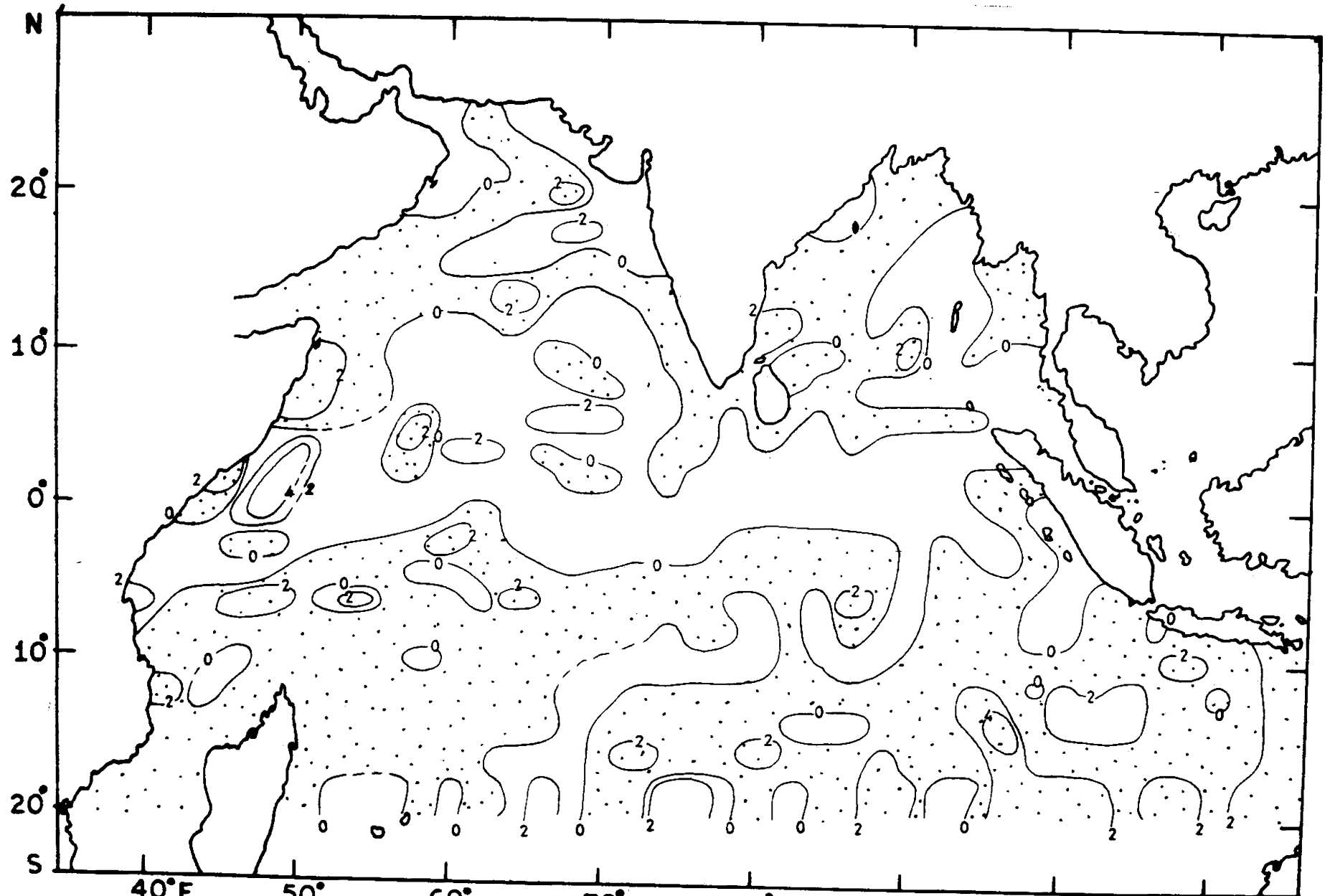

FIG: 14 CURL OF THE WIND STRESS (10^{-8} dynes cm^{-3}) IN FEBRUARY

coastal strip of positive curl is found along the northeastern part of the Arabian coast and along the northeastern coast of India. A relatively wide zone of positive curl is observed near the northwest coast of India with lower values mostly below the order of +1.

The width of the band of negative curl of the southern hemisphere is slightly reduced. The most predominant value is of the order -1 while the maximum value is of the order of -5 which is observed at 96°E. The number of positive cells are slightly increased in this zone of negative curl.

MARCH

In March (Fig.15), the zonal belt of positive curl north of the equator is not running along the width of the ocean like the previous month but is interrupted by an area of negative curl in the central region. A major part of the Arabian Sea is covered by positive curl and it extends upto the Somali coast as a narrow strip. The maximum value is reduced from +4 in February to +2 in March. Relatively a large strip of negative curl is found to be extended from the Somali coast with values as high upto the order of -5. As a result, the area of the positive curl off the Somali coast is considerably reduced and lies between 2°N and 2°S.

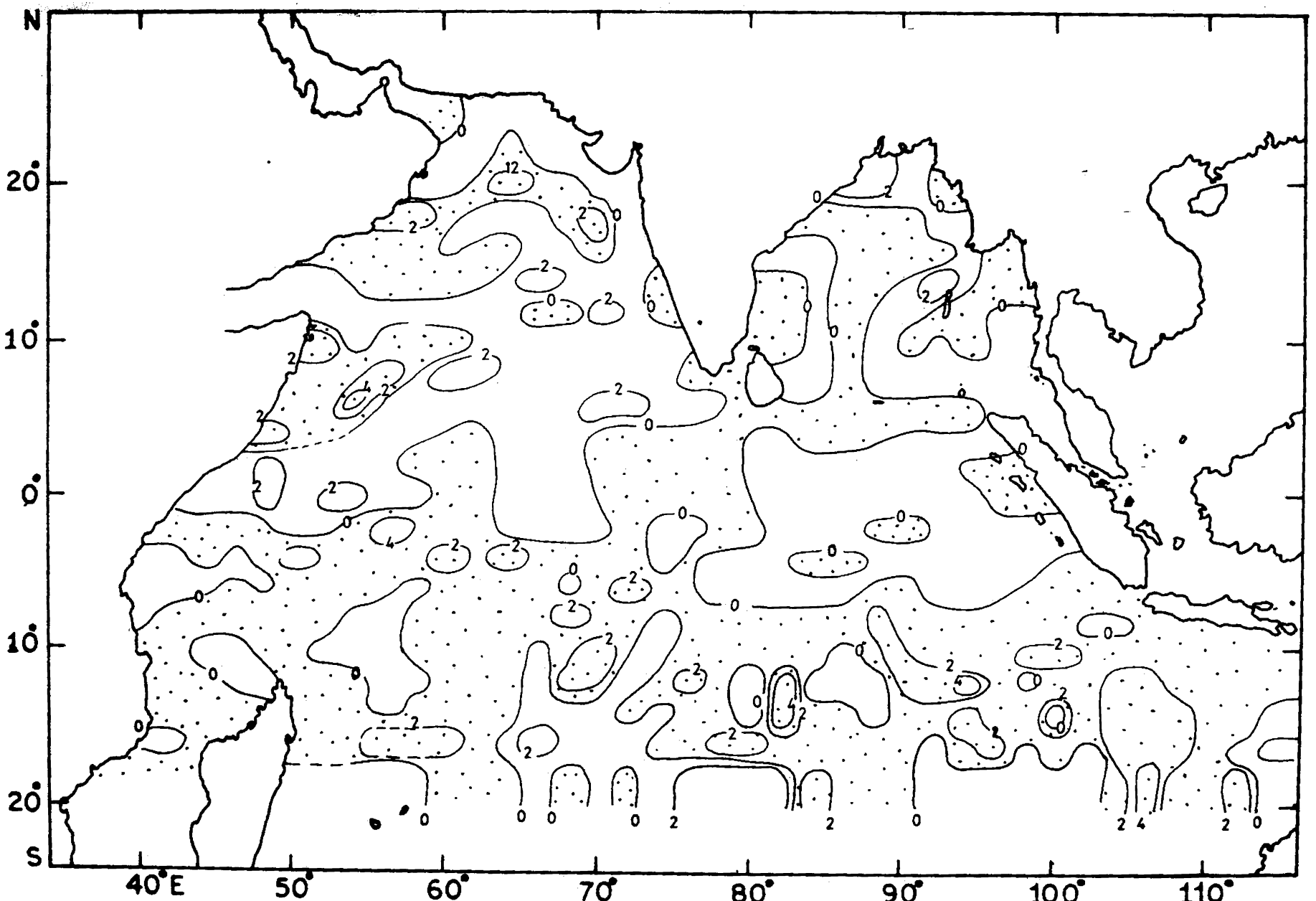

FIG: 15 CURL OF THE WIND STRESS(10^{-8} dynes cm^{-3}) IN MARCH

Another zone of positive curl is found between 4°N and 7°S, east of 80°E. This zone extends into the head of the Bay of Bengal through the eastern most parts of the Bay of Bengal. The values of this positive curl field are slighly lower than those in the Arabian Sea eventhough, the maximum value ocsured is of the order +2.

The narrow strips of negative curl, found in February in the central Arabian Sea and along the west coast of India disappeared by March while it still persists in the Bay of Bengal upto 19°N with values of the order of -1. The sign of the curl field at the head of the Bay of Bengal is reversed by March and the intensity is remarkably strengthened upto a maximum of the order of +3. A narrow belt of weak positive curl is appeared between 83°E and 85°E in the Bay of Bengal which is almost parallel to the longitude. The relatively narrow strip of negative curl, found in the eastern-most part of the Bay of Bengal is slightly extended to west.

The area of the negative curl in the western Arabian Sea is slightly reduced by March and as a result, positive values completely occupy the northernmost parts of the Arabian Sea. The southern boundary of this negative zone is changed from 5°N in February to 13°N in March with highest value of the order of -2. In general, the zones of positive and negative curl in the western parts of the ocean are shifted further north by March.

The width of the zone of negative curl in the southern Indian Ocean is widened by March, especially, in the central region. A number closed cells of positive curl are also found in this region. The width of this zone is widest between 70°E and 80°E where it reaches the southern tip of India and extends into the central parts of the Bay of Bengal. The most predominant value is of the order of 0.5 and values increase upto -4 in the easternmost parts of the southern Indian Ocean. But its width is slightly reduced in the eastern region where its northern boundary lies along 7°S. The Mozambique channel is completely covered by the negative curl.

APRIL

The pattern of the curl field (Fig.16) varies considerably in April. The zone of positive curl in the Arabian Sea is markedly contracts and the maximum value occured is of the order of +2 only. This zone doesnot run along the width of the ocean, but is interrupted between 88° and 92°E in the southern parts of the Bay of Bengal. Negative curl prevails in the entire Bay of Bengal except in a narrow strip near Burma. The value of the negative curl in the western Arabian Sea is slighly increased as it extends into south and east with most predominating value of the order of-0.5. The zone of positive curl in the Arabian Sea is very much reduced by

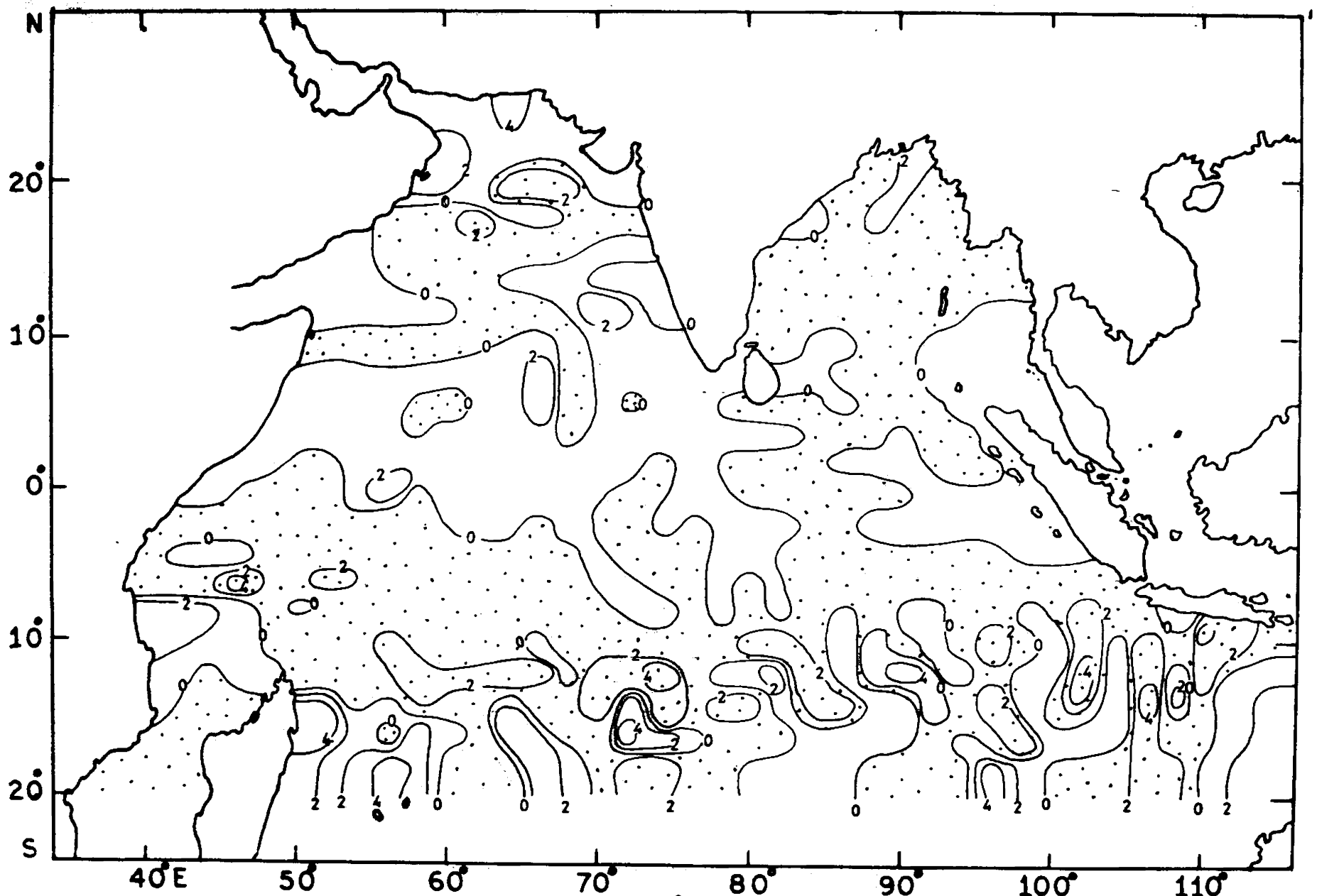

FIG: 16 CURL OF THE WIND STRESS (10^{-8} dynes cm^{-3}) IN APRIL

April and the maximum value occured is of the order of +2 only. However, the area of positive curl in the northern parts of the Arabian Sea expands and extends upto 17°N.

The zone of negative curl in the southern hemisphere runs along the width of the ocean eventhough its width is considerably reduced in the central region. But its width in the eastern region is considerably increased and extends upto the head of the Bay of Bengal. As a result, the area of the positive curl in the eastern region is reduced from that in the previous months and lies east of 86°E between 3°N and 3°S. The values of the negative curl are as high as low as of the order of -7 in the western region while the most predominant values are of the order between -1 and -2. The intensity of this negative curl field is, generally, lower in the eastern region than that in the western region. The number of closed cells of positive curl are increased in the southern Indian Ocean. A relativity large strip of positive curl is observed just north of the Mozambique channel with maximum value of the order of +3. Meanwhile, the Mozambique channel is completely covered by negative curl.

The width of the positive curl field in the Somali region is widened in April compared to that in March and is found to exist between 8°N and 1°S. But the intensity of this curl field is slightly reduced.

MAY

In May (Fig.17), the zone of negative curl in the southern Indian Ocean is not running along the width of the ocean, but is terminated at 48°E. Its width is considerably widened in the eastern and western regions where it extends upto 18°S and 12°N respectively. The most predominant value is of the order of -1 and the highest value, observed is of the order of -5. Relatively large strips of positive curl are observed south of this zone of negative curl with values as high as +5 x 10^{-8} dynes cm^{-3}. Positive curl prevails west of 48°E along the east coast of Africa between 16°N and 18°S. As a result, the Somali region is almost covered by positive curl and its intensity is remarkably strengthened by a factor of +6 at least from the previous months.

The mouth of the Red Sea is also covered by positive curl and it extends upto the southwest coast of India through the south central Arabian Sea. From there it continues upto the northern parts of the Bay of Bengal, completely covering the western half of the Bay of Bengal. Higher values are observed in the Bay of Bengal while lower values are encountered in the south central Arabian Sea. Positive values prevail in the northern parts of the Arabian Sea with values as high as +6 while, negative values prevail at the head of the Bay of Bengal.

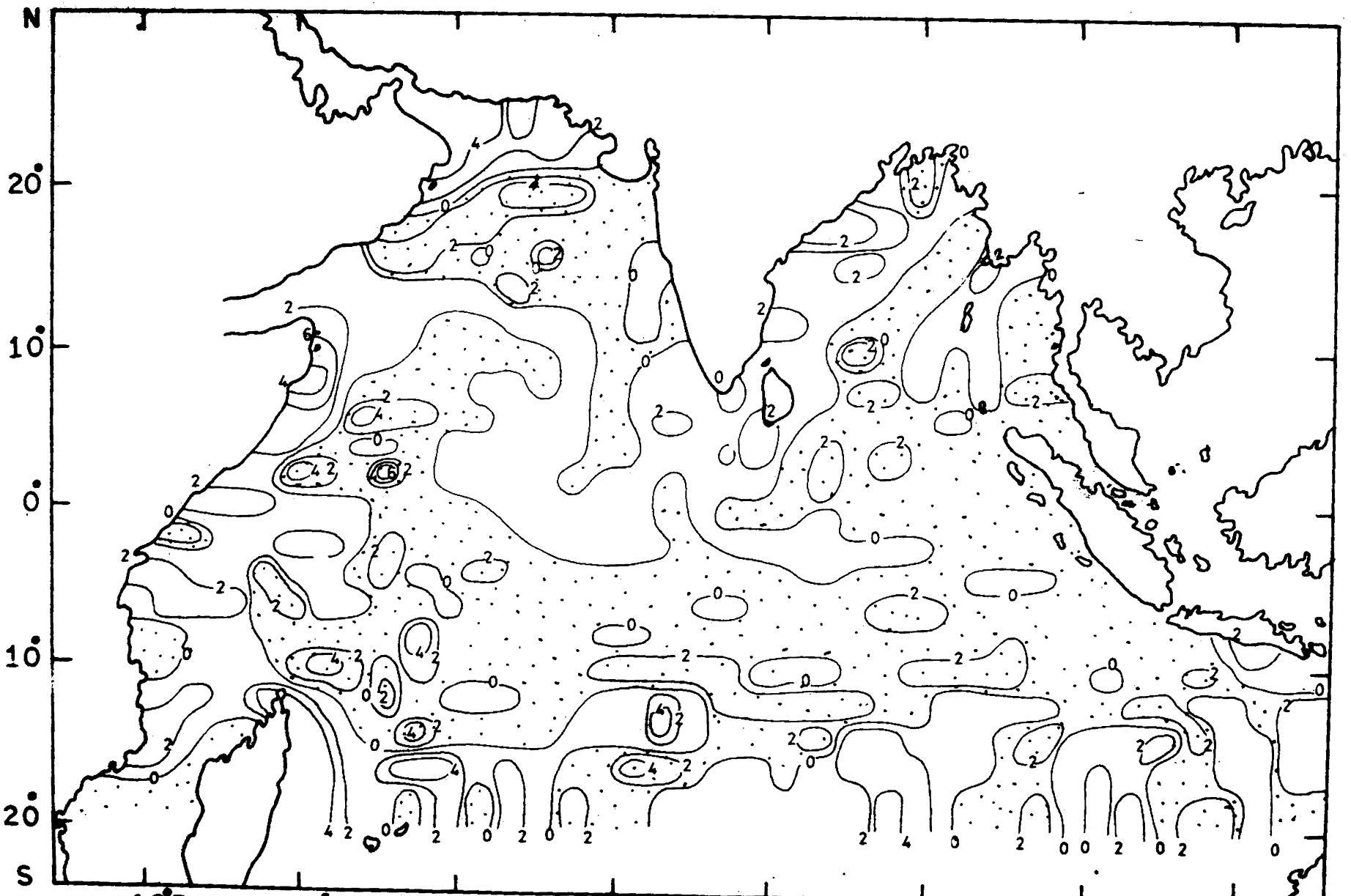

FIG: 17 CURL OF THE WIND STRESS(10^{-8} dynes cm^{-3}) IN MAY

A relatively large belt of negative curl runs from the Arabian coast to the west coast of India, across the Arabian Sea between 13°N and 21°N. This belt extends into the southern parts of the Arabian Sea at 12°N and 70°E. The values found in this belt are lower than those in April and the maximum value is of the order of -4.

JUNE

The curl pattern of June (Fig.18) shows considerable variations from the previous months. The eastern and southern parts of the Arabian Sea exhibit negative curl and it extends as a narrow strip upto 6°N. The most predominant value is of the order of -1 and the highest value observed is of the order of -6. Another zone of negative curl prevails in the eastern region from 80°E to 100°E between 2°S and 10°S with values as high as -5×10^{-8} dynes cm^{-3}.

The northern and northeastern parts of the Bay of Bengal record positive curl. A narrow strip of positive curl extends from the east coast of India upto 90°E with values of the order of +2 only. A relatively narrow strip of negative curl runs from Sri Lanka to the eastern parts of the ocean through the central parts of the Bay of Bengal. The western and northern parts of the Arabian Sea are completely covered by positive curl and its intensity is remarkably strengthened.

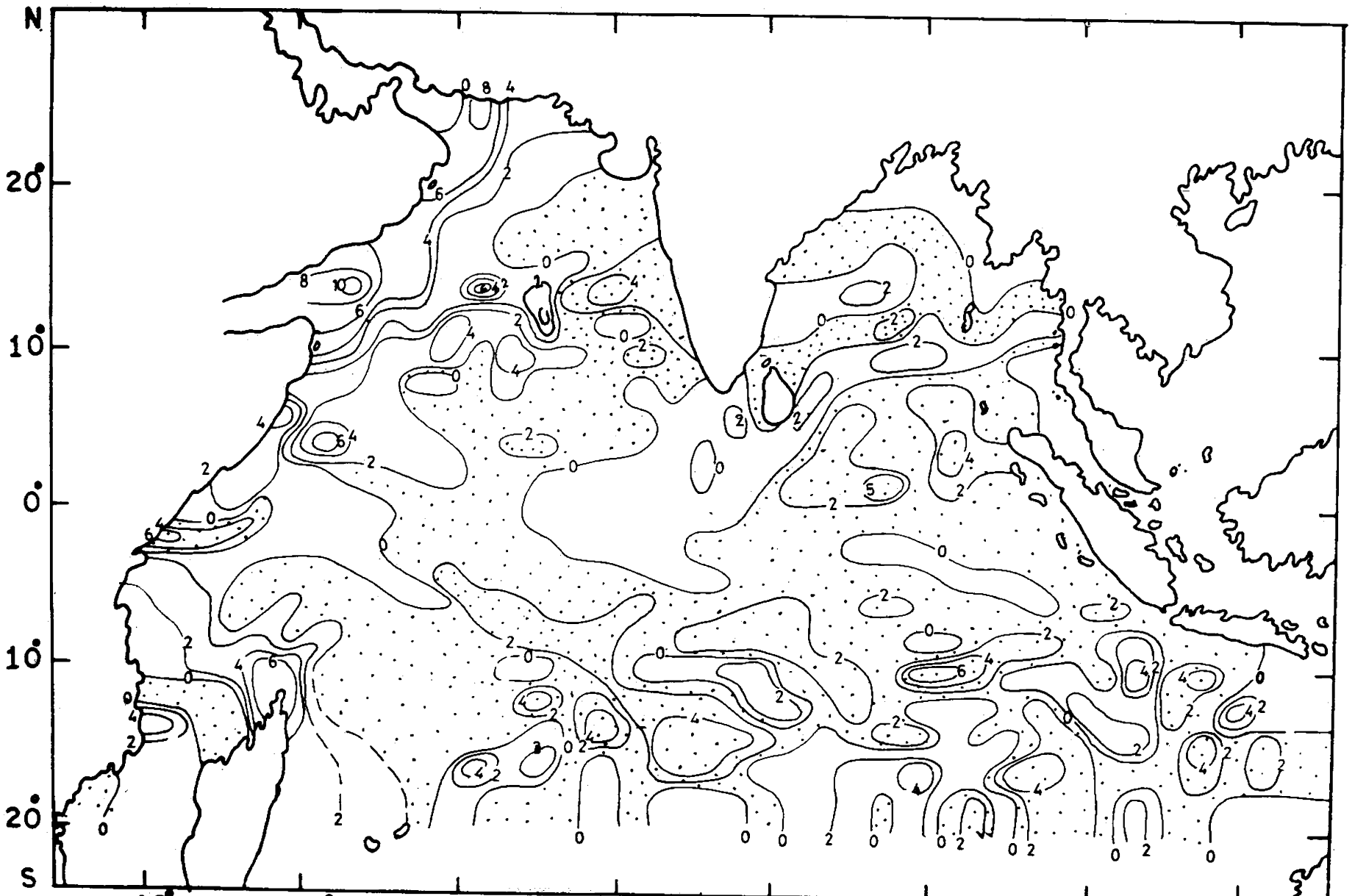

FIG: 18 CURL OF THE WIND STRESS(10^{-8} dynes cm^{-3}) IN JUNE

The most predominant value is of the order of +5 and the maximum value observed is as high as +10 x 10^{-8} dynes cm^{-3}. The Somali region is covered by positive curl except in a narrower strip between 7°N and 9°N. A general increase of values are observed in the Somali region with +3 as the most predominating value.

A major part of the Indian Ocean is covered by negative curl, especially south of the equator. This zone of negative curl extends to north and almost cover the whole Arabian Sea and Bay of Bengal. The intensity of this curl field is very much strengthened compared to that of the previous months. The maximum value of the order of -7 is occured at 10°S between 90°E and 92°E. Unlike the previous months, the cells of positive curl, which are distributed in the broad zone of negative curl show higher values as indicated by the maximum value of the order of +4.

Positive curl prevails along the east coast of Africa between 7°N and 11°S. The head of the Bay of Bengal and the northern parts of the Arabian Sea are completely covered by positive curl.

JULY

The pattern of curl in July (Fig.19) is similar to

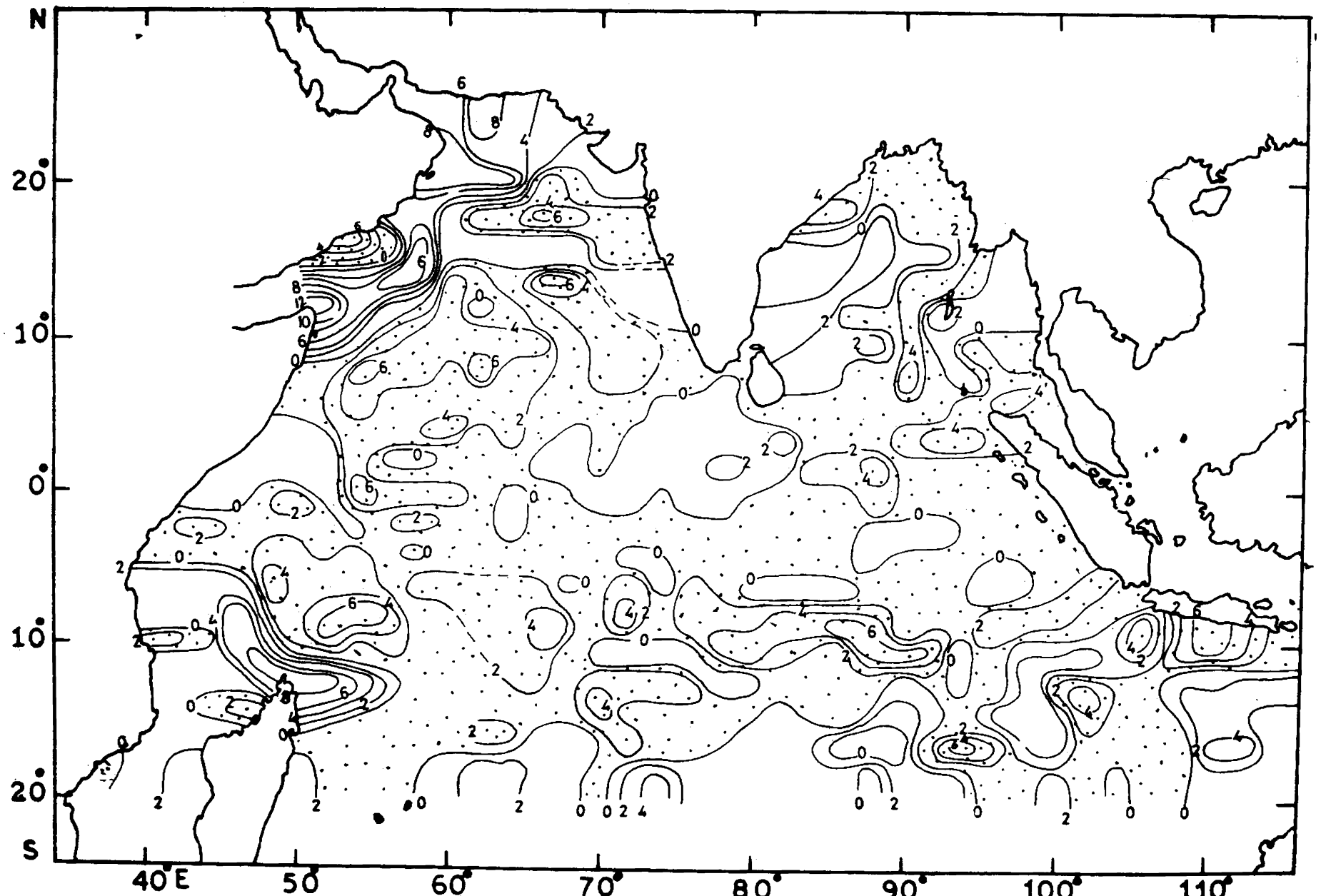

FIG: 19 CURL OF THE WIND STRESS (10^{-8} dynes cm^{-3}) IN JULY

that in June with some slight differences. The eastern and south central parts of the Arabian Sea are covered by negative curl and it extends upto 2°S. The intensity of this negative curl field is slightly strengthened in this region where values as high as -6×10^{-8} dynes cm^{-3} are found. Another zone of negative curl is found between 80°E and 100°E north of 6°N with values as high -4×10^{-8} dynes cm^{-3}. This zone is extended upto the head of the Bay of Bengal as a narrow strip through the central parts of the Bay. Higher values of the order of -4 are again encountered at the head of the Bay. However, a major part of the Bay of Bengal is covered by positive curl, especially in the western half and in the easternmost parts, where the most predominant value is of the order of +2.

A major part of the Somali region is covered by positive curl except in a narrow strip between 5°N and 8°N. The most predominant value between 5°N and 6°S is of the order of +1 and the maximum value is about $+6 \times 10^{-8}$ dynes cm^{-3}. A strong positive curl field prevails in the northern and western parts of the Arabian Sea. This field starts from the tip of Somali and covers about three fourth area of the Arabian Sea. Its intensity is remarkably strengthened and as a result, values as high as +20 are observed. All most all the values present in this zone are of the order greater than +5. A narrow strip of negative curl occurs near southwest coast of Arabia while

while another one extends from the west coast of India between 16°N and 20°N upto 60°E with values as high as -7 x 10^{-8} dynes cm^{-3}.

A relatively large strip of positive curl is observed south of the southern tip of India with maximum value of the order of +2.

A major part of the Indian Ocean is covered by negative curl. The area prevailed by the negative curl is increased from that of June. The zone of negative curl extends upto 15°N in the Arabian Sea and upto the head of the Bay of Bengal as a narrow strip. The intensity of this curl field is very much strengthened compared to that of the previous months. The highest value occured is of the order of -7.

A strong field of positive curl is found in the Mozambique channel and in the nearby regions with values as high as +11 x 10^{-8} dynes cm^{-3}. Similar to the previous months, a number of cells of positive curl are observed in this wide zone of negative curl. The intensity of the curl field is maximum in July during the year.

AUGUST

The curl field of August (Fig.20) is similar to that of July.A relatively large area of negative curl prevails in the southwestern and south central parts of the Arabian Sea

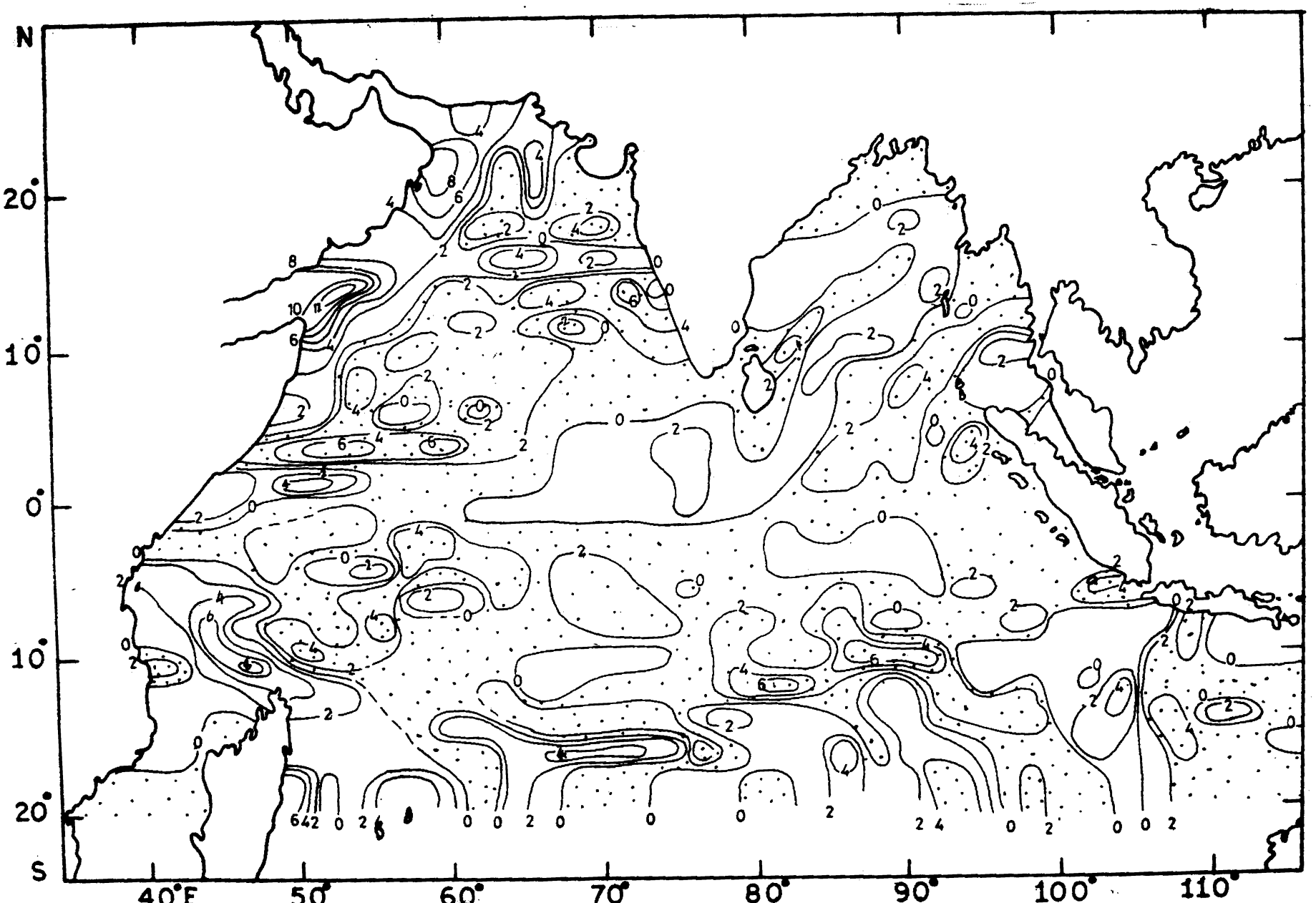

FIG: 20 CURL OF THE WIND STRESS(10^{-8} dynes cm^{-3}) IN AUGUST

between 15°N and 1°S. This zone is extended into the Bay of Bengal as a narrow belt along the southern tip of India. The most predominant value is of the order of -3 and values as high as -7 are observed. Similar to the case of July, strip of negative curl is again extending from the west coast of India, north of 16°N with values of the order of -4.

Another zone of negative curl prevails in the eastern region east of 80°E and north of 5°S. This zone further extends to north and completely covers the southeastern part of the Bay of Bengal. The intensity of the curl field in this area is approximately similar to that in July. The head of the Bay of Bengal exhibits negative curl, eventhough the area is slightly reduced.

The Somali region is almost covered by positive curl. A relatively large zone of positive curl is running to north from 5°N along the coasts of Somali and Arabia and covers the northern parts of the Arabian Sea. This zone reaches the east coast of India, as a narrow strip of 200 km width through the central Arabian Sea. The intensity is very much weakened from July as indicated by the maximum value of the order of +12 observed north of Somali.

The zone of negative curl runs along the width of the ocean and extends upto 15°N in the Arabian Sea. This zone extends also into the Bay of Bengal covering the eastern half

of the Bay the highest value observed is of the order of -8. There is not much variation in the intensity of the curl field in August from that in July, especially in the western region. As in the previous months, a number of positive cells are observed in the southern parts of this negative curl zone. The Mozambique channel and the nearby regions exhibit remarkably strong positive curl with values as high as +8.

A relatively large strip of positive curl is found south of the southern tip of India. It extends into the Bay of Bengal and covers the western half of the Bay. The intensity of this curl field is much lower, compared to the positive curl field in the Arabian Sea.

SEPTEMBER

The general pattern of the curl field in September (Fig.21) is similar to that in August. The eastern half of the Arabian Sea is covered by negative curl and this zone extends to south upto the equator and to west upto 53°E. The most predominating value is of the order of -1 and the highest value observed is about -4×10^{-8} dynes cm^{-3}. A relatively small area of positive curl is found almost in the middle of this zone, while another strip of positive curl is observed near the west coast of India.

Another zone of negative curl is found north of 8°N

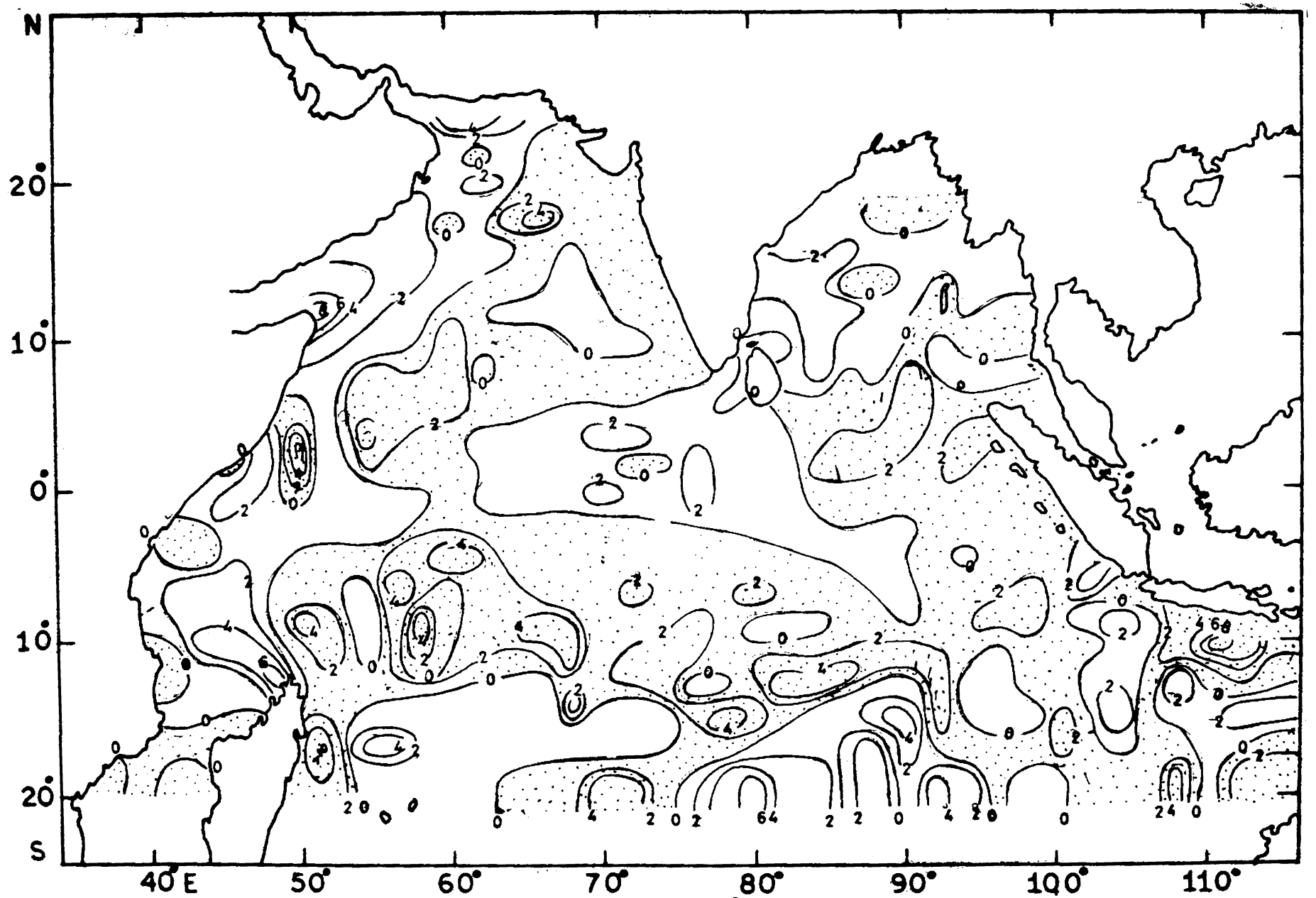

FIG: 21 CURL OF THE WIND STRESS (10^{-8} dynes cm^{-3}) IN SEPTEMBER

and east of 83°E. This zone extends into the southeastern parts of the Bay of Bengal with values slightly lower than those in August. Positive curl prevails in the western, southern and central eastern parts of the Bay of Bengal except in a small strip in the central region. However, the intensity is slightly weakened and the maximum value observed is of the order of +3 only. Eventhough sufficient data are not available, a tendency of negative curl field is observed in the northern parts of the Bay of Bengal.

A major part of the Somali region is covered by positive curl except in a narrow belt between 2°N and 6°N. The intensity of this curl field is slightly weakened by September. Positive curl prevails in the southwestern parts of the Arabian Sea. The intensity of this curl field is very much reduced in the southwestern Arabian Sea from a maximum of the order of +12 in August to +8 in September. However, the area covered by the positive curl in the northern parts of the Arabian Sea is remarkably reduced.

The negative curl field of the southern Indian Ocean runs from the eastern boundary of the ocean upto 50°E. This zone extends into the Arabian Sea upto 24°N between 52°E and 62°E and upto 14°N in the Bay of Bengal. As in the previous months, a number of positive cells are also observed especially, south of 6°S. A relatively large area of positive curl is

occured between 4°S and 20°S and it extends upto 60°E as a narrow belt with highest value of the order of +6.

OCTOBER

The pattern of the curl field is changed markedly in October (Fig.22) from that in the summer months.

A zonal belt of positive curl is observed along the width of the ocean in the northern Indian Ocean. This belt starts from the Somali region and reaches the eastern parts of the Bay of Bengal through the southern parts of the Arabian Sea. The most predominant value is of the order of +0.5 while the maximum observed is of the order of +2 only. The curl field in the western and southwestern Arabian Sea is reversed in sign and as a result, a major portion of the Arabian Sea north of 12°N is covered by negative curl. However, two patches of positive curl having lower values are observed in the Arabian Sea north of 12°N.

The Somali region between 12°N and 6°S is completely covered by positive curl. The intensity of this curl field is markedly weakened as indicated by the maximum value of the order of +2.

The area of the negative curl of the southern Indian Ocean is slightly reduced from that in the previous months. The northern boundary of this zone lies approximately along 2°S

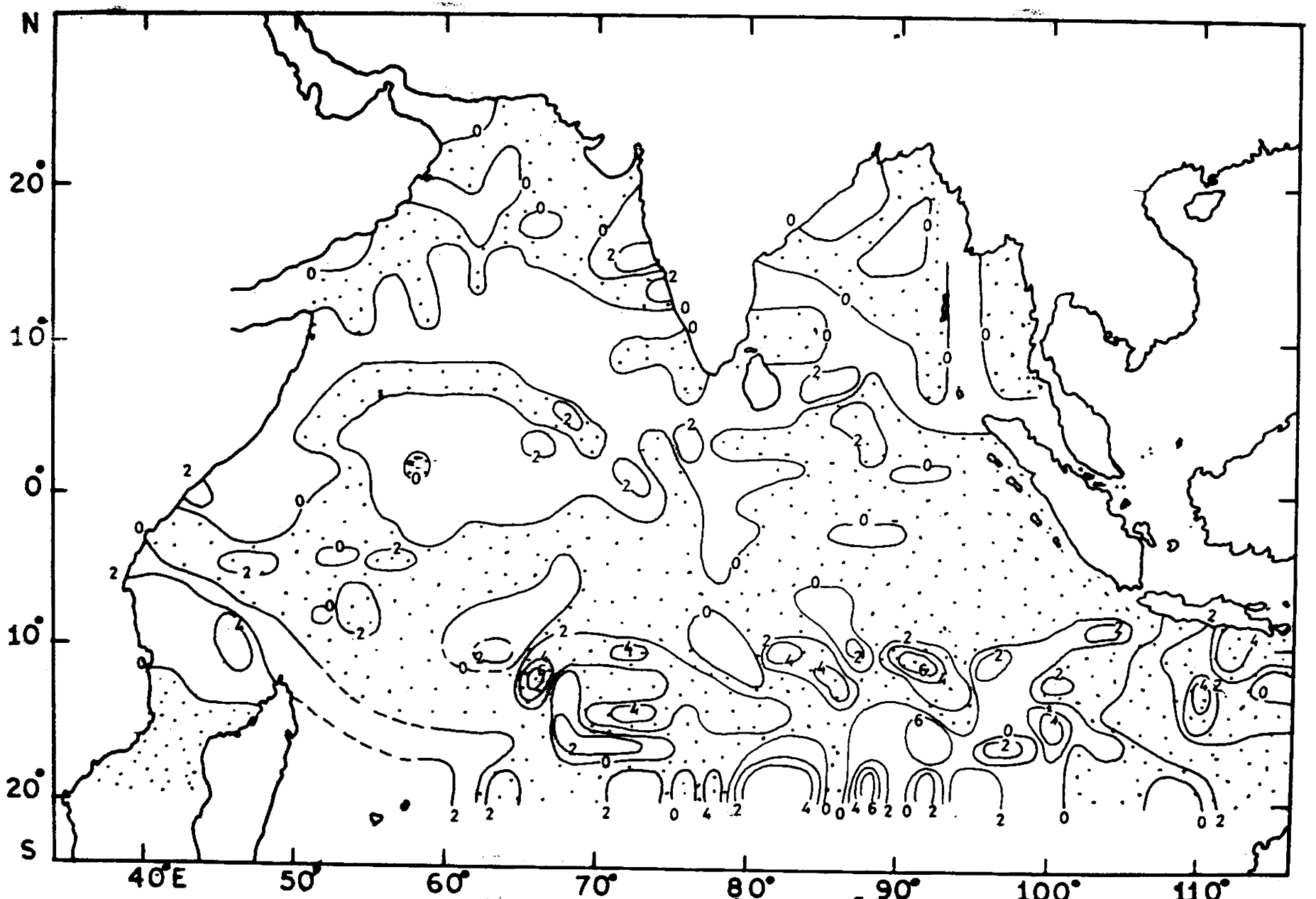

FIG: 22 CURL OF THE WIND STRESS(10^{-8} dynes cm^{-3}) IN OCTOBER

in the western half of the ocean. In the eastern parts of the ocean, the field of negative curl is extended upto 6°N. The values are generally higher east of 65°E as indicated by the highest value of the order of -6. The intensity of the curl field is slightly weakened in this region compared to that in the previous month. The total area of the positive curl cells south of the equator are markedly reduced by October from that in September. The Mozambique channel with most predominating value of the order of +2.

NOVEMBER

The curl field of November (Fig.23) is similar to that of October with slight deviations.

A zone of positive curl is found in the north Indian Ocean, from the Somali coast to the northern parts of the Bay of Bengal. This zone covers the entire region of the Bay of Bengal and the eastern half of the Arabian Sea. The values are relatively higher than those in October and the maximum value observed is of the order of +3.

Unlike in October, the positive curl field in the Somali region is not continuous but is interrupted at two regions by negative curl. However, a slight increase in the

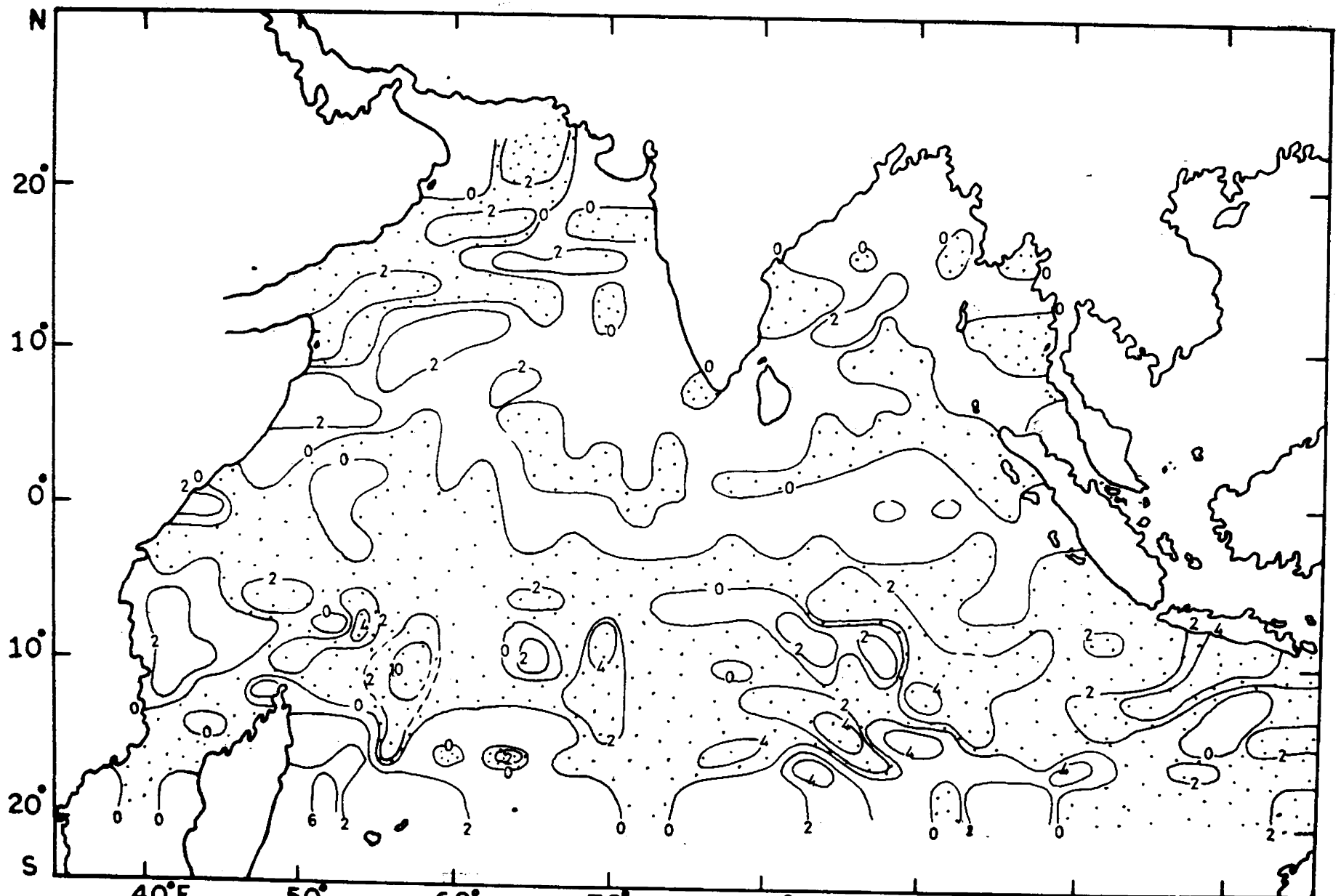

FIG: 23 CURL OF THE WIND STRESS(10^{-8} dynes cm^{-3}) IN NOVEMBER

magnitude of the positive curl field is noticed as indicated by the most predominating value of the order of +2.

The area of the negative curl in the Arabian Sea is slightly reduced and is limited north of 12°N and west of 66°E. The values are generally higher than those in October as indicated by the most predominating value of the order of -2.

The zone of negative curl of the southern Indian Ocean occurs as in the previous months eventhough its width is markedly reduced. The values are generally higher than those in October, with maximum value of the order of -10. The northern boundary of this negative curl field lies approximately along 2°S. The area of the positive cells in the southern Indian Ocean are markedly reduced in November. The Mozambique channel north of the 20°S is completely covered by negative curl, while a zone of positive curl with most predominating value of the order of +2 is observed just north of it.

DECEMBER

The pattern of the curl field in December (Fig.24) is almost similar to that in November with stright deviations. The zone of positive curl north of the equator starts from the Somali region and continuous upto 16°N in the Bay of Bengal through the Arabian Sea.

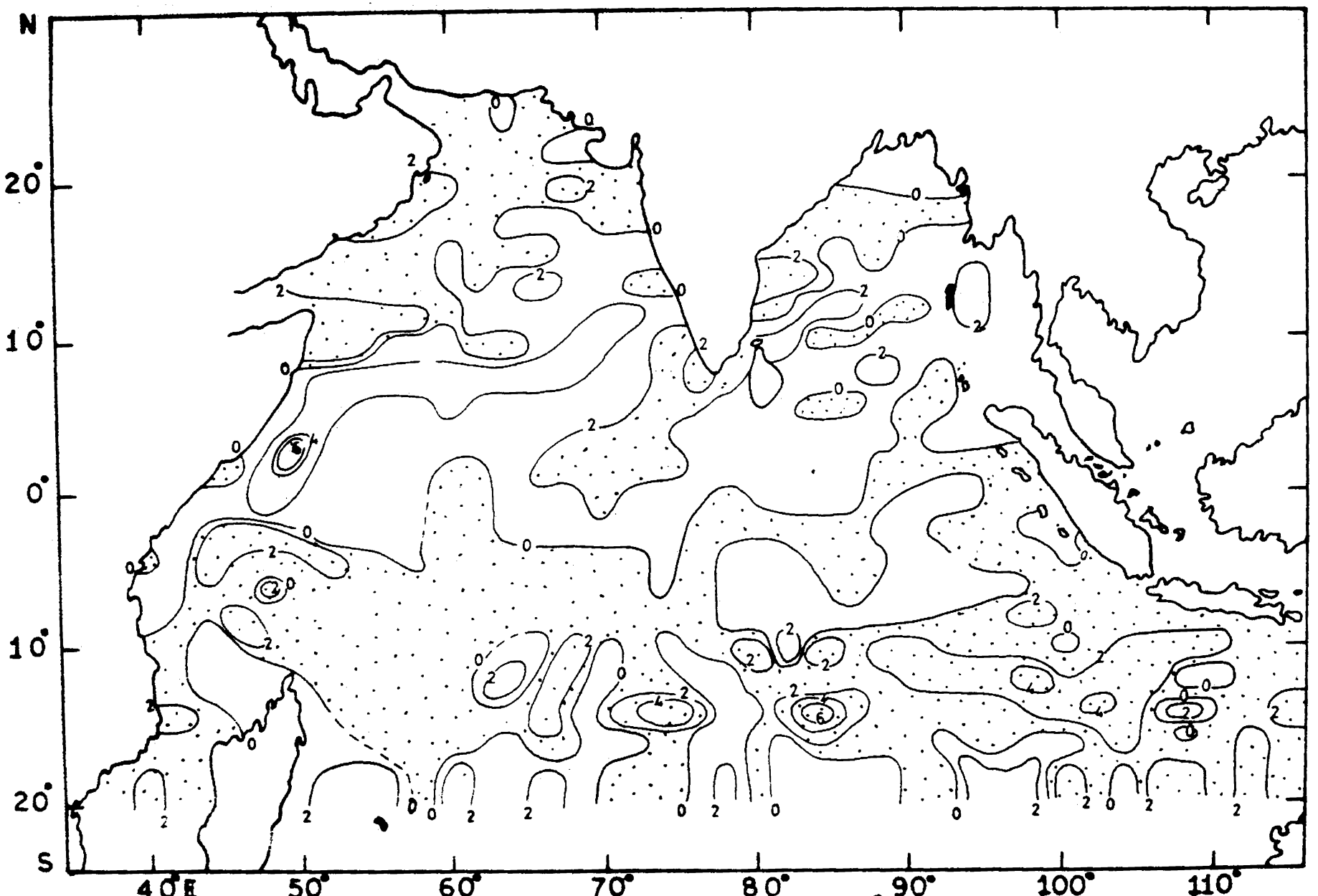

FIG: 24 CURL OF THE WIND STRESS(10^{-8} dynes cm^{-3}) IN DECEMBER

A major portion of the Bay of Bengal is covered by positive curl. Similarly, the southcentral and south of 15°N of the eastern parts of the Arabian Sea is covered by positive curl. The intensity of this curl field is slightly strengthened from that in November. Negative curl prevails along the east coast of India and it extends upto the eastern boundary of the ocean between 16°N and 20°N. The head of the Bay of Bengal exhibits positive curl as in the previous month.

The Somali region between 9°N and 9°S is completely covered by positive curl. An increase in the intensity of the curl field is noticed in this region with maximum value of the order of +6.

The northern and southwestern parts of the Arabian Sea is completely covered by positive curl. The most predominating value is of the order of -1 and the highest value observed is of the order of -3. A narrow zone surrounding the southern tip of India exhibits negative curl.

The negative curl field of the southern Indian Ocean is slightly reduced in area. The intensity of this curl field is slightly strengthened by December compared to that in November as indicated by the maximum value of the order of -6.

In the eastern region, this belt of negative curl extends upto 8°N. The occurrence of the positive cells south of the equator are reduced from that in the previous month. The Mozambique channel is completely covered by negative curl with reduced intensity.

CHAPTER 4

GENERAL FEATURES OF THE SURFACE CIRCULATION IN THE INDIAN OCEAN

The streamline pattern of the circulation of surface waters for all the months are presented in Figs.25 to 36. A large number of singular points, including lines of convergence and divergence, are observed in the streamline pattern. Lines of convergence and divergence in most cases represent the boundaries between different watertypes moving in relation to each other. They are generated when heavy water meets lighter water or when lighter water spreads out over heavier water that sinks. The occurrence of divergence and convergence lines is a general phenomena closely connected with oceanic circulation. Points of convergence and divergence represent the meeting of an infinite number of streamlines. To satisfy the continuity equation, horizontal movements associated with these must be related to the movements perpendicular to the sea surface. Thus, a divergence point in a water layer near the surface indicates upwelling and a convergence point indicates sinking. Hyperbolic (neutral) point occur when

currents flowing in opposite direction meet each other and spread. At neutral points, vertical motions may but do not necessarily have to occur. The only requirement is, that at neutral points the horizontal velocity becomes zero. The singularities are closely connected with the velocity field. When the streamlines intersect, the velocity must be zero and the isolines of velocity must be closed around the point singularities.

From the distribution of streamlines it can be seen that May, June, July and August fall under the southwest monsoon, while conditions of the northeast monsoon prevail from November through February. March-April and September-October can be considered as the transition period. The eastward flowing Equatorial Countercurrent and the westward flowing South Equatorial Current exist throughout the year. But during the southwest monsoon, the eastward flowing Southwest Monsoon Current replaces the North Equatorial Current and merges with the Equatorial Countercurrent. The southern boundary of the Monsoon current extends into south from May through August. The Somali Current is well developed and flows to northeast, during this season. A number of point singularities are observed at the boundary between the Monsoon Current and the South Equatorial Current. The strength of the currents are higher in July and the Somali Current records

the maximum speed. A high velocity core in the central equatorial region in April-May and October-November indicates the presence of the Equatorial Jet. A number of cyclonic and anticyclonic eddies are formed during the northeast monsoon. The number of point singularities are high especially in November which is due to the seasonal reversal of the direction of the currents. The eastward flowing North Equatorial Current is well developed by November. The southern boundary of the North Equatorial Current shifts to south of the equator by February and as a result, the width of the Equatorial Countercurrent is considerably reduced. The Equatorial Countercurrent is found to exist in the southern hemisphere, eventhough the northern boundary of this current lies just north of the equator in November. During the north-east monsoon the current off the Somali coast flows to south. The Mozambique Current, which is mostly confined to the coastal regions of Africa flows to south between Mozambique and Malagasy throughout the year.

The number of point singularities are considerably increased during the transition periods. From February to April, while the northeast monsoon is still blowing but with less force, the coastal circulation of the Arabian Sea and Bay of Bengal is reversed. At the head of the Bay, the coastal circulation is reversed even in January. Well

developed anticyclonic circulation prevails in the Arabian Sea and Bay of Bengal in March and April. The current off the Somali coast starts to flow to north by March and is well developed by April. The circulation pattern south of the equator in March is similar to that during the northeast monsoon while April shows mainly the characteristics of the southwest monsoon. The circulation pattern in September is similar to that during the southwest monsoon except at the head of the Bay of Bengal where the currents are reversed. The reversal of the currents in the Arabian Sea starts by October. The Somali Current still flows to northeast in October with weakened intensity. It is clear from the streamline pattern that October is the typical month of transition from the southwest monsoon to the northeast monsoon.

The circulation pattern of each month is discussed in the foregoing paragraphs in detail.

JANUARY

In January (Fig.25) the current follows along the coast lines and has a southerly component on the east coast of India, the Arabian and Somali coasts. It becomes northerly on the west coast of India. There is an anticyclonic converging point at the head of the Bay of Bengal near the northeast coast of India. Since it is very near to the coast, the

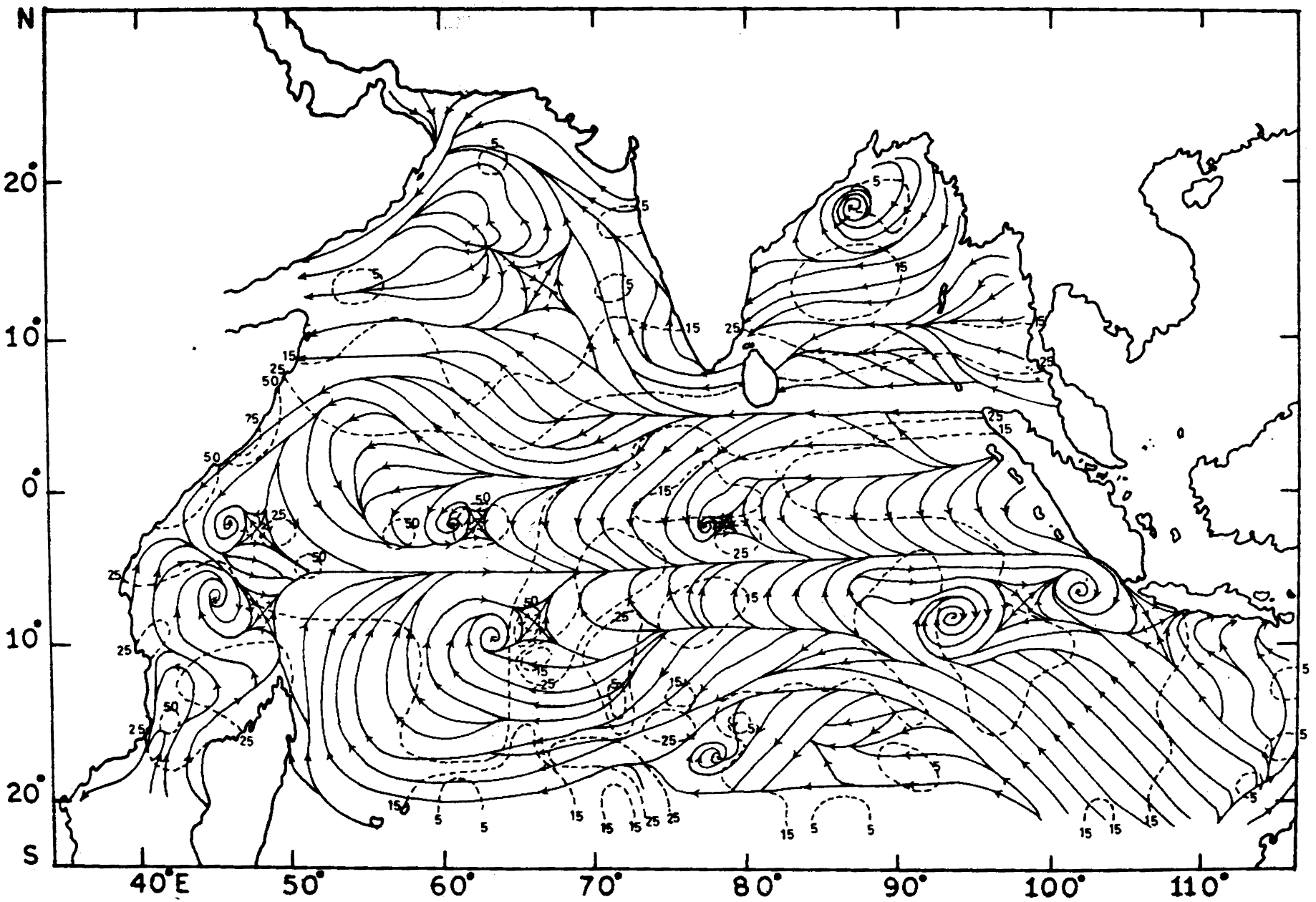

FIG. 25 STREAMLINES AND ISOTACHS (cm. sec^{-1}.) IN JANUARY.

associated hyperbolic point is not observed. A strong diverging point is found in the central Arabian Sea with the associated hyperbolic point very near to it. The North Equatorial Current flows westward north of 2°S. The Equatorial Countercurrent flows eastward between 2°S and 5°S. In the eastern region of this current system, there are two cyclonic converging points with a common hyperbolic point. The westward flowing South Equatorial Current predominates south of 5°S. A strong anticyclonic converging point is observed with the associated hyperbolic point at the boundary between the South Equatorial Current and the Equatorial Countercurrent. A strong converging line is observed along 6°S and a diverging line is found at the boundary between the Equatorial Countercurrent and the South Equatorial Current. A cyclonic converging point with the associated hyperbolic point is observed at 2°S and 60°E at the boundary between the North Equatorial Current and the Equatorial Countercurrent. A cyclonic and an anticyclonic converging points with a common hyperbolic point are observed south of the Somali coast. A diverging line is found south of the southern tip of India. From the streamline pattern it can be confirmed that the South Equatorial Current and the North Equatorial Current together feed the Equatorial Countercurrent. In the eastern region of the Indian Ocean the West Australian Current feeds the South Equatorial Current. The speed of the North Equatorial Current exceed 50 cm sec $^{-1}$ in

the central region of the Indian ocean. The current off the Somali Coast records higher velocities and the maximum speed is noticed just north of Malagasy. The strength of the South Equatorial Current is lower in the eastern region compared to that in the western region where velocities higher than 40 cm sec^{-1} are recorded.

FEBRUARY

In February (Fig.26), the North Equatorial Current flows westward north of 2°S with increased speed particularly in the western region. The Equatorial Countercurrent flows between 2°S and 8°S and the South Equatorial Current flows south of 8°S. There is not any variation of the position of the currents in February from that in January. The anticyclonic converging point in the Bay of Bengal is well developed by February. The corresponding hyperbolic point is not present because of the land boundary. The reversal of the currents which set in January at the head of the Bay of Bengal is further established and extended with northerly flow in the western region and southerly flow in the eastern region. While the circulation is cyclonic in the Arabian Sea in January, it changes into anticyclonic by February. The converging ing point in the Arabian Sea shifts further to north by February. An anticyclonic converging point is also observed

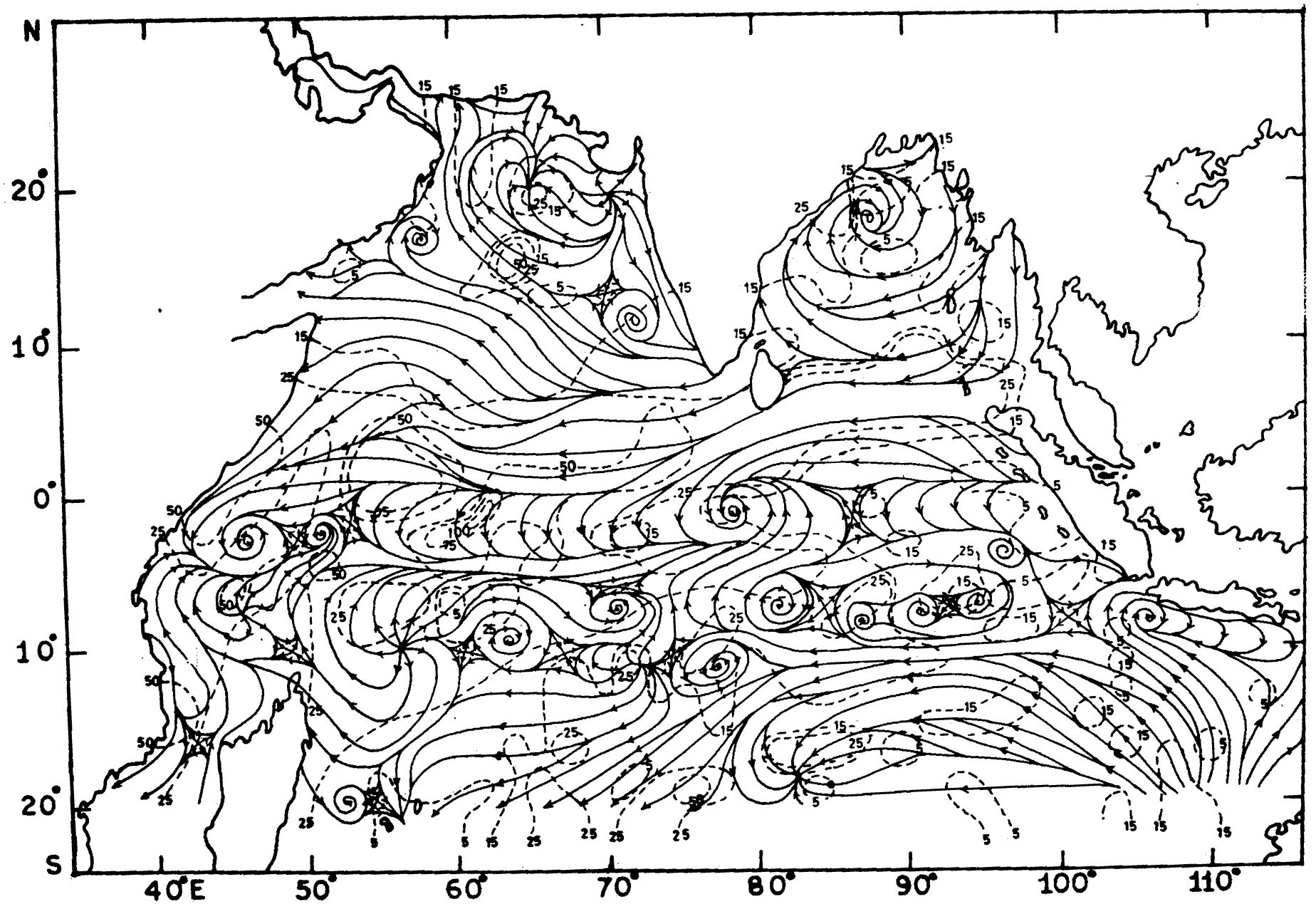

FIG. 26 STREAMLINES AND ISOTACHS (cm. sec^{-1}) IN FEBRUARY.

near the southwest coast of India. A well developed hyperbolic point separates this singular point from the earlier mentioned anticyclonic converging point. It seems that the reversal of current direction is established in the Arabian Sea and Bay of Bengal much ahead of the wind reversal. However, the zonal components of the wind stress are changed to positive at the head of the Bay of Bengal and Arabian Sea, while the meridional components still remain negative. The values of both the components of the wind stress are lower in these regions. So, the changes in the circulation seem to have been the consequence of the weakening of the northeast monsoon. An anticyclonic converging point is found in the western part of the Arabian Sea near the coast but the associated hyperbolic point is not present due to the land boundary. The cyclonic converging point at 2°S and 80°E found in January strengthened further near the boundary between the North Equatorial Current and the Equatorial Countercurrent with a well developed hyperbolic point. Similarly, two cyclonic converging points are found in the western region separated by a common hyperbolic point. The anticyclonic converging point, which is found in January, south of these converging points in the western region of the Indian Ocean is replaced by a strong diverging point. A series of singular points are observed near the boundary between the Equatorial Countercurrent and the South Equatorial Current along the width of the ocean. Particular mention may be made about the strong diverging point at 10°S and 56°E

which was not present in January. The strong hyperbolic point found in January near Java has disappeared by February. In general, a considerable increase in the number of point singularities is observed in February. The isotachs show that the speed of the currents in February is slightly higher than that in January. The western half of the Indian Ocean records higher velocities than the eastern half. Velocities about 75 cm sec^{-1} are observed in the Somali Current region.

MARCH

The surface circulation in the Bay of Bengal and Arabian Sea is almost reversed by March (Fig.27). But the northeast monsoon circulation still persists in the equatorial region. The anticyclonic converging point in the Bay of Bengal moved further south accompanied by an increase in current speed by about 10 cm sec^{-1}. A well developed anti-cyclonic converging point is observed in the Arabian Sea, but the associated hyperbolic point is not observed due to the land boundary. The anticyclonic converging point found in February near the southwest coast of India shifts to west due to the complete reversal of the circulation. Unlike in the previous months, a part of the Equatorial Countercurrent lies in the northern hemisphere east of 80°E. The distribution of the zonal components of the wind stress also

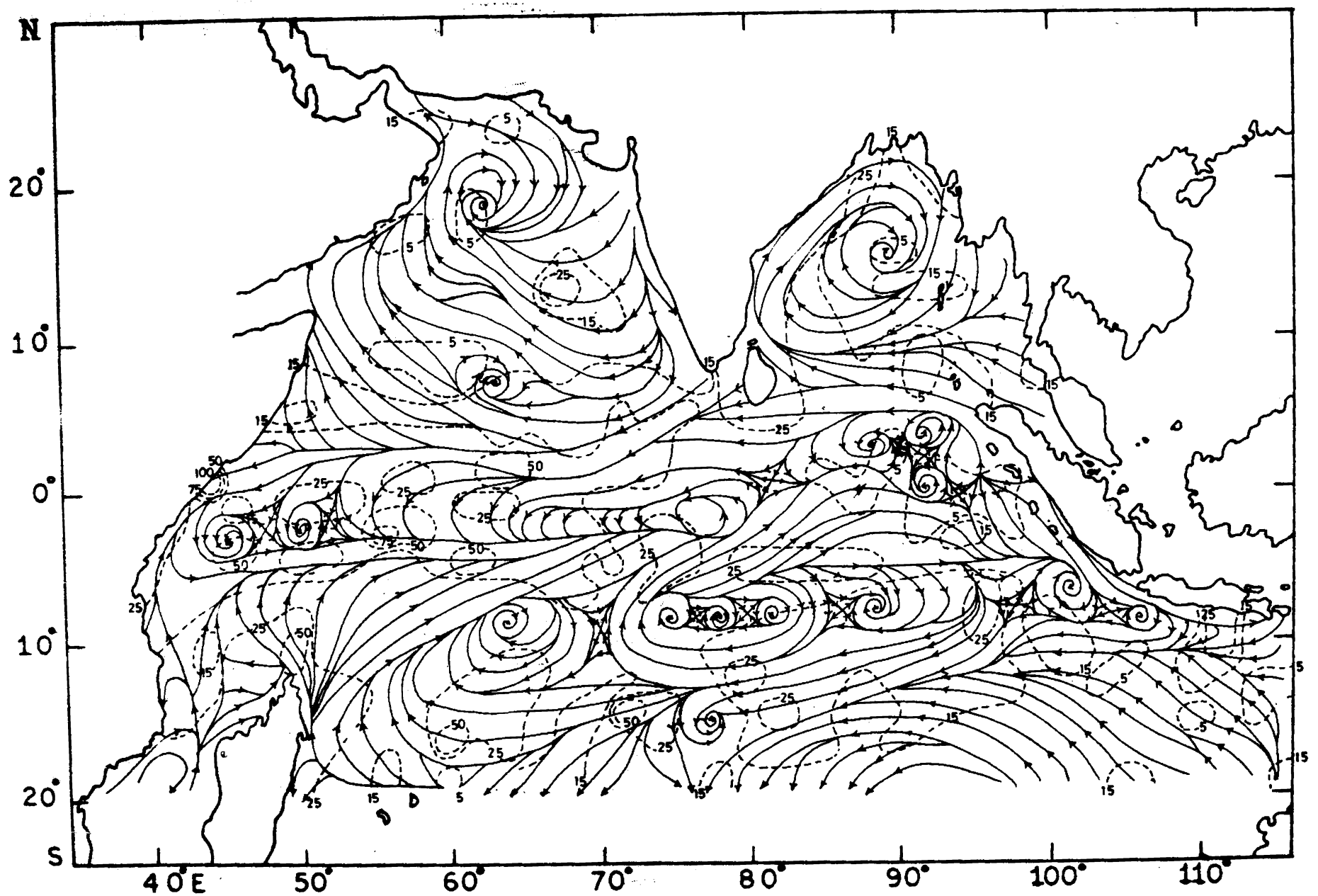

FIG. 27 STREAMLINES AND ISOTACHS(cm. sec^{-1}) IN MARCH.

confirm the above conclusion. Between 70°E and 80°E, the Equatorial Countercurrent is present between 2°S and 8°S, while west of 70°E it is further extended into the southern hemisphere. The northern boundary of the South Equatorial Current lies along 8°S east of 65°E and 4°S west of 65°E. A number of point singularities are observed at the boundaries between different currents. Three cyclonic converging points and one diverging point are present in the eastern region of the Indian Ocean separated by three hyperbolic points. These singular points represent the confluence of the North Equatorial Current and the Equatorial Countercurrent. The strong cyclonic converging point found at 2°S and 80°E in February reduces to a small cyclonic converging point by March. A hyperbolic point which is gradually developed by March separates the present singular point from the group of point singularities in the eastern part of the ocean. Similarly, the two cyclonic converging points in the western part of the ocean dissipate considerably while no change is noticed in the associated hyperbolic points. The two strong converging points and the associated hyperbolic point found in February in the eastern region, south of 6°S disappeared by March. The anticyclonic converging point observed at 10°S and 64°E strengthens by March while the two cyclonic converging points east of it disappeared. The diverging point which is present at 12°S in February shifts further

south and dissipates. There is not much variation in the position and size of the point singularities east of 75°E, except in the eastern parts of the ocean where the anticyclonic converging point dissipates. But, another anticyclonic converging point appears just west of the previous one separated each other by a neutral point. A diverging point is observed in the South Equatorial Current just east of the Malagasy island. Apart from the point singularities, lines of convergence and divergence are also present in the streamline pattern, eventhough they are not prominent as in the previous month. It can be seen from the streamline pattern that the Equatorial Countercurrent is fed by the North Equatorial Current and the South Equatorial Current. In turn the Equatorial Countercurrent feeds the South Equatorial Current. At 3°N and 52°E, the North Equatorial Current branches into two, one branch flows to north as the Somali Current while the other flows to the south. Part of the southward flowing branch feeds the Equatorial Countercurrent. The speed of the currents is much reduced especially in the Arabian Sea while the speed of the current near the Somali coast is higher than that in February. There is no conspicuous variation in the strength of the currents in other parts of the ocean.

APRIL

Compared to the previous months, the number of

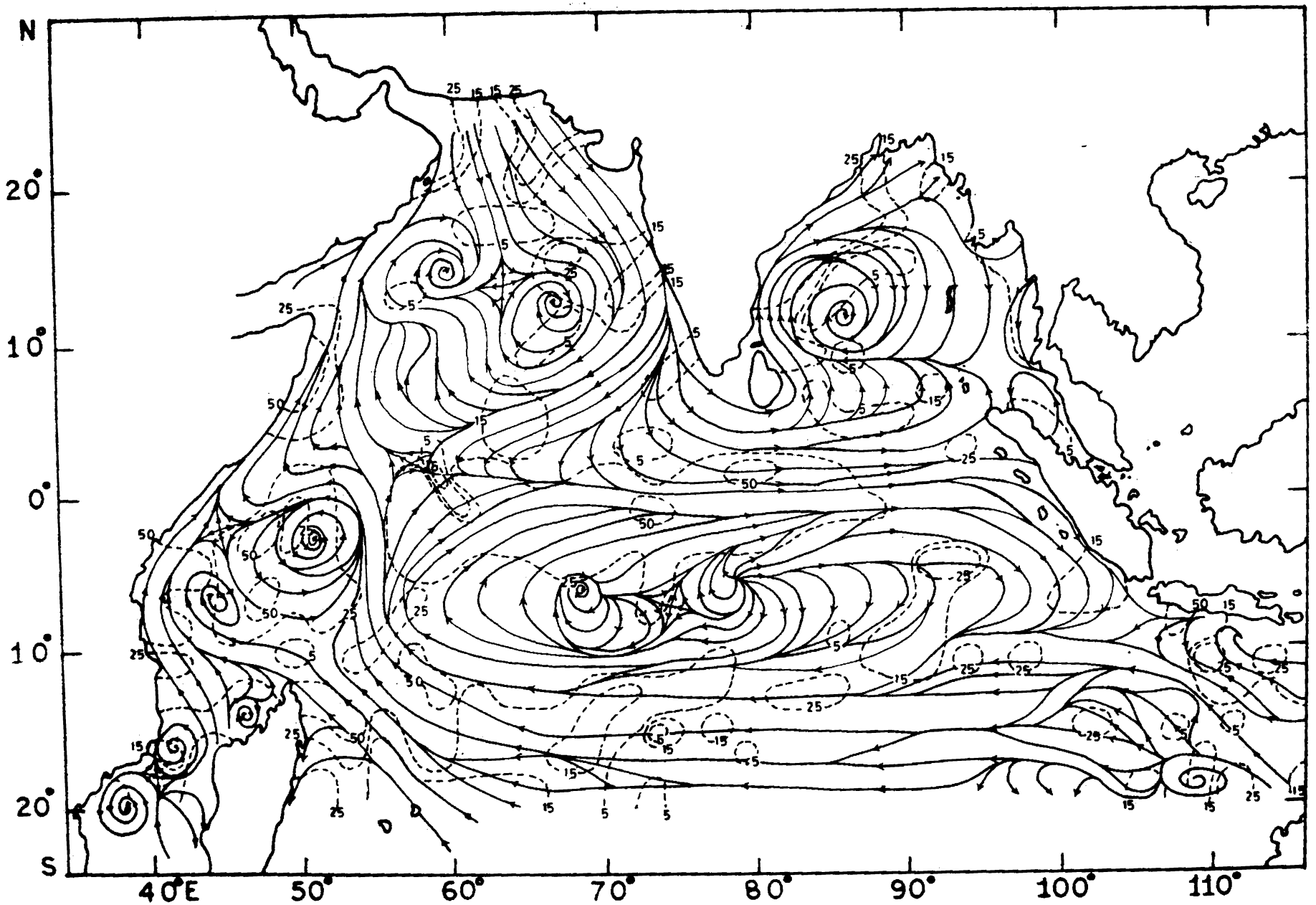

FIG. 28 STREMLINES AND ISOTACHS (cm. sec^{-1}) IN APRIL

singular points are too high in April (Fig.28) in the northern and western parts of the ocean. The large number of singular points may be due to the transition from the northeast monsoon to the southwest monsoon and the associated unsteady conditions in the circulation. The reversal of the surface circulation is completed by April. The North Equatorial Current is completely replaced by the eastward flowing Southwest Monsoon Current which merges with the Equatorial Countercurrent. This broad current extends approximately upto 8°S along the width of ocean except west of 58°E. The Somali Current is well developed west of 58°E and flows to northeast. The South Equatorial Current exists south of 8°S. The South Equatorial Current feeds the Somali Current and the Monsoon Current in the western region of the ocean. In turn, the South Equatorial Current is fed by the Monsoon Current in the eastern parts of the ocean. Thus, the Monsoon Current, the Somali Current and the South Equatorial Current form the part of a large anticyclonic circulation system. The anticyclonic converging point in the Bay of Bengal intensifies and shifts further south by April. The associated neutral point is not present due to the land boundary. A converging line is also found associated with the above singular point. The two anticyclonic converging points in the Arabian Sea become stronger and come closer and are separated by a well developed hyperbolic point. The number of singular

points east of 60°E along 10°S reduces compared to that in the previous months. One antieyclonic converging point and another antieyclonic divering point are observed along 10°S between 65°S and 75°E. A well developed hyperbolic point is observed near Java. The eyclonic converging point south of the Somali Coast is considerably strengthened and another antieyclonic converging point replaces the previous eyclonic converging point, just south of the above singular point. A well developed eyclonic point is also observed west of the Malagasy island. Unlike the previous months, no point singularities are observed in the South Equatorial Current, and along the equator, east of 60°E. The streamlines are parallel and symmetrical to the equator, east of 60°E. The above characteristics indicate that the Equatorial Jet starts to flow to east by April. This conclusion is also confirmed by the distribution of the isovels. A high velocity core with values exceeding 60 cm sec^{-1}, is observed in the equatorial region from 60° to 85°E. The speed of the currents near the Somali Coast is reduced considerably by April. This may be due to the complete reversal of the surface circulation. There is no conspicuous change in the speed of the currents in other parts of the ocean.

MAY

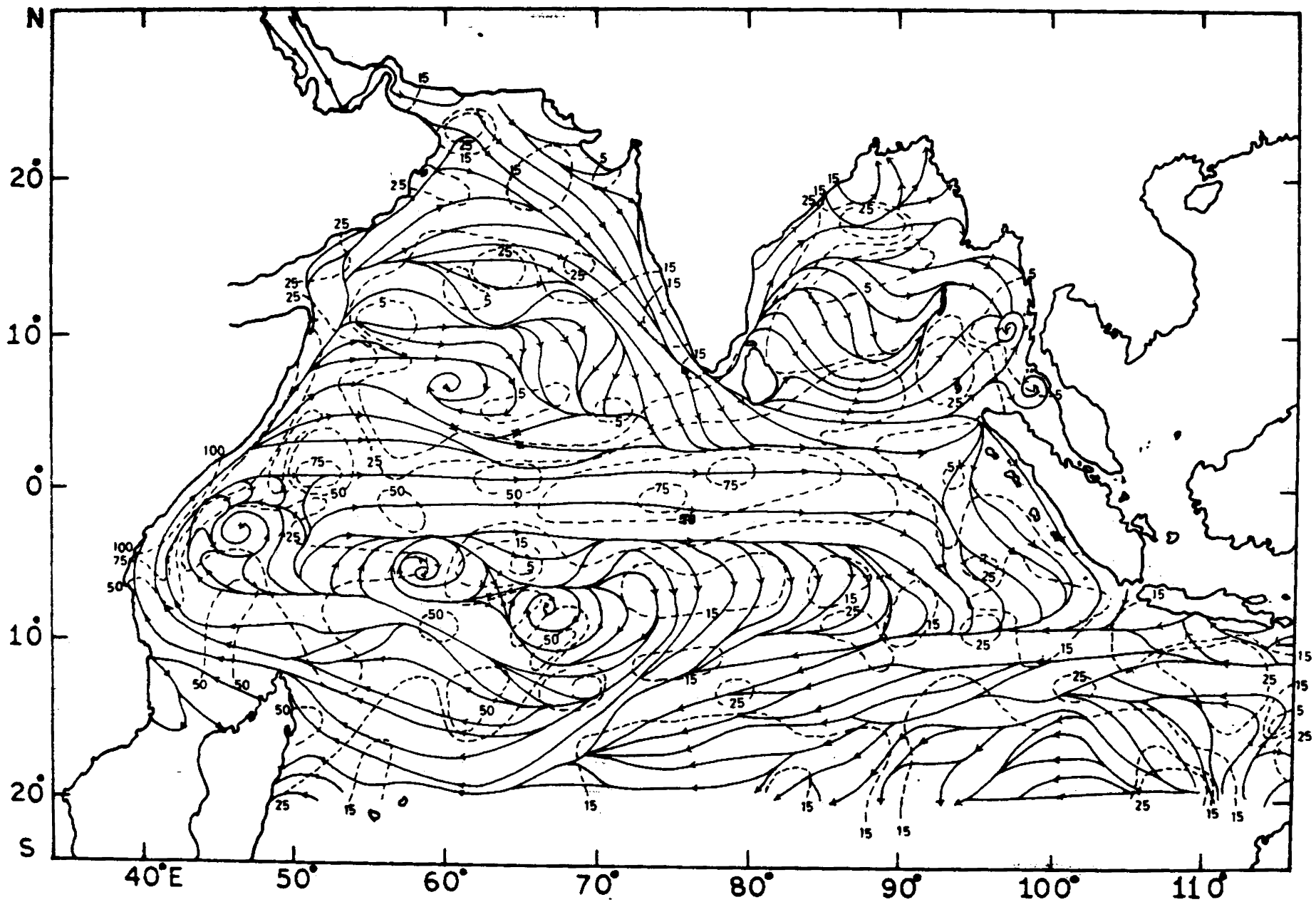

FIG. 29 STREAMLINES AND ISOTACHS (cm. sec^{-1}) IN MAY

over the area. As a result, the Southwest Monsoon Current is fully developed and extends upto 8°S. The Somali Current is also well established and continues to flow northeastward. The South Equatorial Current is observed south of 8°S and feeds the Somali Current. The anticyclonic eddy, comprising of the Monsoon Current, the Somali Current and the South Equatorial Current further intensifies and extends almost along the width of the ocean. The streamlines are straight and parallel to the equator from 65° to 90°E. This character indicates the presence of the Equatorial Jet. The high velocity core in the isoval pattern also confirms the above conclusions. The number of singular points are considerably reduced by May. All the anticyclonic converging points disappeared from the Bay of Bengal and the Arabian Sea. All other singular points disappeared except one cyclonic converging point south of the Somali Current and two anticyclonic converging points at the boundary between the Monsoon Current and the South Equatorial Current. In addition to the above point singularities, lines of convergence and divergence are also observed in the streamline pattern. The circulation in the open ocean is mainly zonal, while meridional components predominate near the coasts. Northerly components prevail near the coasts of East Africa, Somali, Arabia and the east coast of India, while southerly components predominate near the west coast of India, Burma and Sumatra. The isotachs show considerable increase

in the speed of the currents in the entire Indian Ocean, especially in the central equatorial region and in the western region. The Equatorial Jet records speed exceeding 75 cm sec^{-1} while the Somali Current records values greater than 100 cm sec^{-1}.

JUNE

The streamline pattern considerably changes by June (Fig.30). The Monsoon Current extends further south, from 8°S in May upto 10°S in June and turns to south in the eastern region of the equatorial Indian Ocean. The Monsoon current feeds the South Equatorial Current which in turn feeds the Somali Current and the Monsoon Current. The large anticyclonic eddy comprising of the above three major currents becomes stronger and steady by June. The number of the point singularities are further reduced. The cyclonic converging point south of the Somali Current disappeared. The two anticyclonic converging points found in May at the boundary between the Monsoon Current and the South Equatorial Current dissipate and shift westward. A cyclonic converging point is observed at 18°S and 100°E along with the neutral point. A converging point is present at 12°S and 112°E which is separated from the nearby cyclonic singular point by a well developed hyperbolic point. The reduction in the number of the singular points is due to the strengthening of the south-

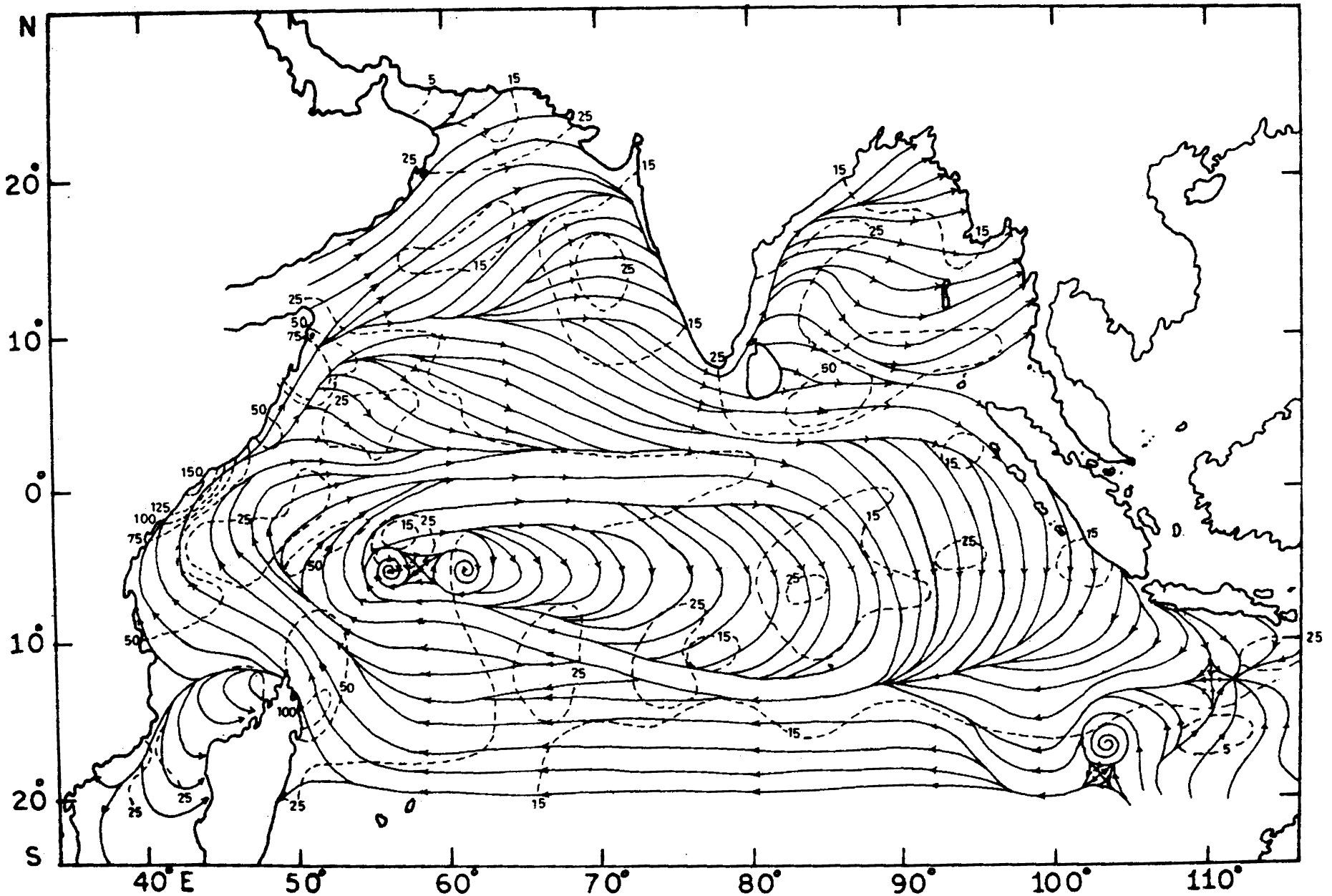

FIG. 30 STREAMLINES AND ISOTACHS(cm. sec^{-1}) IN JUNE.

west monsoon over the Indian ocean. The streamlines are oriented zonally in the open ocean but, meridional components exist near the coasts. It is evident from the streamline pattern that the Equatorial Jet disappears by June. The speed of the Somali Current increases further from 100 cm sec^{-1} in May to 175 cm sec^{-1} in June. The isovels show an increase of the speed in the Arabian Sea and Bay of Bengal. The speed of the currents in the central equatorial region is considerably reduced from 75 cm sec^{-1} in May to about 25 cm sec^{-1} in June. The peculiar pattern of the streamlines in the eastern region of the equatorial Indian Ocean may be due to the anticyclonic shear developed between the fast moving Monsoon Current and the slower Equatorial Countercurrent.

JULY

There is not much variation of the basic current structure in July (Fig.31) from that in June. East of 60°E, the Monsoon Current turns completely to south from the equator itself and feeds the South Equatorial Current. Within the large anticyclonic eddy of the southern hemisphere, two anti-cyclonic converging points and one cyclonic converging point which are separated by the associated hyperbolic points are observed. The formation of a cyclonic converging point at the head of the Bay of Bengal indicates that the currents along the east coast of India are reversed. A cyclonic converging

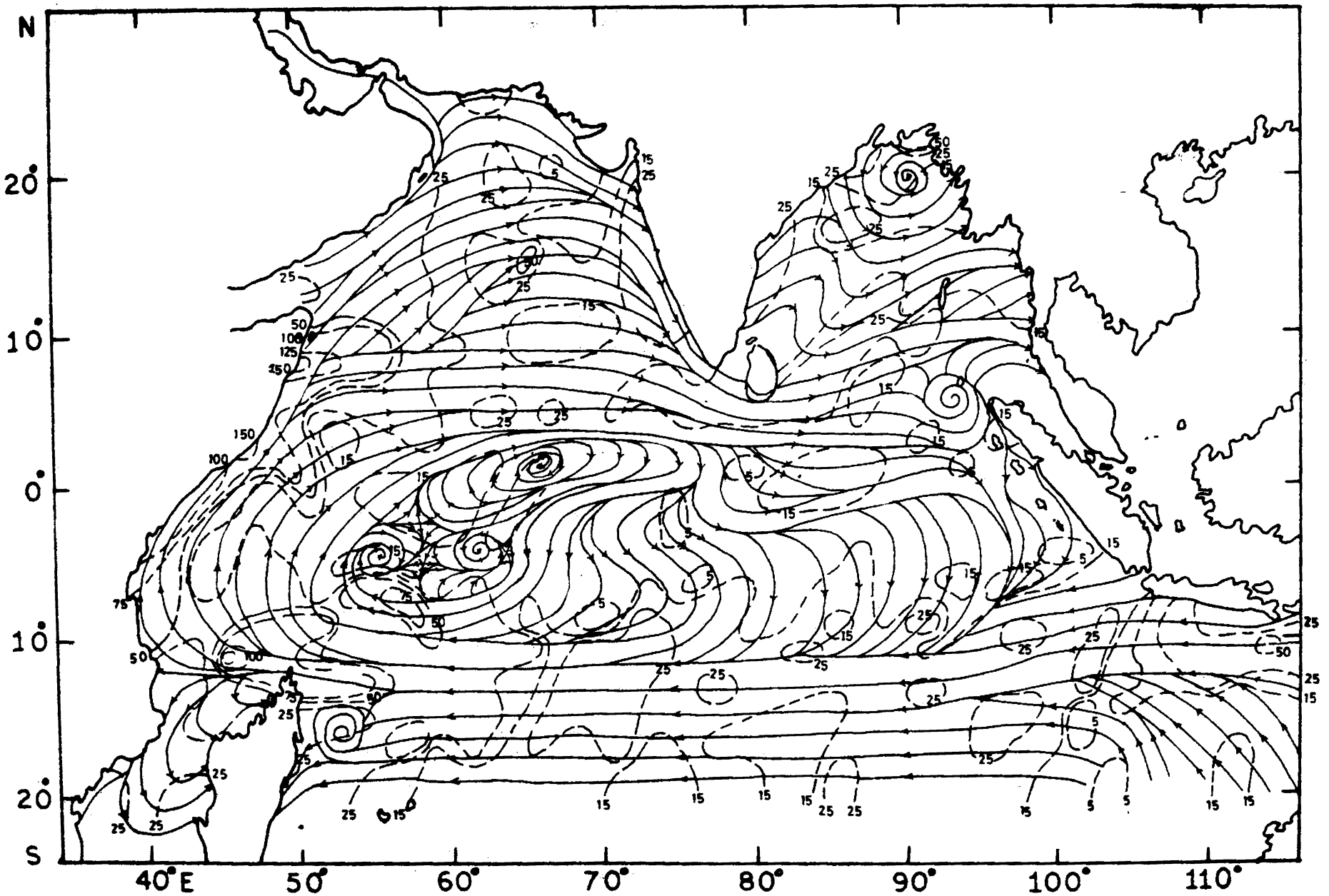

FIG. 31 STREAMLINES AND ISOTACHS(cm. sec^{-1}) IN JULY.

point is observed north of the Sumatra Coast along with the neutral point. An anticyclonic converging point is observed east of the Malagasy Island. The South Equatorial Current branches into two parts, northwest of Malagasy. One branch flows southward and feeds the Mozambique Current, while the other branch flows northward and feeds the Somali Current. Apart from the point singularities, lines of convergence and divergence are noticed in the streamline pattern. The flow is mainly zonal in the open ocean but follows the coasts near the land boundaries. The streamline pattern clearly reveals that the Somali Current turns offshore at about 4°N. In the eastern region, south of 8°S, water comes from south indicating that the West Australian Current also feeds the South Equatorial Current. The isovels show a general increase of the speed of the currents in the entire Indian ocean, especially, in the Somali region. However, the equatorial region experiences a decrease of the current speed.

AUGUST

The streamline pattern in August (Fig.32) is similar to that in July with slight differences. The anticyclonic eddy comprising of the Monsoon Current, the Somali Current and the South Equatorial Current is not much pronounced as that in the previous months. The point singularities are more concentrated in the western region than in the eastern region. This may be

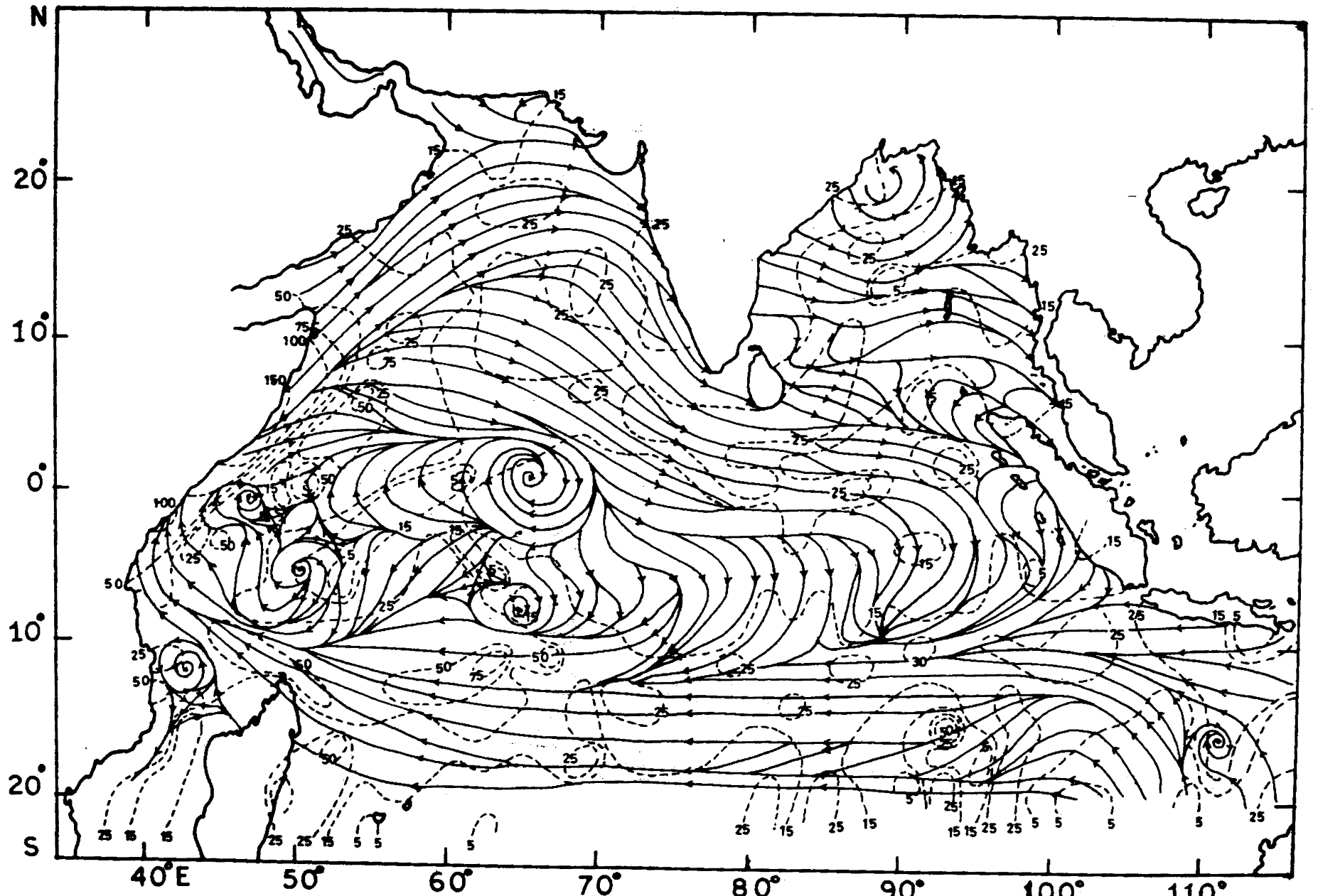

FIG. 32 STREAMLINES AND ISOTACHS (cm. sec^{-1}) IN AUGUST.

due to shifting of the South Equatorial Current to north, approximately upto 4°S, west of 70°E. The antieyclonic converging point at 2°S and 65°E strengthens, while the cyclonic converging point south of it disappears. One antieyclonic converging point and another antieyclonic diverging point are observed south of the Somali Current, separated by a neutral point. A cyclonic converging point is also observed west of the Malagasy Island. An antieyclonic converging point and an associated neutral point are observed at 10°S and 88°E where the Monsoon Current, after turning south, joins with the South Equatorial Current. The well developed cyclonic converging point, found at the head of the Bay in July weakens slowly by August. Generally, the currents follow the coasts except in the east coast of India and the west coast of Sumatra. The speed of the currents in the Arabian Sea is reduced while the equatorial region experiences an increase. There is not much variation of the speed of the currents in the Somali region and in the other parts of the ocean from that in July.

SEPTEMBER

The streamline pattern in September (Fig.33) clearly reveals the weakening of the southwest monsoon. The reversal of current sets in at the head of the Bay of Bengal. The antieyclonic eddy formed by the Monsoon Current, the Somali Current and the South Equatorial Current is less prominent

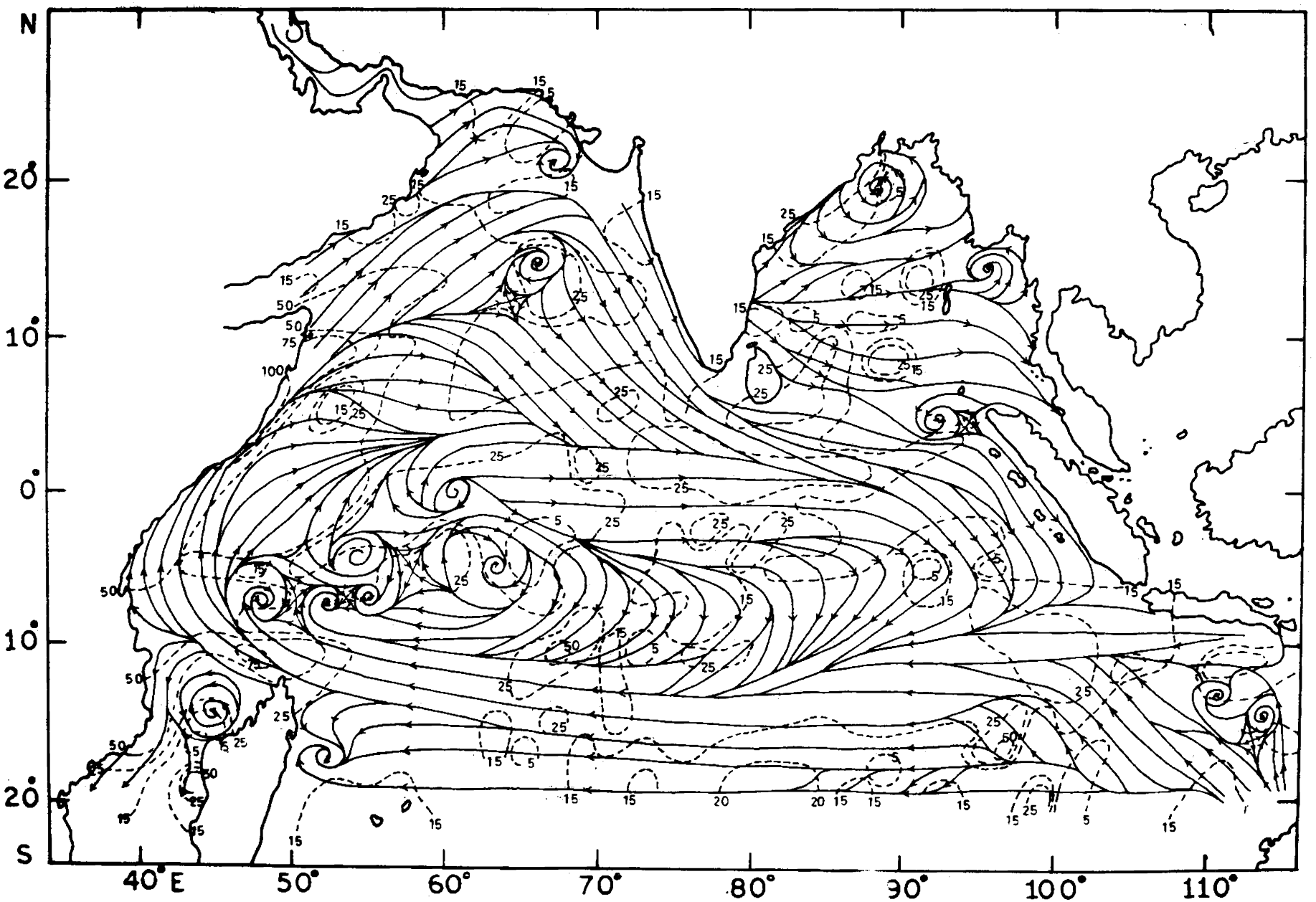

FIG.33 STREAMLINES AND ISOTACHS n. sec^{-1}) IN SEPTEMBER.

than that in the previous months. The South Equatorial Current shifts to north in the western region as in the case of August. The number of point singularities increase in September which may be dpe to the weakening of the southwest monsoon. Two anticyclonic converging points are observed in the Arabian Sea itself. The cyclonic converging point at the head of the Bay of Bengal intensifies but, the associated hyperbolic point is not observed due to the land boundary. A small cyclonic converging point is observed near the coast of Burma, while another one is present northeast of Sumatra. In the western part of the large scale eddy circulation, a number of point singularities five anticyclonic converging points and one anticyclonic diverging point, are observed. They are all separated each other by well developed hyperbolic points. An anticyclonic diverging point is observed between the African coast and Malagasy island where a part of the South Equatorial Current flows southward as the Mozambique Current. Two less prominent point singularities - one cyclonic converging point and another anticyclonic converging point, are observed in the eastern part of the southern Indian Ocean. Lines of convergence and divergence are also present in the streamline pattern. The currents flow zonally in the open ocean, but they follow the coasts except along the east coast of India where the current makes an angle with the coast line. The streamline pattern in the eastern region, west of 10°S indicates that part of the South

Equatorial Current is fed by the West Australian Current. The streamlines in the central equatorial region run almost parallel and symmetric to the equator. In addition to it, the strength of the currents in the equatorial region increases from an average of 15 cm sec^{-1} in August to 25 cm sec^{-1} in September. The above characteristics clearly reveal that the Equatorial Jet starts to flow in September itself. The isovels record a decrease of current strength in the Somali Current region. There is not any conspicuous variation of current speed in other parts of the ocean.

OCTOBER

This is the typical transition period from the southwest monsoon to the northeast monsoon (Fig.34). So, the unsteady conditions similar to those existing in April prevail in this month too. A large number of singular points are formed in the whole region consistent with this unsteady conditions. The Equatorial Countercurrent predominates in the place of the Monsoon Current. The Somali Current still flows toward northeast with relatively weakened intensity. The anticyclonic eddy south of the equator weakens considerably. The number of point singularities are large in the western region than in the eastern region. Two well developed anticyclonic converging points are observed in the western part of the Arabian Sea separated by a neutral point. A cyclonic converging point is

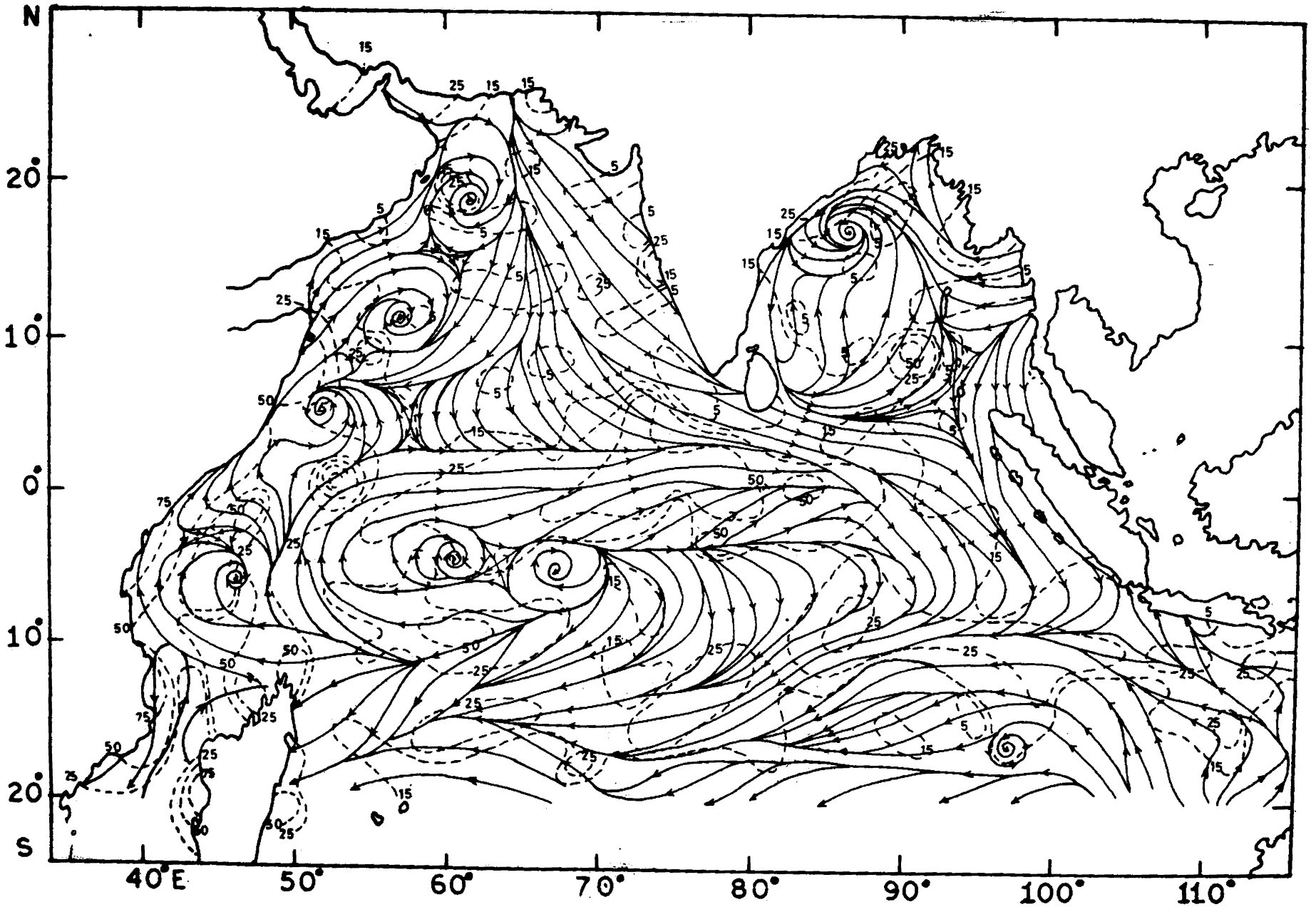

FIG.34 STREAMLINES AND ISOTACHS (cm. sec^{-1}) IN OCTOBER.

present near the Somali Coast, which is separated from the nearby anticyclonic converging point by a hyperbolic point just north of it. Apart from this, another well developed hyperbolic point is also found east of this singular point which separates it from the eastward flow. An anticyclonic converging point is observed at 8°S and 48°S. A hyperbolic point separates this singular point from the westward flow just north of it. Two anticyclonic converging points, separated by a well developed hyperbolic point are observed at about 6°S, between 60°E and 70°E. The cyclonic converging point at the head of the Bay of Bengal is intensified by October and the surface circulation in the Bay of Bengal is established as a cyclonic flow. Eventhough, anticyclonic circulation is developed in the western Arabian Sea, flow is towards south in the eastern regions. The currents follow the coasts near the land boundaries except along the Burma Coast. The singular point between Malagasy and the African Coast disappeared. The streamlines are parallel and symmetric to the equator from 60° to 88°E. This pattern and the higher values of velocity indicate the presence of the Equatorial Jet. The strength of the Equatorial Jet considerably increases while the Somali Current records a decrease of current speed from an average of 125 cm sec^{-1} in September to 75 cm sec^{-1} in October.

NOVEMBER

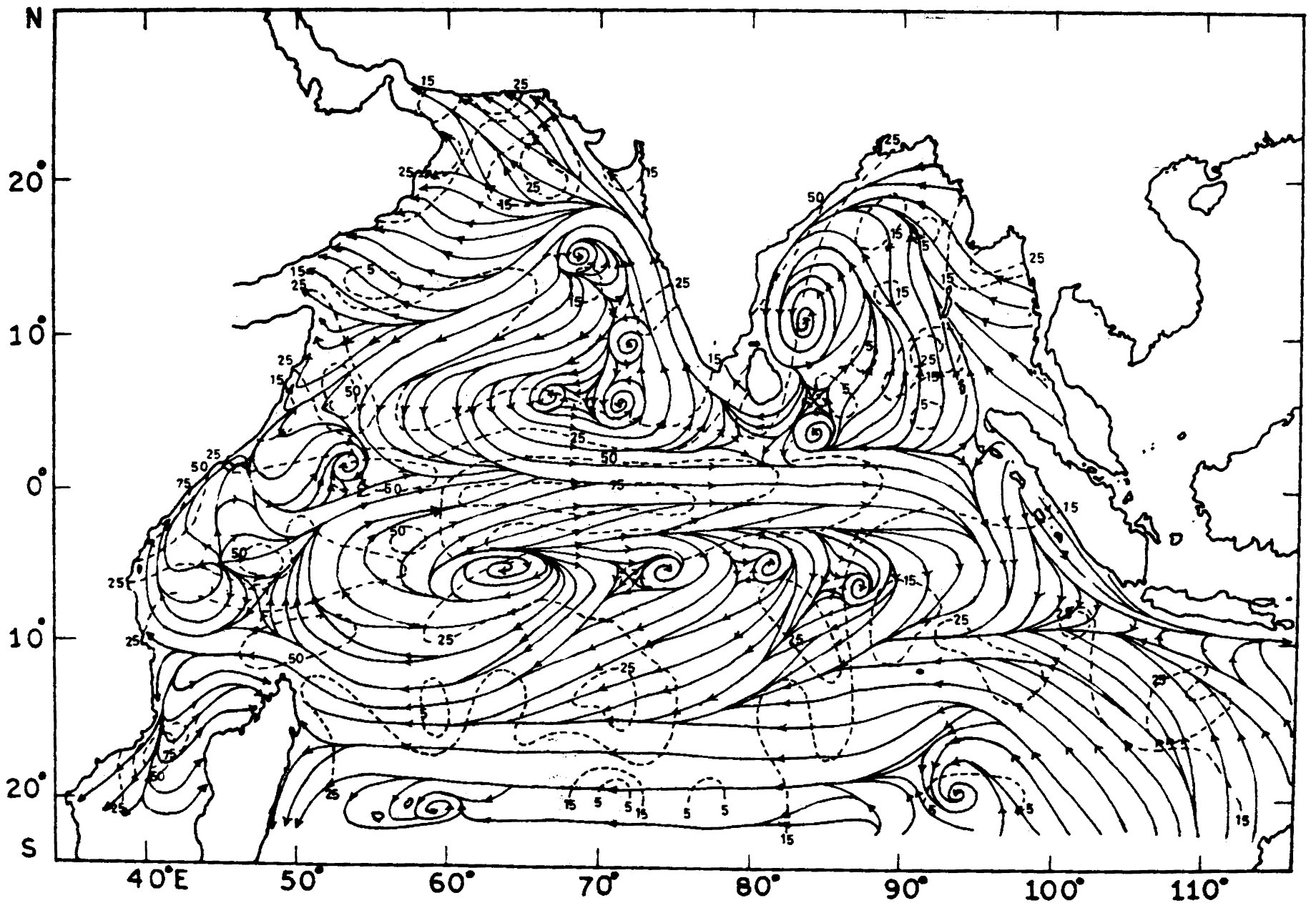

FIG. 37 STREAMLINES AND ISOTACHS (cm. sec^{-1}) IN NOVEMBER.

established in November (Fig.35). Strong cyclonic circulation exists in the Bay of Bengal while westward flow exists in the Arabian Sea. The Equatorial Countercurrent is found to exist between 3°N and 6°S. The Somali Current disappears and a current flows to south, off the Somali Coast. The Equatorial Jet is observed from 55° to 88°E, between 2°N and 2°S. The number of point singularities are decreased in the western region but an increase is noticed between 6°S and 8°S where the Equatorial Countercurrent comes nearer to the South Equatorial Current. The strong cyclonic converging point, found in the Bay of Bengal further intensifies and shifts to the south. Two cyclonic converging points are observed in the eastern part of the Arabian Sea, separated by a neutral point. These two converging points form the centre of the large cyclonic flow, still existing in the eastern part of the Arabian Sea. A well developed diverging point is present south of the Somali Coast. A hyperbolic point separates it from the large anticyclonic flow formed by the South Equatorial Current and the Equatorial Countercurrent. A series of converging points are observed at the middle of this major eddy circulation system. The anticyclonic converging point, found at about 8°S and 64°E is the most developed one. The other singular points, observed in a line east of the above singular point are not well developed. A cyclonic converging point is found in the

eastern region where the West Australian Current joins with the South Equatorial Current. In addition to the point singularities a large number of lines of convergence and divergence are noticed in the streamline pattern. From the distribution of the isovels, it can be seen that the strength of the current in the central equatorial region is considerably increased from an average of 50 cm sec^{-1} in October to 75 cm sec^{-1} in November. The strength of the currents in the northern parts of the Arabian Sea and Bay of Bengal increases by November. The currents off the Somali Coast records an average of 50 cm sec^{-1}. There is no conspicuous variation in the strength of the currents, south of the equator.

DECEMBER

The North Equatorial Current is well established by December (Fig.36) and extends from 3°N in November approximately upto the equator. Eventhough, singular points are absent in the Bay of Bengal and Arabian Sea, a number of singular points are observed at the boundary between the different currents. A small anticyclonic converging point is found in the northwestern part of the Arabian Sea which is separated from the coast by a neutral point. Another anticyclonic converging point is depicted in the central region of the Bay of Bengal. Two cyclonic converging points are formed at the boundary between

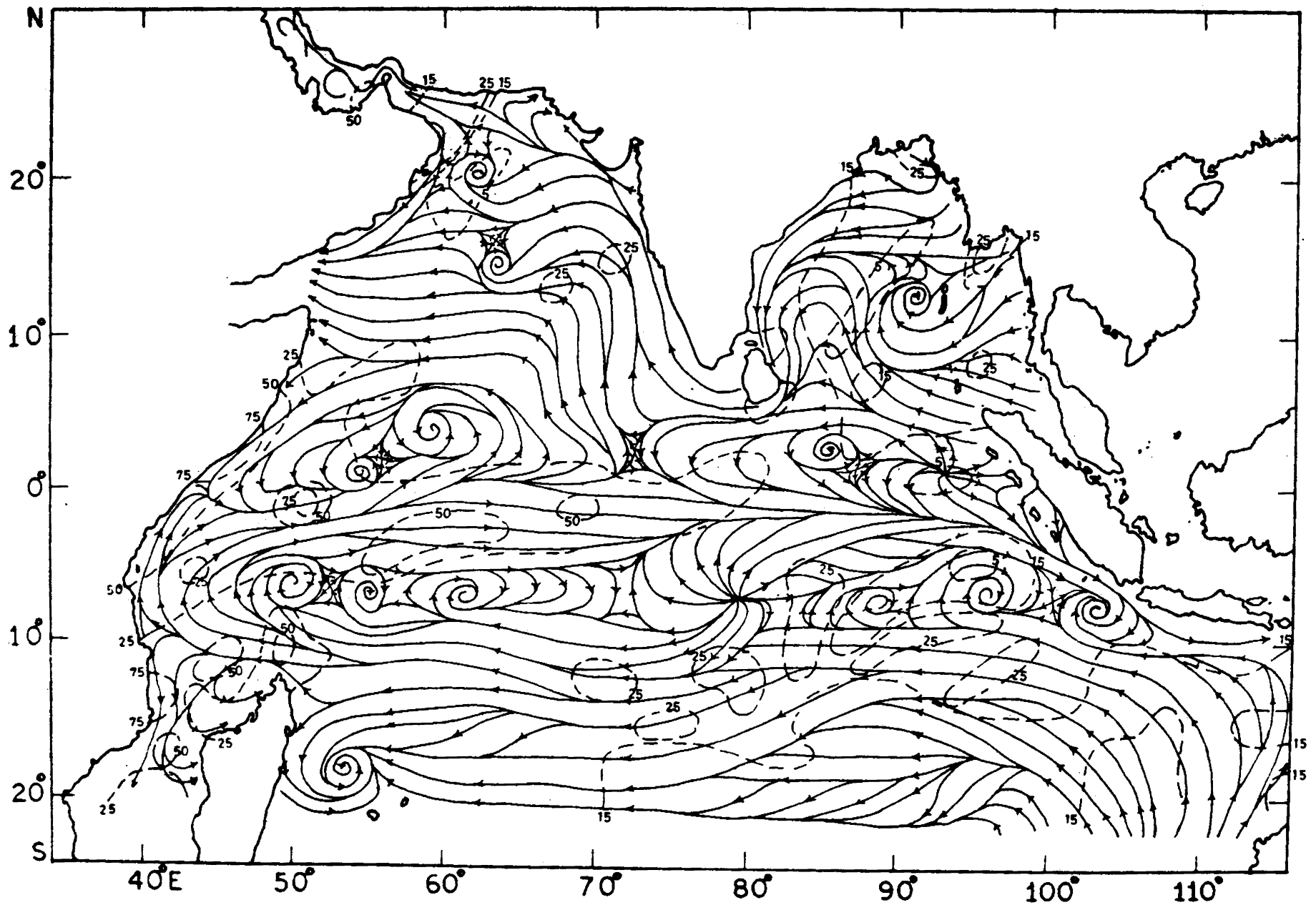

FIG. 36 STREAMLINES AND ISOTACHS (cm. sec^{-1}) IN DECEMBER.

the North Equatorial Current and the Equatorial Countercurrent, east of Somali Coast. Similarly, a diverging point is formed in the eastern region near the boundary between the North Equatorial Current and South Equatorial Current, and is separated from a nearby cyclonic converging point by a neutral point. A part of the North Equatorial Current turns to east and a part of the Equatorial Countercurrent turns to northwest at 1°N and 73°E. As a result, a well developed hyperbolic point is formed between these flows. Similarly, a series of point singularities are noticed at the boundary between the Equatorial Countercurrent and the South Equatorial Current at about 8°S. Out of the above singular points, the most pronounced is the diverging point at about 8°S and 80°E. The anticyclonic eddy in the southern hemipshere slowly dissipates by December. A part of the South Equatorial Current flows to south between the African Coast and Malagasy as the Mozambique Current. The streamlines are mainly zonal in the open ocean but they are meridional along the coasts. The strength of the current is considerably decreased in the central equatorial region. The absence of the high velocity core in the central equatorial region indicates the disappearance of the Equatorial Jet. The same conclusion can be derived from the pattern of the streamlines. The strength of the current off the Somali Coast is increased. No noticeable variation is observed in the strength of the currents in other parts of the ocean.

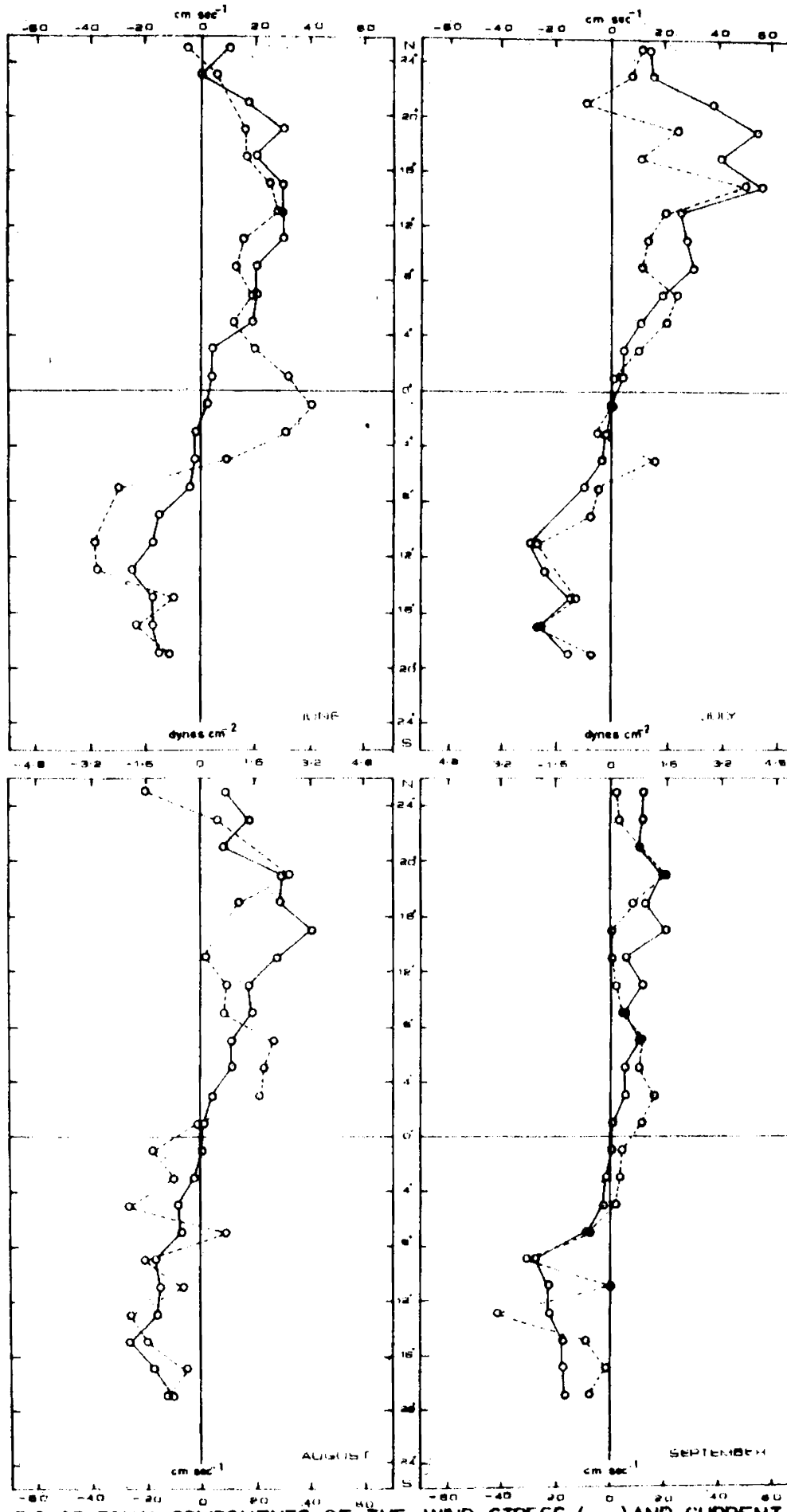

FIG. 37. ZONAL COMPONENTS OF THE WIND STRESS (—) AND CURRENT VELOCITY (---) ALONG 65°E

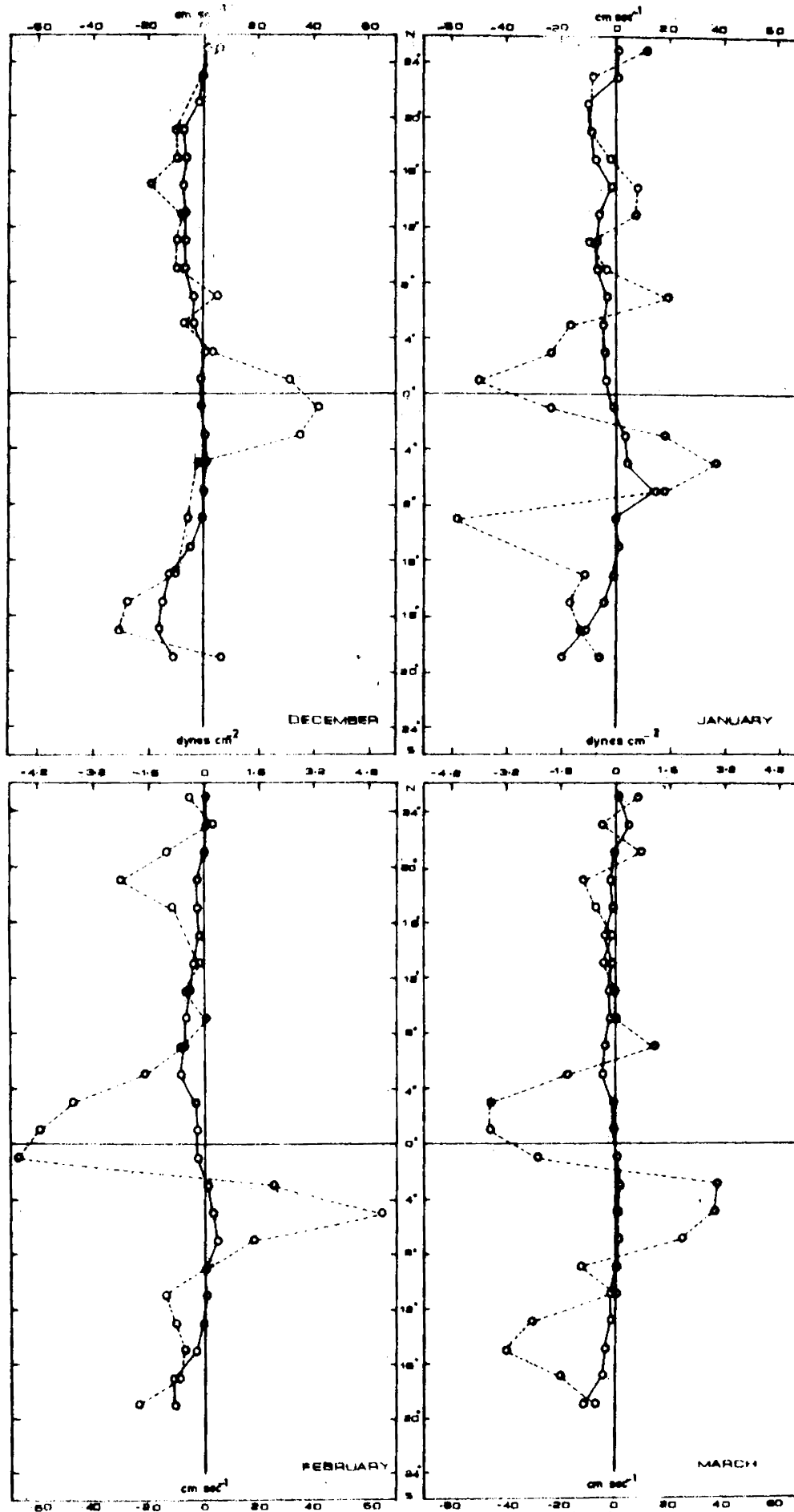

FIG. 38 ZONAL COMPONENTS OF THE WIND STRESS (—) AND CURRENT VELOCITY (---) ALONG 65°E

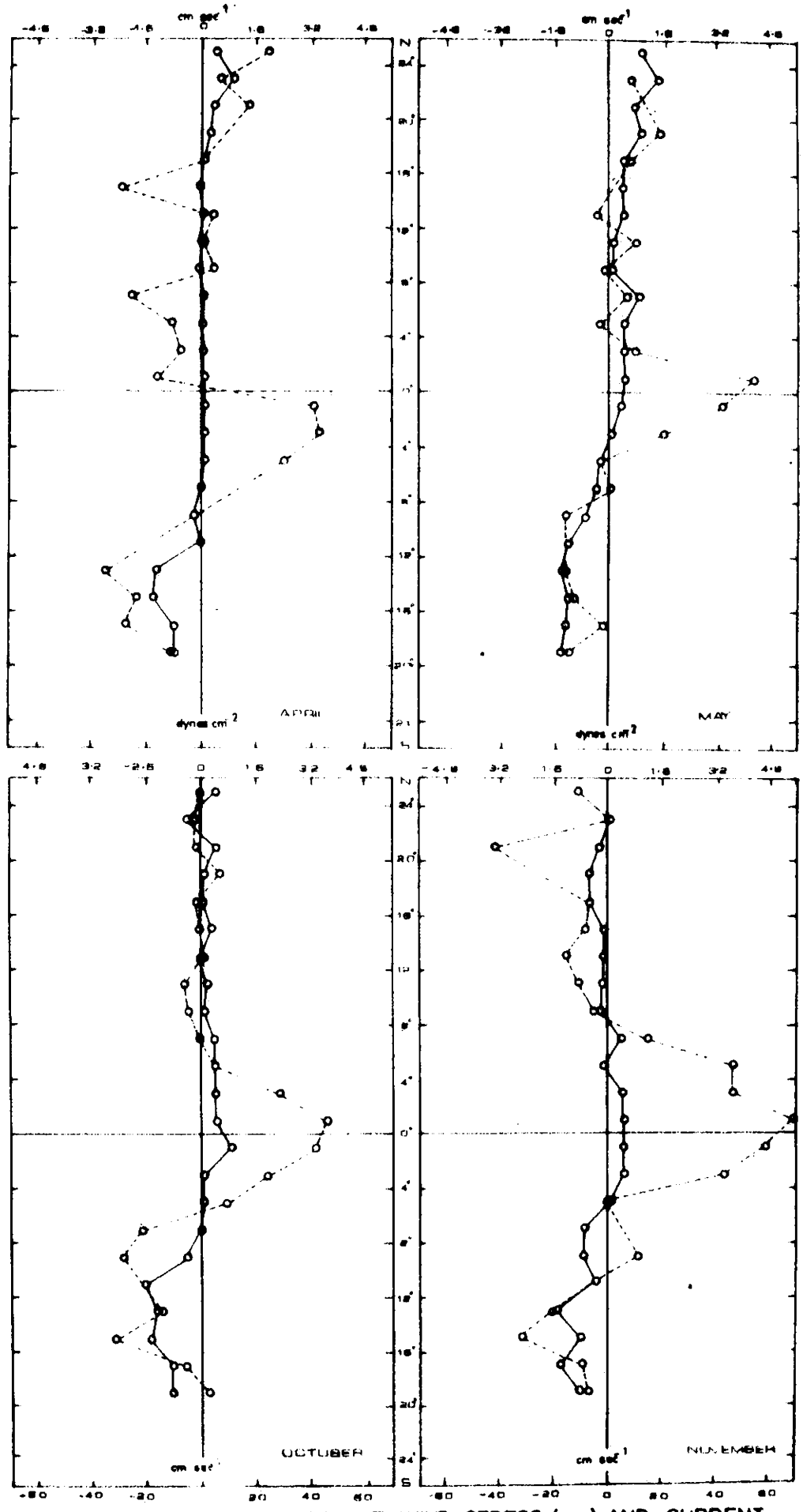

FIG:39 ZONAL COMPONENTS OF THE WIND STRESS (—) AND CURRENT VELOCITY (---) ALONG 65°E

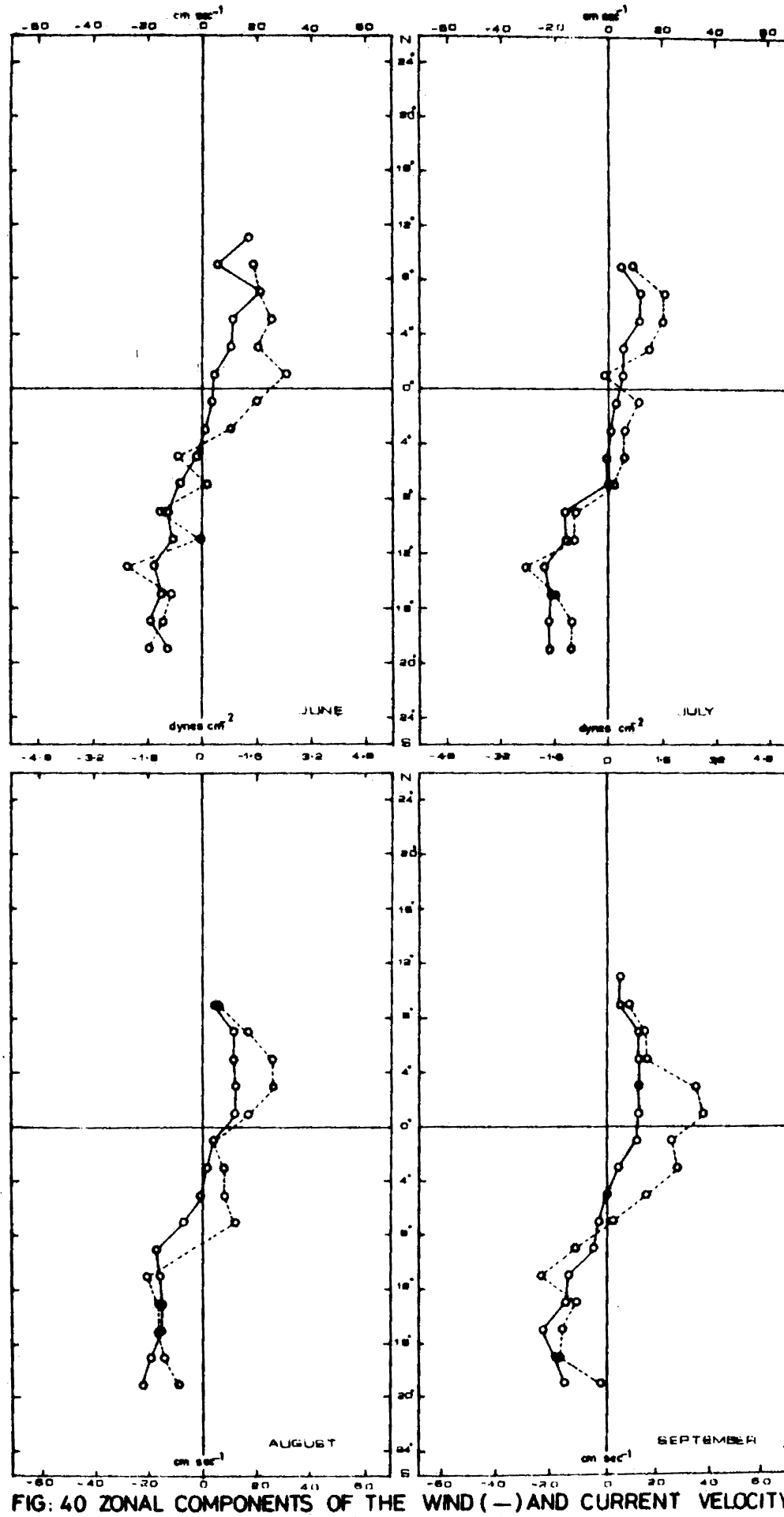

FIG: 40 ZONAL COMPONENTS OF THE WIND (—) AND CURRENT VELOCITY (---) ALONG 77°E

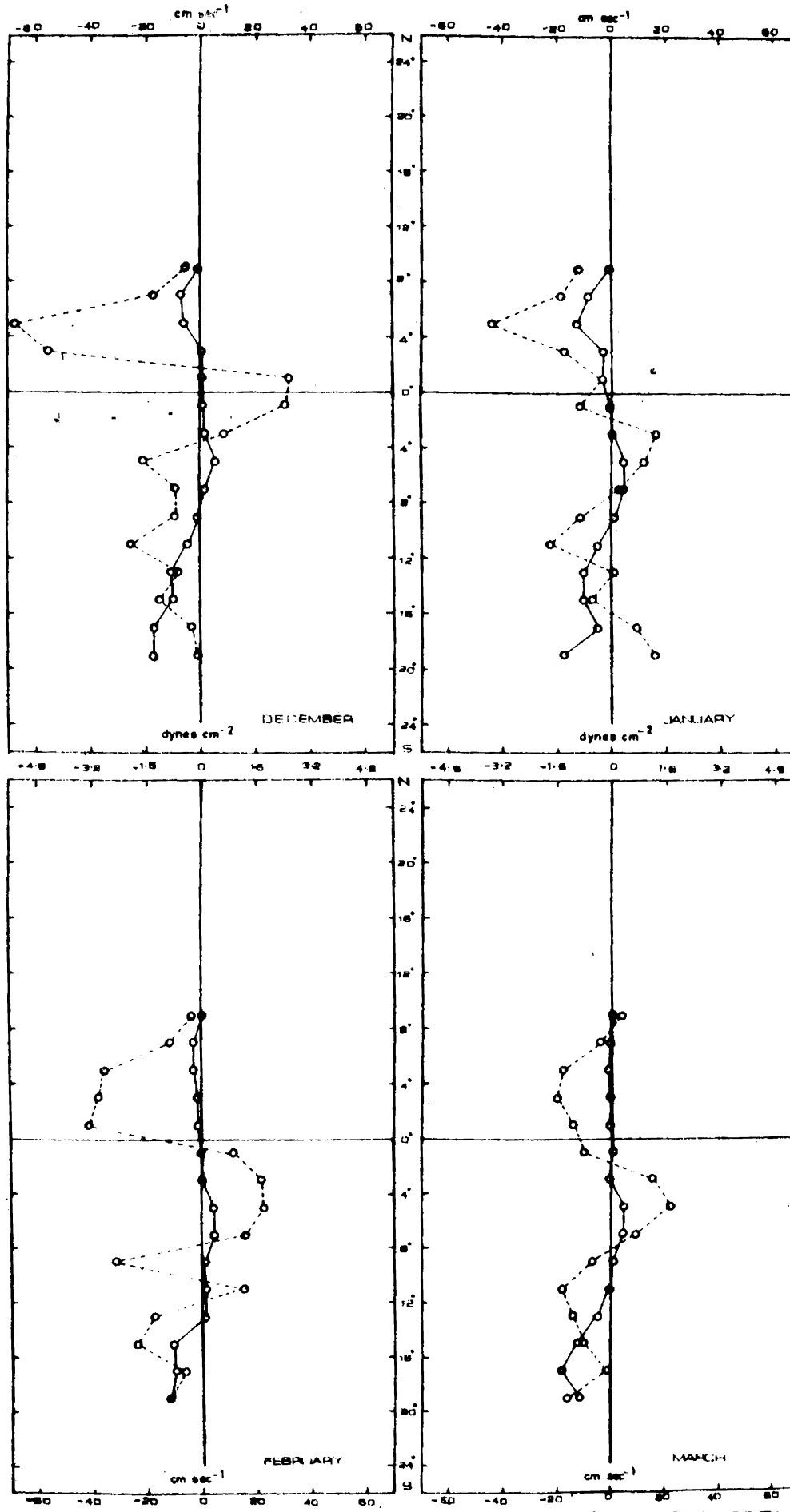

FIG: 41 ZONAL COMPONENTS OF THE WIND STRESS (—) AND CURRENT VELOCITY (---) ALONG 77° E

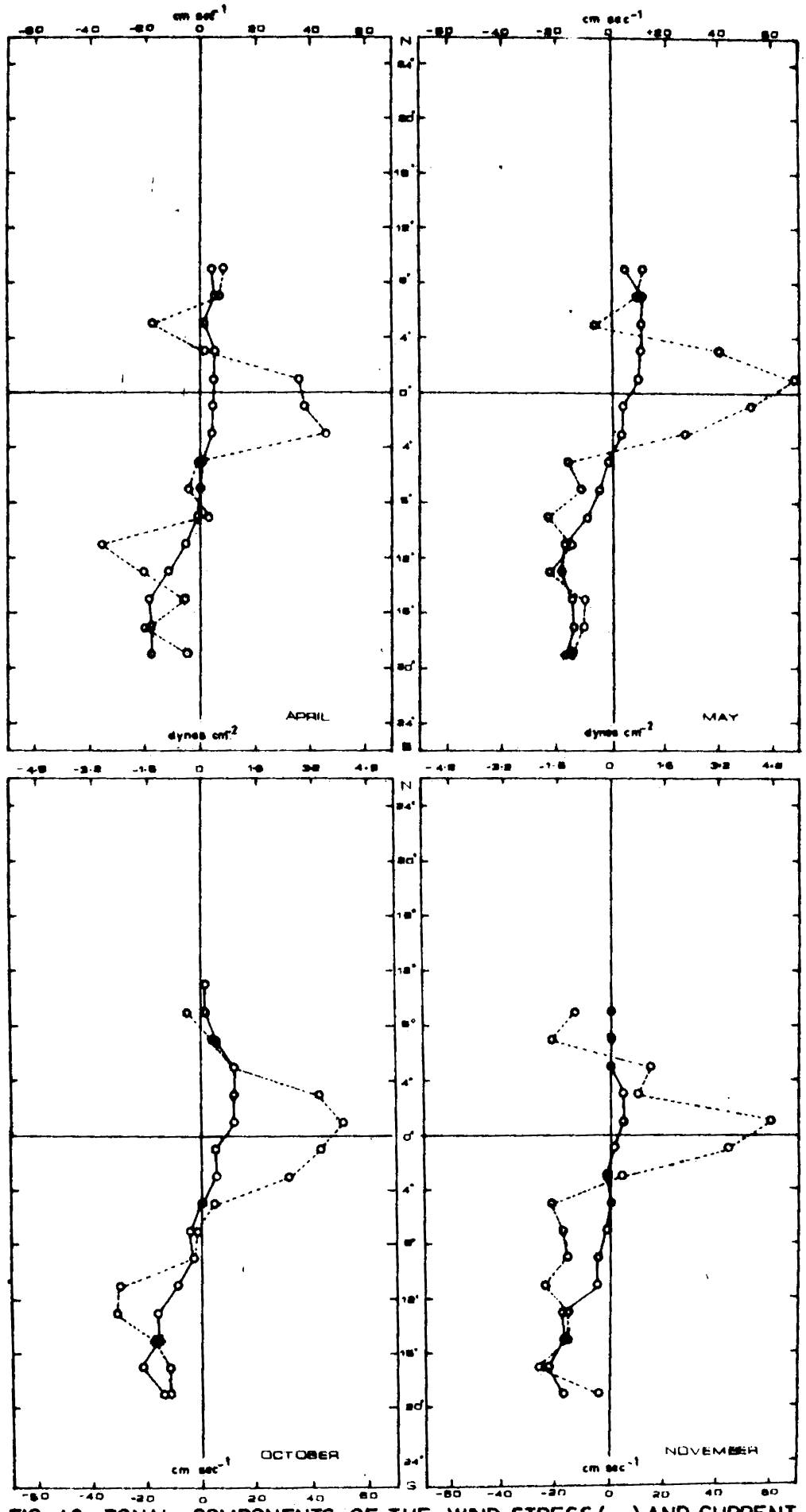

FIG: 42. ZONAL COMPONENTS OF THE WIND STRESS (—) AND CURRENT VELOCITY (---) ALONG 77° E

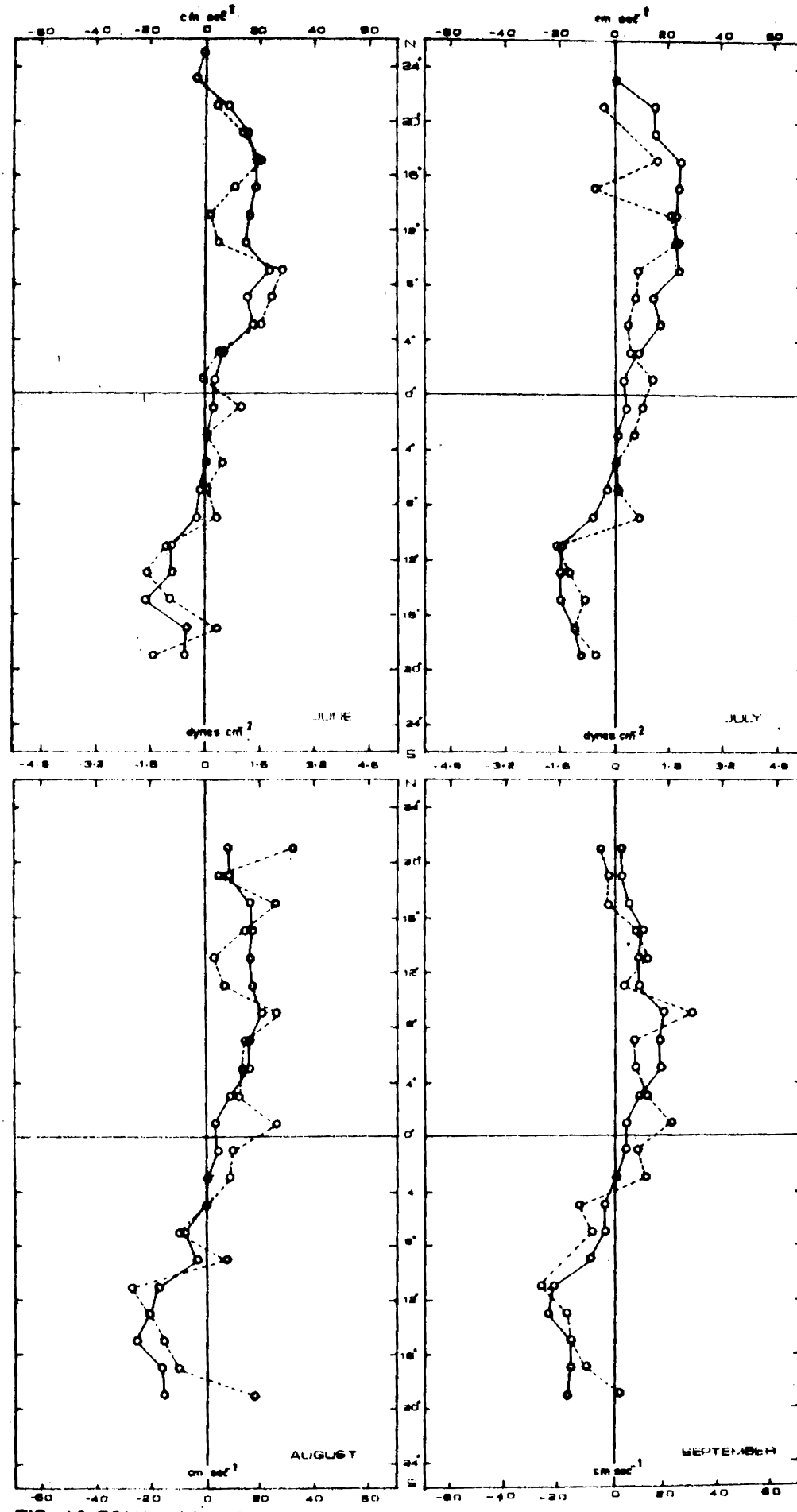

FIG: 43 ZONAL COMPONENTS OF THE WIND STRESS (—) AND CURRENT VELOCITY (---) ALONG 89°E

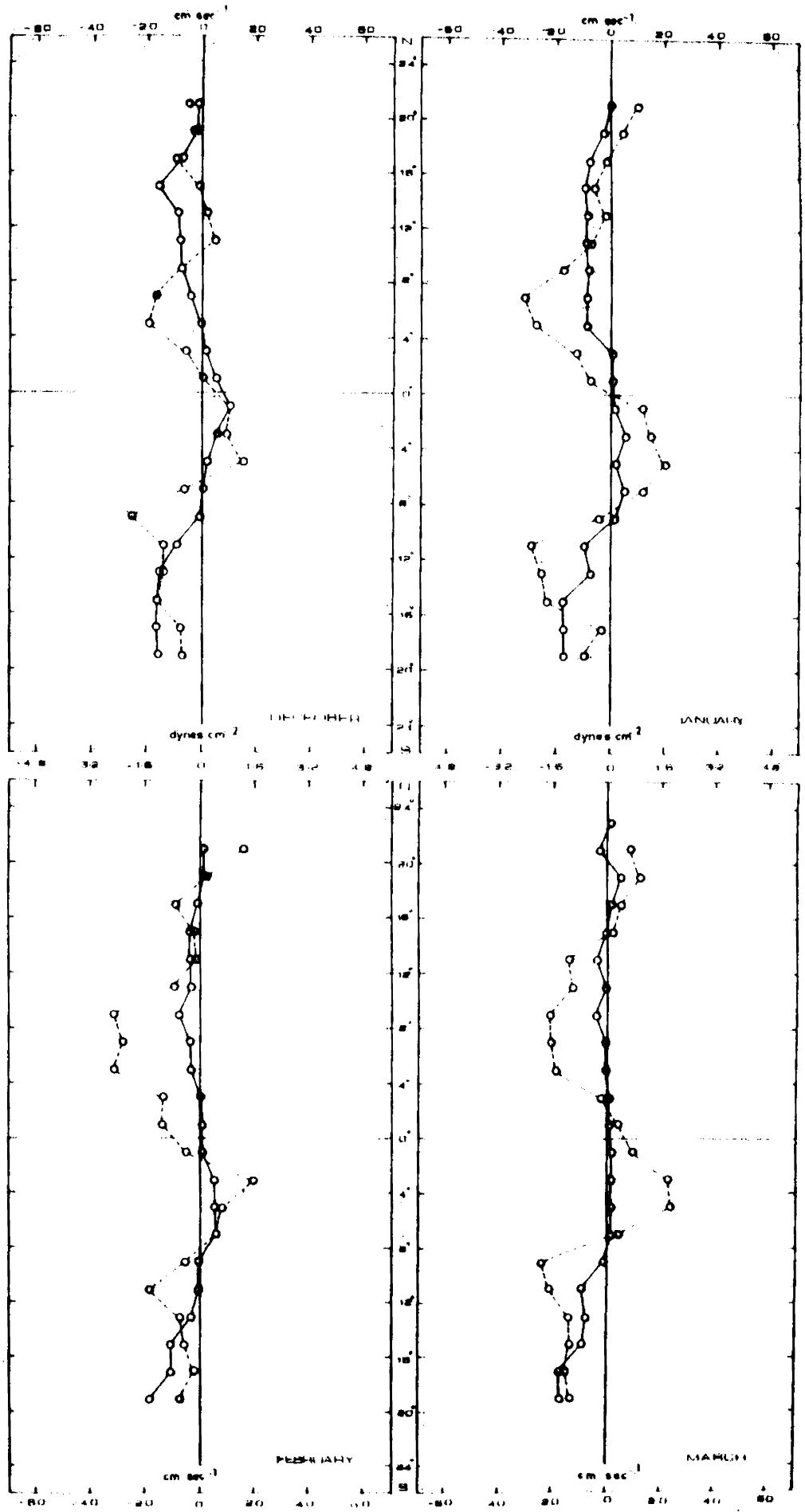

FIG. 44 ZONAL COMPONENTS OF THE WIND STRESS (—) AND CURRENT VELOCITY (---) ALONG 89° E

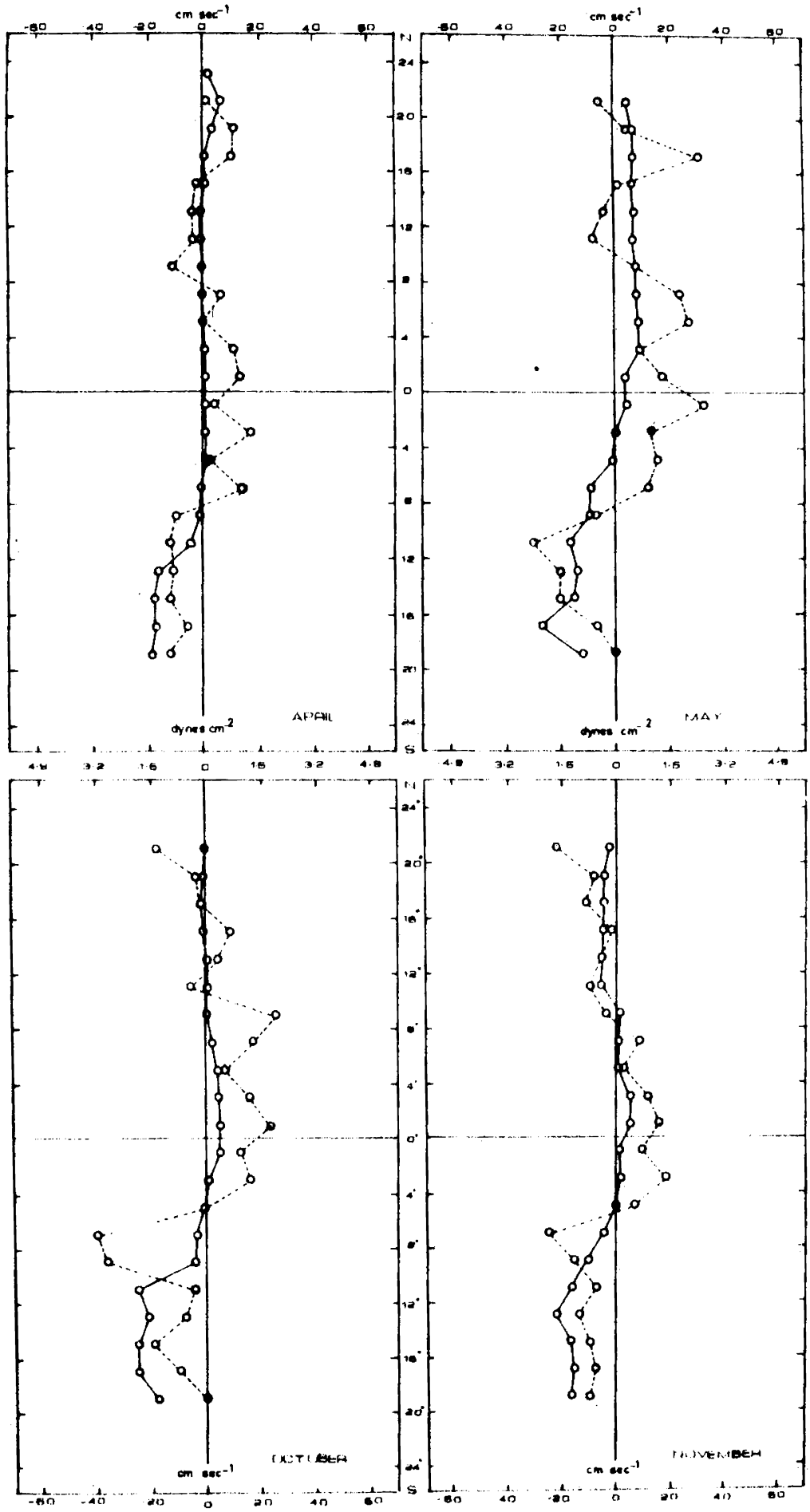

FIG. 45 ZONAL COMPONENTS OF THE WIND STRESS (—) AND CURRENT VELOCITY (---) ALONG 89° E

The zonal components of the wind stress and current velocity along 65°, 77° and 89°E are presented from fig. 37 to 45, which enables for a direct comparison of both the parameters. A good correlation between them are observed as the zones of easterly currents are found in the regions of eastward wind stress while the zones of westerly current are found in the regions of westward wind stress. The Equatorial Jet is present at 65°E and 77°E with maximum velocity in May and November. The Jet almost disappears as it reaches 89°E.

CHAPTER 5

5.1. SURFACE CIRCULATION OF THE INDIAN OCEAN IN RELATION TO THE WINDSTRESS AND ITS VORTICITY

The surface circulation of the oceans is mainly induced by the prevailing winds over the oceans. The strength of the ocean currents is closely related to the curl of the windstress as the mass transport is mainly controlled by the vorticity of the windstress. In the earlier chapters the surface circulation pattern, the distribution of the windstress and its vorticity are presented. In the present chapter it is attempted to correlate the surface circulation pattern with the distribution of the windstress and its vorticity. Ofcourse, it should be borne in mind that a comprehensive discussion in this regard is not possible because of certain discrepancies (Munk, 1950). Of the discrepancies, the undertainty in the drag coefficient, the inadequacy of wind data over the oceanic region and the contribution to the circulation due to thermohaline processes are some of the important ones. Nevertheless, it is always noticed that the circulation, being mainly driven by the winds, is closely associated with the windstress and its vorticity.

During the southwest monsoon the curl of the windstress in the northern hemisphere is positive off the

coasts of Somali and Arabia and east coast of India which is responsible for the northerly flow off these coasts. The negative values off the west coasts of India, Burma and Malayasia is responsible for the southerly flow. A close examination of the circulation pattern and curl of the windstress indicates a relationship of a cyclonic flow in the regions of positive curl and anticyclonic flow in the regions of negative curl. This peculiar feature is predominant not only during the southwest monsoon but throughout the year. In general, the curl of the windstress is relatively weak during the northeast monsoon and it is very well reflected in the weak circulation pattern.

During the southwest monsoon the strong meridional components of the windstress and the associated curl of the windstress off the Somali Coast cause an intense current with a northerly flow. The cell structure in the circulation pattern in August is obviously the consequence of isolated closed cells in the curl of the windstress distribution. Similar features are observed on the dynamic topography charts of Bruce (1973). Thus, it can be concluded that the cell structure is not only a synoptic phenomena but a permanent feature on the eastern side of the Somali Current. This can also be caused by current shear apart from the wind effect. The increase in the strength of the Somali

Current towards north is a result of the northward increase of the curl of the windstress off the Somali Coast.

A major part of the Somali Current region is covered by positive curl from April to October. When curl of the windstress is positive the circulation off the Somali Coast is northerly and it is southerly when curl of the windstress is negative. In general, it is noticed that the negative vorticity is relatively weak and this is very well reflected in the relatively weak southerly current off the Somali Coast during the northeast monsoon compared to that of the southwest monsoon. The variation of the curl of the windstress off the Somali Coast during the northeast monsoon is much less compared to that during the southwest monsoon. A similar observation is noticed in the strength of the current off the Somali Coast. The above observations are in confirmation with the theoretical study of Higgins (1965) which states that positive curl exists in regions of western boundary currents.

Intensity of the curl field is remarkably strengthened from May to July in the Arabian Sea. Such a remarkable increase in the intensity of the curl is not observed in the Bay of Bengal. The maximum strength of the currents in the Arabian Sea occurs when the intensity of the curl is maximum.

Since there is not any conspicuous variation of the curl in the Bay of Bengal, the average strength of the currents remains almost constant.

One of the most conspicuous features during the southwest monsoon is a major anticyclonic circulation comprising of the Monsoon Current, the South Equatorial Current and the Somali Current. This eddy circulation starts by April and its size increases through the succeeding months upto August and decreases by September due to the reversal of winds. The eddy circulation is most predominant in July and August when the intensity of the negative curl field is maximum. The intensity of the negative curl field increases from -2×10^{-8} dynes cm^{-3} in May to -8×10^{-8} dynes cm^{-3} in August and then it decreases to -4×10^{-8} dynes cm^{-3} in September. Thus, it is clear that the major anticyclonic circulation is a result of the anticyclonic vorticity of the surface winds.

The zone of negative curl reduces considerably during the northeast monsoon. Almost the entire northern part of the ocean exhibits a positive curl. The zone of negative curl lies approximately south of the equator, as a result, the major anticyclonic eddy of the southwest monsoon is replaced by a cyclonic eddy in the north and

another anticyclonic eddy in the south. The cyclonic eddy in the northern hemisphere comprises of the westward flowing North Equatorial Current, part of the eastward flowing Equatorial Countercurrent and the southerly flow along the Somali Coast. The anticyclonic eddy in the southern hemisphere consists of the South Equatorial Current and part of the Equatorial Countercurrent.

The meridional components of the windstress off the Somali Coast are changed from negative to positive value by April eventhough the zonal components still remain negative. The magnitude of both the components decrease from March to April. The decrease in the windstress results in a retarding force on the surface and causes the reversal of the current. Thus, it confirms that the Somali Current commences with the wind forcing (Leetma, 1972). In the northern hemisphere the highest values of the positive components of the windstress are observed in July in the western Arabian Sea off the northeast region of the Somali Coast. An examination of the circulation pattern indicates that the current strength is highest during July and August off the Somali Coast, thus, revealing a time lag of less than one month between the occurrence of the strongest wind and current.

Both zonal and meridional components of the windstress in the northern hemisphere, generally, change from

negative to positive sign during March-April, indicating the transition period between the northeast and southwest monsoons. Positive values of the windstress continue to prevail till August beyond which the transition from southwest to northeast monsoons takes place in September-October. Negative values are predominant during the period November to February indicating conditions of the northeast monsoon. Consistent with the wind distribution, the surface circulation is cyclonic in the Arabian Sea and Bay of Bengal during he northeast monsoon. During the spring transition, the surface circulation preceeds the reversal of the wind. This is mainly because of the gradient current that is developed initially off the southwest coast of India and due to weakening of the northeast monsoon. This is one of the instances where a deviation in the relationship between the distribution of winds and the circulation occurs due to thermohaline processes.

During the transition periods with a time lag of about one month strong easterly current called the Equatorial Jet (Wyrtki, 1973) is present. During this period the zonal components of windstress along the equator are positive and consistently high while the meridional components are inconsistent and relatively weak. Thus, it is obvious that the zonal windstress is the main driving force for the Equatorial Jet. With regard to the curl of the windstress,

it is not possible to correlate with the circulation along the equator as its sign changes on either side of the equator and there is no data plotted along the equator, but only along 2°N and 2°S. It is also interesting to note that the positive values of the zonal components of windstress during the transition period are highest along the equator, while higher values are observed in the eastern Arabian Sea during the southwest monsoon.

The meridional components of the windstress are positive in the entire Indian Ocean during the southwest monsoon except near the westcoast of India. But, during the northeast monsoon, the northward windstress is mostly confined south of 8°S Easterly Currents predominate in the regions of northward windstress north of the equator and westerly currents in the regions of northward windstress, south of the equator.

The isolines of the windstress and its vorticity in the southern hemisphere are mostly oriented parallel to the latitudes giving rise to zonal flow. The isolated closed isotachs are obviously the result of the closed cells of windstress as well as its vorticity in the region, south of the equator. There is not much variation of the magnitude of the windstress and its vorticity, south of 8°S which indicates that the South Equatorial Current is a steady flowing current compared to other currents in the Indian Ocean.

5.2. COMPARISON OF THE RESULTS OF WINDSTRESS AND ITS CURL WITH EARLIER WORKS

The main features of the global surface vorticity are anticyclonic vorticity in the middle and subtropical latitudes and cyclonic vorticity in the tropics (Mintz and Dean, 1952). The present study clearly reveals an exception to this general pattern in the Indian Ocean. The vorticity in the Indian Ocean during summer shows considerable variations from the normal pattern. Areas of anticyclonic vorticity cover almost the entire Indian Ocean during the southwest monsoon. These observations demonstrate that the Indian Ocean displays an impressive anomaly of the vorticity distribution and has stronger seasonal changes than any other area of the world ocean.

Hidaka (1958) tabulated the components of the mean windstress for four seasons and their annual mean using 5° latitude-longitude quadrangle. Although, the order of magnitude of his computations agree with the present as 10^{-1} dynes cm^{-2}, their absolute values are relatively higher in the present investigation, mainly because of a smaller grid used. The annual mean of the windstress is not tabulated in the present study as it will not be representative because of the temporal variations of the windstress in the Indian Ocean.

Stommel (1965) computed the annual mean of the curl of the windstress components from Hidaka (1958) for the whole world oceans. Because of the large scale representation, both in space and time, made by him, it would not be possible to compare his results with the present, in the northern hemisphere. According to him, south of 30°S the Indian Ocean experiences the maximum curl of the windstress of about $+15 \times 10^{-9}$ gm sec^{-2} whereas the North Pacific records about $+10 \times 10^{-9}$ gm sec^{-2}. Stommel's study reveals that negative curl prevails in the Indian Ocean north of 10°S.

The order of magnitude of the curl of the windstress obtained in the present investigation (10^{-8} dynes cm^{-3}) agrees with that of Mintz and Dean (1952), Holopainen (1967), Evenson and Veronis (1975) and Sastry and Ramesh Babu (1979). The distribution of the windstress in the present study is consistent with the findings of Hellerman (1967). The slight discrepancies may be due to the differences in the grid size and drag coefficient. Hellerman adopts a C_D value with a 40 percent jump at Beaufort 4 and takes into account the latitudinal variations of air density as he did compute for the whole world oceans where the variations of wind strength and the density of the air are relatively high. For the present study, a constant drag coefficient and air density are used. The curl of the windstress in the present

investigation records higher values than those of Hellerman.

The pattern and intensity of the vorticity are almost similar to that of Hantel (1970) except the maximum values.

In the North Atlantic and Pacific, the windstress is higher during winter and lower during spring and summer (Evenson and Veronis, 1975). On the other hand, in the Indian Ocean greater stresses are noticed during the northern hemisphere summer.

5.3. ANOMALOUS FEATURES IN THE SURFACE CIRCULATION OF THE INDIAN OCEAN

The South Equatorial Current is a permanent feature in the Indian Ocean as that of the other major oceans. This is mainly because the atmospheric circulation south of the equator comprises the southeasterly trades which drive the South Equatorial Current throughout the year. But in the northern region the northeasterly trades which drive the North Equatorial Current are present only during a part of the year. During the northern hemisphere summer, the northeasterly trades are replaced by the southwesterlies which drive the Southwest Monsoon Current. Since the Southwest Monsoon Current flows in the same direction as that of the Equatorial Countercurrent, the former merges with the

latter. The equatorial current system has a latitudinal shift. The South Equatorial Current shifts from 8°S in May to 12°S in June and 14°S in July and August, while it moves to the northernmost boundary during northern hemisphere winter. The strength of the South Equatorial Current reaches the maximum during the southwest monsoon. As the South Equatorial Current reaches the northeastern part of Malagasy, the current is further strengthened due to convergence and the boundary effects, reaching the highest values of this current.

The North Equatorial Current is present only from December to March with maximum strength in January. During this period because of the shear developed between the trades which drive the South Equatorial Current and North Equatorial Current respectively, an Equatorial Countercurrent which flows to the east is formed.

The most conspicuous feature that is unknown in any part of the world oceans is the Equatorial Jet which is for the first time pointed out by Wyrtki (1973). This Jet is noticed during the months of April-May and October-November. During the periods of occurrence, the strength of the current increases from April to May and October to November. The Equatorial Jet flows to east along the equator between 2°N and 2°S from 65°E to 90°E. Out of the four months November

records the maximum speed of the Jet.

Another important anomalous feature of the surface circulation in the North Indian Ocean is that when the atmospheric circulation is almost similar to that over the Pacific and Atlantic the northward flowing western boundary current is absent. In the Atlantic and Pacific the western boundary currents in both the hemispheres are fed by the corresponding equatorial currents. In other words, the North Equatorial Current feeds the northward flowing boundary currents in the northern hemisphere and the South Equatorial Current feeds the southward flowing boundary currents in the southern hemisphere.

The northward flowing western boundary current in the Indian Ocean appears to be absent during the northeast monsoon because of the continental boundary on its northern side. In the Indian Ocean the northward flowing western boundary current, namely, the Somali Current is present only during the southwest monsoon when the wind distribution over the North Indian Ocean is dissimilar to that of the other major oceans. It is fed by the South Equatorial Current. It is also noted that the Somali Current is the strongest (350 cm sec^{-1}) ever observed in any part of the world oceans (Swallow and Bruce, 1966).

There is an evidence of eastern boundary current in the Indian Ocean along the west coast of Sumatra between

2°N and 6°S. The streamlines turn to south at about 2°N near Sumatra Coast by April itself. This pattern becomes more conspicuous during the succeeding months, especially, in June and July and slowly dissipates by the end of November. The width of this current is greater and its strength is considerably lower compared to that of the Somali Current.

According to Wooster and Reid (1963), the eastern boundary currents are slow, broad and shallow with relatively small transport of water. It is evident from the streamline pattern and isotachs that the southward flowing current along the Sumatra Coast fully satisfies these characteristics.

Since this eastern boundary current is found near Sumatra, it can be called the Sumatra Current. It is formed when the eastward current is blocked by the landmass of Sumatra. All the other eastern boundary currents are also formed when the eastward flowing currents are blocked by the continents. For example, the California Current in the Atlantic Ocean is formed when the West Wind Drift is blocked completely by the continent (Wooster and Reid, 1963). In the South Pacific and South Atlantic the continents extend far south to interupt at least a part of the flow of the West Wind Drift which turns north as Peru and Benguela Currents respectively. In the North Atlantic, the principal eastern boundary current is the Canary Current which flows along the northwest coast of Africa.

The GEK measurements indicate that the average speed of the eastern boundary current is about 25 cm sec^{-1} or less in contrast to the extreme speeds of more than 200 cm sec^{-1} in the western boundary currents (Stommel, 1958). The present investigation indicates that the speed of the Sumatra Current is lower than that of the eastern boundary currents in the other oceans.

The Sumatra Current is very weak in April, October and November. Its presence during these months can be attributed to the occurrence of the strong eastward flowing Equatorial Jet instead of the Monsoon Current. The turning of the Monsoon Current in the eastern region of the Indian Ocean is evident from the streamline charts of Sharma (1971), and Varadachari and Sharma (1967).

During the northeast monsoon the streamlines in the southeastern region of the present study run in a north-south direction. Such a well oriented pattern is not observed during the southwest monsoon which clearly reveals that the West Australian Current is weak during the southern hemisphere winter. According to Wyrtki (1961), the West Australian Current is a steady and strong current in the southern hemisphere summer, reaching the maximum velocity of 0.4–0.7 knot north of $3^{\circ}S$. During the southern hemisphere winter the currents are weakened and are seperated by several branches of the southward current.

CHAPTER 6

SUMMARY AND CONCLUSION

The present thesis is an attempt of the author to investigate the surface circulation of the Indian Ocean, north of 20°S in relation to the atmospheric circulation over the ocean. The aim is achieved by working out the circulation pattern and correlating it with the computed wind stress and its vorticity.

The monthwise surface circulation is arrived by drawing the streamlines, using freehand method with superimposed isotachs. The zonal and meridional components of the windstress and the curl of the windstress are computed for each month over 2° latitude-longitude quadrangle from the bulk aerodynamic formula, using a computer programme. The data for drawing the surface circulation and for computing the windstress and its curl have come from the Dutch Atlas (K.N.M.I.Publ.No.135,1952).

From the distribution of the zonal and meridional components of the windstress, it is clear that the southwest monsoon dominates in the North Indian Ocean from May to August and the northeast monsoon prevails from November to February. March-April and September-October represent the transition periods. Further, it should be emphasised that

the duration of any one of the monsoons is not constant throughout the area under study but it varies from place to place. In fact, while the southwest monsoon is dominant in the Arabian Sea, the northeast monsoon plays a major role in the Bay of Bengal. In the equatorial region the variation of the windstress is more frequent than semi-annual. Thus the transition periods also vary from region to region. South of $10^{\circ}S$ there appears to have been no seasonal variation.

During southwest monsoon, in the Arabian Sea, higher values of eastward windstress is prominent in July while lower values are observed in May and September. The meridional components are strong off the Somali Coast. In general, the positive windstress predominates in the entire region under study during the southwest monsoon. During the northeast monsoon a prominent belt of positive zonal windstress in the equatorial region is sandwiched by two belts of westward windstress in the north and south of it. Off the Somali Coast negative zonal windstress is noticed throughout the season with higher values in January, whereas negative meridional windstress is prominent in December and January only. In general, the components of the windstress are considerably higher during the southwest monsoon than the northeast monsoon in the region of the monsoon influence. The reversal of the southwest monsoon starts earlier in the north while that of the northeast monsoon starts earlier from the south.

During the transition periods the zonal components are positive and strongest at the equator and the meridional components are either nonexistent or weak, except in the western region.

Generally, the curl of the windstress has opposite sign off the east and west coasts in the North Indian Ocean. Off the east coast of Africa and India, during the southwest monsoon, the vorticity is positive while it is negative during the northeast monsoon. The highest value of the curl of the windstress is observed in July in the Arabian Sea. The North Indian Ocean exhibits the most spatial and time variation of the curl of the windstress. In the southern hemisphere the negative curl of the windstress is predominent during the whole year. The Indian Ocean records greater curl of the windstress during the northern summer whereas the North Atlantic and Pacific Oceans record higher values in winter.

The surface circulation, south of the equator, does not vary much and it is conspicuously covered by the westward flowing South Equatorial Current. North of the South Equatorial Current is the eastward flowing Equatorial Countercurrent which has a meridional shift with season. It has its southernmost extent during the southwest monsoon and this in turn pushes the South Equatorial Current southward. The circulation in the northern region changes semiannually

while that along the equator changes four times in an year. The North Equatorial Current is present only during the northeast monsoon and it is replaced by the eastward flowing Southwest Monsoon Current. Therefore, during the southwest monsoon the Equatorial Counter Current and the Southwest Monsoon Current flow as a single eastward current. In the region bordering the continent the circulation is clockwise during the southwest monsoon and anticlockwise during the northeast monsoon. The reversal of the current along the boundaries preceeds the wind reversal during the spring transition. The conventionally persistent western boundary current of the northern hemisphere is absent in the Indian Ocean during the northeast monsoon but it is present as the strongest current ever observed in any part of the world oceans as the Somali Current during the Southwest monsoon. The most interesting feature along the equator in the central Indian Ocean is the presence of the strong eastward flow called the Equatorial Jet, during April-May and October-November. The present investigation shows an evidence of the presence of an eastern boundary current in the Indian Ocean from April to November along the west coast of Sumatra between 2°N and 6°S.

The South Equatorial Current which flows westward throughout the year is essentially driven by the southeasterly trades and its seasonal meridional shift is closely associated

with the variation in the strength of the southerly trades of the southern hemisphere. This is obvious from the distribution of the components of windstress and the curl of the windstress. South of the equator there is not much variation in the direction of the wind but only the magnitude.

Along the equator, the variation of the wind is not merely semiannual but varies four times. Such a variation results in the presence of the Equatorial Jet along the equator when the zonal components of the windstress is maximum in the central region. From a close examination of the occurrence of the maximum strength of the wind and that of the maximum current it can be concluded that the time response of the surface water to the wind is about one month in the North Indian Ocean.

The North Equatorial Current which is driven by the northerly trades is present in the Indian Ocean only during part of the year. With the reversal of the northeasterly trades to southwesterlies, the North Equatorial Current is replaced by the Southwest Monsoon Current that is driven by the southwesterlies towards east. During this period, the Equatorial Countercurrent and the South West Monsoon Current flow as a combined one without a conspicuous boundary between them. Besides the southwesterly winds the shear of the South Equatorial Current also acts as a driving force for the combined current.

The positive curl of the windstress and the positive windstress components are responsible for the western boundary current in the Indian Ocean namely the Somali Current during the southwest monsoon. During the northeast monsoon, the curl of the windstress is negative off the Somali Coast. A negative curl in the northern hemisphere with a continental boundary on one side gives rise to a southerly flow. That is why the conventional western boundary current is absent in the North Indian Ocean, although the atmospheric circulation over the North Indian Ocean is almost similar to that over the other major oceans. Because of the boundaries, the surface circulation in the Arabian Sea and Bay of Bengal is clockwise and counterclockwise during the southwest and northeast monsoons respectively. The surface circulation in the northern region of the North Indian Ocean, sometimes indicates the reversal of the currents ahead of the wind reversal, thus, indicating the influence of thermohaline circulation which is controlled by other factors of the energy exchange between the atmosphere and ocean.

Most of the monsoon depressions originate in the Bay of Bengal and Arabian Sea in the low latitudes. These cyclones cause a lot of energy exchange between the sea and atmosphere. This exchange drastically changes the thermohaline effects over the surface circulation. In order to have a

a complete understanding of the surface and subsurface circulations, it would be necessary to work out the energy exchange in the Arabian Sea and Bay of Bengal.

The success of the numerical models to simulate the oceanic circulation depends on the feed back of the physics fed to the model. Unlike in the other major oceans, the time response of the ocean to the winds is an important factor to be considered in the North Indian Ocean where the winds vary semiannually. From the present investigation it is found that the time of response of the ocean to the wind should not be more than one month. While considering the numerical model of the Equatorial Indian Ocean the frequent variation of the wind particularly the zonal components should be considered instead of the semiannual variation.

REFERENCES

Aleem, A.A. (1967). Concepts of currents, tides and winds among medieval Arab geographers in the Indian Ocean. Deep Sea Res., 14, 459–464.

Anderson, D.L.T. and P.B. Rowlands (1976). The Somali response to the southwest monsoon; the relative importance of local and remote forcing. J. Mar. Res., 34, 395–417.

Anderson, D.L.T. and D.W. Moore (1979). Cross-equatorial inertial jets with special relevance to very remote forcing of the Somali Current. Deep Sea Res., 26A, 1–22.

Badgley, F.I., Paulson, C.A. and M. Miyake (1972). Profiles of wind, temperature and humidity over the Arabian Sea. Inter. Indian Ocean Exped. Meteor. Monogr. No.6. East West Center Press, Honolulu 84 pp.

Barlow, E.W (1934). Current of the Arabian Sea and Bay of Bengal. Marine Observer, 11, 19–22.

Barlow, E.W (1935). The 1910–1935 survey of the currents of the Indian Ocean and China Seas. Marine Observer, 12, 153–163.

Basil Mathew, R.N.Nair and G.S.Sharma (1982). The Tropical Countercurrent in the Indian Ocean. Indian J. Mar. Sci., 11, 208–211.

Belyae, V.S (1967). The dependence of the spectra of the velocity components of a wind-driven current on the spectrum of the tangential wind force Izv. Atmos. and Oceaneo Phys. 3, 1217–1226.

Bishop, J.M. (1979). A note on surface wind-driven flow. Ocean Eng., 6, 273-284.

Bishop, J.M (1980). A note on the seasonal transport on the middle Atlantic shelf. J. Geophys. Res., 85, 4933-4936.

*Bolizon, E (1922). Vergleichende Betrachtung des Klimas undderkatton Auftriebestromungen an der sudwesta-frilkanishen and suddarabishchen Kuste. Dstsch. Ubers. Mikbeole Hft., 23, 1-18.

Brocks, K and L. Kugermeyer (1972). The hydrodynamic roughness of the sea surface. In Studies Phys. Oceanogr., Ed.A.L.Gordon, 75-92.

Brown, O.B., Bruce, J.G. and R.H. Evans (1980). Evolution of sea surface temperature in the Somali basin during the south west monsoon of 1979. Science, 209, 595-592.

Bruce, J.G (1969). A further estimate of maximum transport of the Somali Current. Deep Sea Res., 16, 227-228.

Bruce, J.G. and G.H.Voskmann (1969). Some measurements off the Somali Coast during the northeast monsoon. J. Geophys. Res., 74, 1958-1967.

Bruce, J.G (1973). Large scale variations of the Somali Current during the southwest monsoon. Deep Sea Res., 20, 837-846.

Bryan, K (1963). A numerical investigation of a nonlinear model of a wind-driven Ocean. J. Atmospheric Sci., 20, 594-606.

Bryan, K (1969). A numerical model of the study of the circulation of the world oceans. J. Computat. Physics, 4, 347-376.

Bryan, K and Cox M.D (1967). A numerical investigation of the oceanic general circulation. Tellus, 19, 54-80.

Bryan, K and Cox M.D (1968). A non-linear model of an ocean driven by wind and differential heating. J. Atmos.Sci., 25, 945-967, 968-978.

Bunker, A.F (1976). Computations of surface energy flux and annual air-sea interaction cycles of the North Atlantic Ocean. Mon. Wea. Rev., 104, 1122-1139.

Burt, W.V., Cummings, T and C.A. Paulson (1974). The mesoscale wind field over an ocean. J. Geophys. Res., 79, 5625-5632.

Busalacchi, A.J and J.J.O'Brien (1980). The seasonal variability in a model of the tropical Pacific., J. Phys. Oceanogr., 10, 1929-1951.

Bye, J.A., Noyc, B.J and Sag (1975). A monthly analysis of global wind stress and the ocean transports predicted from a numerical model. Quart. J.R.Met. Soc., 101, 749-762.

Cane, M.A and E.S.Sarachek (1976). Forced Baroclinic ocean motions: I The linear equatorial unbounded case. J. Mar. Res., 34, 629-665.

Cane, M.A (1979a). The response of an equatorial ocean to simple windstress patterns: I Model formulation and analytic results. J. Mar. Res., 37, 233-252.

Cane, M.A (1980). On the dynamics of the equatorial currents with application to the Indian Ocean. Deep Sea Res., 27A, 525-544.

Cane, M.A (1979b). The response of an equatorial ocean to simple windstress patterns: II Numerical results, J. Mar. Res., 37, 253-299.

Cane, M.A and E.S.Sarachek (1976). Forced baroclinic ocean motions: I The linear equatorial unbounded case. J. Mar. Res., 34, 629-668.

Carrier and A.R.Robinson (1962). On the theory of the wind-driven ocean circulation. J. Fluid Mech., 12, 49-80.

Charney, J.G (1955). The generation of oceanic currents by wind. J. Mar. Res., 14, 477-498.

Charney, J.G (1960). Non-linear theory of a wind-driven homogeneous layer near the equator. Deep-Sea Res., 6, 303-310.

Charney, J.G and S.Spiegal (1971). Structure of wind-driven equatorial currents in homogeneous oceans. J. Phys. Oceanogr., 1, 149-160.

Clowes, A.J. G.E.R.Deacon (1935). The Deepwater circulation of the Indian Ocean. Nature, 136, 936-938.

Colon, J.A (1964). On interactions between the southwest monsoon current and sea surface over the Arabian Sea. Indian J. Met. Geophys., 15, 185-200.

Cox, M.D (1970). A mathematical model of the Indian Ocean. Deep-Sea Res., 17, 47-75.

Creigan, A and J.A. Johnson (1978). An advective mixed layer model with imposed surface heating and windstress. Deep-Sea Res., 26A, 357-368.

Crutcher, H.L (1959). Upper wind statistics charts of the northern hemisphere NAVER 50-2C-535, Vol.1, U.S. Office of Naval Operations, Washington D.C. 33 pp.

Darbyshire, J (1963). Computered currents off the Cape of Good Hope. Deep-Sea Res., 10, 623-632.

Darbyshire, J (1964). A hydrographical investigations of the Agullas Current area. Deep-Sea Res., 11, 781-815.

*Defant, A (1926). Die Austauschgrosse der atmospharischen und ozeanischen zirkulation. Ann. Hydrograph. Maritime Meteorol, 54, 12.

*Defant, A (1952). Theoretische uberlegungen zum phanomen des wind staus und des Auftriebs an ozeanischen Kusten Dtsch. Hydrogr. Z.5/2-3, 69-80.

Denman, K.L and M.Miyake (1973). Upper layer modifications at ocean station. J. Phys. Oceanogr., 3, 185-196.

de Zzocke, R.A (1980). On the effects of horizontal variability of windstress on the dynamics of the ocean mixed layer, J. Phys. Oceanogr., 10, 1439-1454.

Dongay, J.R and C.Henin (1980). Surface conditions in the eastern equatorial Pacific related to the ITCZ of the winds. Deep-Sea Res., 27, 693-714.

Duing, W (1970). The monsoon regime of the currents in the Indian Ocean East-West Center Press, Honolulu.

Duing, W and K.H.Szhielda (1971). Monsoonal response in the western Indian Ocean. J. Geophys. Res., 76, 4181-4187.

Duing, W., Molinari, R and J.C.Swallow (1980). Somali Current: Evolution of surface flow. Science, 209, 588-590.

Duncon, C.P (1970). The Agulhas Current Ph.D. dissertation. University of Hawai, 76 pp.

Duncon, C.P (1976). Comment on high waves in the Agulhas Current by E.H.Schumann, Marine Wea. Log. 20, 3-5.

Durst, C.S (1924). The relationship between current and wind. Quart. J. Roy. Met. Soc., 50, 113.

Dutches Hydrographisches Institut (1960). Monatskarten fur Indischen Ozean. Publ. No.2422, Hamberg.

Ekman, V.W (1905). On the influence of the earth's rotation on ocean currents, Ark. Math. Astron. Fysik., 2, 1-53.

Ekman, V.W (1923). Uber horizontal zirkulation bei winderzeegten meeresstromungen. Ark. Math. Astron. Fysik., 17, 1-74.

Erikson, C (1979). An equatorial transect of the Indian Ocean. J. Mar. Res., 37(2).

Evenson, A.J. and G. Veronis (1975). Continuous representation of windstress and windstress curl over the world ocean. J. Mar. Res., 33, 131-144.

Findlater, J (1969). A major low-level air current near the Indian Ocean during the northern summer. Quart. J. Roy. Met. Soc., 95,362-380.

Findlater, J (1974). The low-level cross equatorial air current of the western Indian Ocean during the northern summer. Weather, 29, 411-416.

Fofnoff, N.P (1954). Steady flow in frictionless homogeneous ocean. J. Mar. Res., 13, 254-262.

Fofnoff, N.P. and R.B.Montgomery (1956). Equatorial Undercurrent in the light of the vorticity equation. Tellus, 7, 518-521.

Francis, J.R.O (1954). Windstress on a water surface, Q.J.R. Met. Soc., 80, 438-443.

Furnes, G.K (1980). Wind effects in the North Sea. J. Phys. Oceanogr. 10, 978-984.

*Galle, P.H (1924). Klimatdogie van den Indischen Ocean. K. Ned. Met. Inst. Mededeelingen en verhandlingen ser. A, 29a, 87 pp.

*Galle, P.H (1928). Klimatdogie van den Indischen Ocean. K. Ned. Met. Inst. Mededeelingen en verhandlingen ser. A, 29b, 38 pp.

*Galle, P.H (1930). Klimatdogie van den Indischen Ocean. K. Ned. Met. Inst. Mededeelingen en verhandlingen ser. A, 29c, 31 pp.

Gates, W.L (1968). A numerical study of transient Rossby waves in a wind-driven homogeneous ocean. J. Atmos. Sci., 25, 3-12.

Ghosh, S.K., Pant, M.C and B.N. Dewan (1978). Influence of the Arabian Sea on the Indian summer monsoon. Tellus, 30, 117-125.

Gill, A.E (1975). Models of equatorial currents in Proceedings of the symposium of Numerical Models of Ocean Circulation, Washington. National Academy of Science, 364 pp.

Goldbrough, G. R (1933). Ocean Currents produced by evaporation and precipitation. Proc. Roy. Soc. (London), Ser. A., 141, 512-517.

Gorden, A.H., Martinson, D.G and H.W. Taylor (1981). The wind driven circulation in the Weddell-Enderby basin. Deep-Sea Res., 28, 151-163.

*Hantel, M (1969). A numerical investigation of the linear primitive equations applied to the wind-driven circulation of the northwestern Indian Ocean between 16°N-16°S. Annalen da Meteorologic (New Folge) 4, 73-76.

Hantel, M (1970). Monthly charts of surface windstress curl over the Indian Ocean. Mon. Wea. Rev., 98, 765-773.

Hantel, M (1971). Surface wind vergence over the tropical Indian Ocean. J. Appl. Met., 17, 875-881.

Hantel, M (1972). Windstress curl-the forcing function for oceanic motion, in Studies in Physical Oceanography - A Tribute to Georg Wüst on his 80th Birthday. Ed.A.L. Gordon. Gordon and Breach, Science Publishers, New York and London, 1, 121-136.

Harries, T.F.W (1972). Sources of the Agulhas Current in the spring of 1964. Deep-Sea Res., 19, 633-650.

*Hasse, L (1968). Zur Bestimmung der vertikalen transporte von impuls and fuhlbarer warme in der wasernachen Cuftschichet auf see. Hamburger Geophysikalische Einzelschriffen 11, 70 pp.

Hasson, E.M (1968). On the wind driven ocean circulation. Deep-Sea Res., 5, 36-43.

Hellerman, S (1967). An updated estimate of the windstress on the world ocean. Mon. Wea. Rev., 95, 607-626.

Hellerman, S (1968). An updated estimate of the windstress on the world ocean. Correction Notice. Mon. Wea. Rev., 96, 63-74.

Hellerman, S (1978/80). Charts of the variability of the windstress over the tropical Atlantic. Deep-Sea Res., 26A (supply 2), 63-75.

Hidaka, K (1949). Mass transport in ocean currents and lateral mixing. J. Mar. Res., 8, 132-136.

Hidaka, K (1954). Zonal ocean currents driven by winds. Assn. of Phy. Ocn. Rome. Sept. 14-25, Proces-Verbaum Bergan, 253 pp.

Hidaka, K (1955). A theoretical study on the general circulation of the Pacific Ocean. Pacific Sci., 9, 183-220.

Hidaka, K (1958). Computation of the windstress over the oceans. Rec. Oceanogr. Works. Japan, 4, 77-123.

Higgins, M.S.L (1965). Some dynamical aspects of Ocean currents. Quart. J. Roy. Soc., 91, 390.

Hough, S.S (1897). On the application of harmonic analysis to the dynamical theory of the tides. Part I. On Laplace Oscillations of the first species and on the dynamics of Ocean currents. Phil. Trans.(A) 189, 201-258.

Holopainen, E.O (1967). Determination of the wind-driven ocean circulation from the vorticity budget of the atmosphere. Pure and Applied Geophysics, 67, 156-165.

Hughes, R.L (1980). On the equatorial mixed layer. Deep-Sea Res., 27, 1067-1078.

Hurlburt, H.E and J.D. Thomson (1976). A numerical model of the Somali Current. J. Phys. Oceanogr. 6, 646-664.

*Ilyin, A.N and V.M.Kamenkowich (1963). On the influence of friction on Ocean Currents. Dokl. Akad. Nauk. SSSR, 150, 1274-1277.

Johnson, J.A (1979). A wind driven zonal channel with stratification and bottom topography. Atmos. Oceans. 4, 1-13.

Koninklijk Nederlands Meteorologisch Institut (1952). Indian Ocean, Oceanographic and Meteorological Data. Publication No.135, 2nd edition, 2 vols., 24 sheets.

Krauss, E.B (1968). What we do not know about the sea surface windstress. Bull. Amer. Met. Soc., 49, 247-253.

→ *

Knox, R.A (1976). On a long series of measurements of Indian Ocean equatorial currents near Adu. Atoll. Deep-Sea Res., 23, 211-221.

LaFond, E.C (1958). Seasonal cycle of sea surface temperature and salinity along the east coast of India. Andhra Univ. Mem. Oceanogr., 2, 12-21.

Leetma, A (1972). The response of the Somali Current to the southwest monsoon of 1970. Deep-Sea Res., 19, 319-325.

Leetma, A and A.F. Bunker (1979). Updated charts of the mean annual windstress convergences in the Ekman layers. J. Mar. Res., 36(2).

Leetma, A and H.Stommel (1980). Equatorial Current Observations in the western Indian Ocean. J. Phys. Oceanogr., 10, 258.

Lighthill, M.J (1969). Dynamic response of the Indian Ocean to onset of the southwest monsoon. Phil. Trans. of Royal Soc. of London, 265, 45-92.

Lineiken, P.S (1955a). Wind driven currents in the baroclinic layer of the sea. Tr.Gos. Okeanogr. Inst., 29(41).

Lutjeharms, J.R.E. (1976). The Agulhas Current system during northeast monsoon. J. Phys. Oceanogr., 6, 665-670.

Luyten J.R and M.F.J Gonilla (1980). Equatorial Currents in the western Indian Ocean. Science, 209, 600-602.

Masahero, E (1980). The study of ocean circulation dynamics with numerical models. J. Oceanogr. Soc. Japan, 36, 134-140.

McCreary, J.P (1981). A linear stratified ocean model of the Equatorial Undercurrent. Phil. Trans. R. Soc., 298(A), 603-635.

Meku, W.D (1973). The wind-driven equatorial circulation in a homogeneous ocean. Deep-Sea Res., 20, 889-899.

Mintz, Y and G. Dean (1952). The observed mean field of motion of the atmosphere. Geophysical Research Papers. No.17, Geophysics Research Directorate, Cambridge, Mass., 65 pp.

*Michaelis, G (1923). Die Wasserbegung an der oberflache des Indischen Ozeans in Januar and Juli. Veroff. Inst. Mureak. Univ. Berl., 8, 1-32.

*Mollar, L (1929). Die zirculation des Indischen Ozeans. Veroff. Inst. Mureak. Univ. Berl., 21, 1-48.

*Montgomery, R.B (1939). Ein Versuch den verikalen und seitichen Austausch in der Tiefe der sprungschicht im equatorialen Atlantischen ozean see bestimmen. Ann. Hydrograph. Maritimen Meteorol. 67, 242-246.

Montgomery, R.B and E.Palmen (1940). Contribution to the question of the Equatorial Countercurrent. J. Mar. Res., 3, 112-133.

Moore, D.W (1963). Rossby waves in Ocean circulation. Deep-Sea Res., 10, 735-748.

Morgan, G.W (1956). On the wind-driven ocean circulation. Tellus, 8, 301-320.

* Krauss, E.B and R.E. Morrison (1966). Local interactions between the sea and the air at monthly and annual time scales. Q.J.R. Met. Soc., 114-127.

Munk, W.H (1947). A critical wind speed for air-sea boundary processes. J. Mar. Res., 6, 203-278.

Munk, W.H (1950). On the wind-driven Ocean circulation. J. Meteorol., 7, 79-93.

Munk, W.H and G.F.Carrier (1950). On the wind-driven circulation in Ocean basins of various shapes. Tellus, 2, 158-167.

Muraleedharan, P.M., Basil Mathew and R.N.Nair (1980). Some studies on the Undercurrent and Equatorial Jet in the Indian Ocean from the hydrographic characteristics. Bull. Dept. Mar. Sci. Univ. Cochin, XI, 113-126.

Neumann, G (1955). On the dynamics of the wind-driven Ocean Currents. Meteorological papers 2(4). Unty. Series, New York Uni. Press.

Nieler, P.P and P.S. Dubleleday (1970). Circulation in a wind-swept and cooled ocean. J. Mar. Res., 28, 135-149.

O'Brien, J.J and H.E.Hurlburt (1974). Equatorial jet in the Indian Ocean. Science, 184, 1075-1077.

Pearce, A.F (1977). Some feature of the upper 500 m of the Agulhas Current. J. Mar. Res., 35, 731.

Philander, S.G.H and R.C.Pacanowski (1981). Response of equatorial oceans to periodic forcing. J. Geophys. Res., 86, 1903-1916.

Pond, S., Fissel, D.B and C.A.Paulson (1974). A note on bulk aerodynamic coefficients for sensible heat and moisture fluxes. Boundary-Layer Meteorol., 6, 333-339.

Rao, Y.P (1964). Interhemispheric circulation. Quart.J.R. Met. Soc., 90, 190-194.

Reid, R.O (1948a). A model of the vertical structure of mass in the equatorial wind-driven currents of a baroclinic ocean. J. Mar. Res., 7, 304-312.

Reid, R.O (1948b). The equatorial currents of the Pacific as maintained by the stress of the wind. J. Mar. Res., 7, 74-99.

Reid, J.L (1959). Evidence of a South Equatorial Countercurrent in the Pacific Ocean. Nature, 184, 209-210.

Robinson, A.R (1966). An investigation into the wind as the cause of the Equatorial Undercurrent. J. Mar. Res., 24, 179-203.

Rossby, C.G (1936). Dynamics of steady ocean currents in the light of experimental fluid dynamics. Papers Phys. Oceanogr. Meteorol., 5, 1-43.

Saha, K.R (1970). Air and water vapour transport across the equator in the western Indian Ocean during northern summer. Tellus, 22, 681-687.

*Sarkisian, A.S (1954). The calculation of stationary wind currents in an ocean. Izv. Akad. Nauk. SSSR, Ser. Geofiz., 6, 551-561.

Sastry, J.S and V.Ramesh Babu (1979). Convergence of Ekman wind driven layer and surface circulation in the Arabian Sea during southwest monsoon. Mahasagar, 12, 207-211.

*Schott, G (1898). Weltkartezur Uiersicht der Meeresstromungen und Schiffswege. Ann. Hydrograph. Maritimen Meteorol., 26, 409.

*Schott, G (1935). Geographie des Indischen und stillen Ozeans. Hamburg, Boysen, 41.

*Schott, G (1942). Grundlagen einer Weltkar te der Meeresstromungen. Ann. Hydrograph. and Maritimen Meteorol., 70, 329-340.

*Schumacher, P (1940). Monatskarten der oberflachenstromungen im Nordatlantischen Ozean (5°S-50°N). Ann. Hydrograph. Maritimen Meteorol., 68, 109-123.

*Schumacher, P (1943). Monatskarten der obeerflachenstromungen imaguatorialen un sudlichen Atlantischen Ozean. Ann. Hydrograph. Maritimen. Meteorol., 71, 209-219.

Scripps Institution of Oceanography (1948). The mean windstress over the North Pacific Ocean - Scripps. Inst. Oceanogr. Rept.14.

Sewell, R.B.S (1927). Geographic and Oceanographic research in Indian waters. Pt.3, Maritime Meteorology in Indian Sea. Mem. Asiat. Soc. Bengal, 9, 53-102.

Sewell, R.B.S (1928). Geographic and Oceanographic research in Indian waters. Pt.4, The temperature and salinity of the coastal waters of the Andaman Sea. Mem. Asiat. Soc. Bengal, 9, 133-205.

Sewell, R.B.S (1929). Geographic and Oceanographic research in Indian waters. Pt.5, Temperature and salinity of surface waters of the Bay of Bengal and Andaman Sea, with reference to the Laccdiv Sea. Mem. Asiat. Soc. Bengal, 9, 207-355.

Sewell, R.B.S (1932). Geographic and Oceanographic research in Indian waters. Pt.6, Temperature and salinity of the deeper waters of the Bay of Bengal and Andaman Sea. Mem. Asiat. Soc. Bengal, 9, 357-423.

Sharma, G.S (1968). Some inferences on the Equatorial Undercurrent in the Indian Ocean based on the Physical properties of the waters. J. Mar. Biol. Ass. India, 10, 224-236.

Sharma, G.S (1971). Studies on divergence of the surface waters in the North Indian Ocean. Ph.D. thesis, Andhra University, Waltair, 102 pp.

Sharma, G.S (1976). Water characteristics and Current Structure at 65°E during the southwest monsoon. J. Oceanogr. Soc. Japan, 32, 284-296.

Sharma, G.S (1978). Upwelling off the southwest coast of India. Indian J. Mar. Sci., 7, 209-218.

Sharma, G.S., Gouveia, A.D. and Subba Satyendra Nath (1978). Incursion of Pacific Ocean Water into the Indian Ocean. Proc. Indian Acad. Sci., 87A, 29-45.

Sharma, G.S., Narendran Nair, R and Basil Mathew (1982). Current structure in the intertropical Indian Ocean during the northeast monsoon. Indian J. Mar. Sci., 11, 7-14.

Stewart, R.W (1964). The influence of friction on inertial models of oceanic circulation. Studies Oceanog. Hidaka, p. 3-9.

Stewart, R.W (1974). The air-sea momentum exchange. Boundary-Layer Met., 6, 151-167.

Stommel, H (1948). The westward intensification of wind-driven ocean currents. Trans. Am. Geophys. Union, 29, 202-206.

Stommel, H (1957). A survey of ocean current theory. Deep-Sea Res. 4, 149-184.

Stommel, H (1958). The Gulf Stream. 1st Ed. Uni. Calif. Press, Berkeley, Calif. 202 pp.

Stommel, H (1965). Summary charts of the mean dynamic topography and current field at the surface of the ocean and related functions of the mean windstress. In studies on oceanography Ed. K. Yoshida, p. 53-58. University of Washington Press.

Sverdrup, H.U (1947). Wind-driven currents in a baroclinic ocean with application to the equatorial currents of the eastern Pacific. Proc. Natl. Acad. U.S. 33, 318-326.

Swallow, J.C (1964). Equatorial Undercurrent in the western Indian Ocean. Nature, 204, 436-437.

Swallow, J.C (1967). The Equatorial Undercurrent in the western Indian Ocean in 1964. Stud. Trop. Oceanogr. Miami, 5, 15-36.

Swallow, J.C and J.G. Bruce (1966). Current measurements of the Somali coast during the southwest monsoon of 1964. Deep-Sea Res., 13, 861-880.

*Tchernea, R.H.Lecombe and P.Guibout (1958). Sur quelques nou vellus observations hydrologiques relative a la region equatoriole de l' Ocean Indian Bull. Inf. Com. Cont. Oceanogr. Etude Cotes., 10, 115-143.

Taft, B.and J.A. Knauss (1967). Equatorial Undercurrent of the Indian Ocean as observed by the Lusiad Expedition. Bull. Scripps Inst. Oceanogr., 9, 163 pp.

Uda, M and K.Hasunuma (1969). The eastward Subtropical Countercurrent in the western North Pacific Ocean. J. Oceanogr. Soc. Japan, 25, 201-210.

United States Hydrographic Office (1944). Atlas of surface currents. Indian Ocean. H.O.No.566.

Varadachari, V.V.R (1961). On the process of upwelling and sinking on the east coast of India. Prof. Mahadevan Shastyabdapurti Commemoration Volume, 159-162.

Varadachari, V.V.R and G.S.Sharma (1967). Circulation of the surface waters in the North Indian Ocean. J. Indian Geophys. Union 4, 61-73.

Veronis, G (1963). An analysis of wind-driven ocean circulation with a limited number of Fourier components. J. Atmos. Sci., 20, 577-593.

Veronis, G (1966a). Wind-driven circulation Pt.I, Deep-Sea Res., 13, 1-16.

Veronis, G (1966b). Wind-driven circulation Pt.II, Deep-Sea Res., 13, 31-56.

Veronis, G (1973). Models of World Ocean circulation I. Wind-driven two-layer, J. Mar. Res., 31, 228-289.

Warren, B.A (1966). Medieval Arab references to the seasonally reversing currents of the North Indian Ocean. Deep-Sea Res., 13, 167-171.

Warren, Bruce, H.Stommel and J.C.Swallow (1966). Water masses and pattern of flow in the Somali Basin during the southwest monsoon of 1964. Deep-Sea Res., 13, 825-860.

Wealander, P (1959a). On the vertically integrated mass transport in the oceans. In the Atmosphere and Sea in Motion-Rossby Memorial Volume. Ed.B.Bolin. Oxford Uni. Press, New York, p. 95-101.

Wealander, P (1968). Theoretical forms for the vertical exchange coefficients in a stratified fluid with application to lakes and seas. Geophysica, 1, 27.

Weiler, H.S. and K.W. Burling (1967). Direct measurements of stress and spectra of turbulence in the boundary layer over the sea. J. Atmos. Sci., 24, 653-664.

*Witte, E (1879). Uber Meeresstromungen 2. Die stromungenderunzelnen Ocean in Sechstes Programmeder Furstenscheilizu. Plese Schlesien Krummer Press, p. 24-47.

Wooster, W.S. and M.Gilmartin (1961). The Peru-Chile Undercurrent. J. Mar. Res., 19, 97-112.

Wooster, W.S. and J.L. Reid, Jr.(1963). Eastern boundary currents. In The Sea, Ed.M.N.Hill. Interscience Publisher, New York and London, p. 253-280.

Wooster, W.S., M.B.Schaefer and M.K.Robinson (1967). Atlas of the Arabian Sea for fishery oceanography. Uni. Calif. Inst. Mar. Resources, 67, 1-35.

Wyrtki, K (1961). The thermocline circulation in relation to the general circulation in the oceans. Deep-Sea Res., 8, 39-64.

Wyrtki, K (1971). Oceanographic atlas of the International Indian Ocean Expedition. Washington, D.C. National Sci. Foundation, 531 pp.

Wyrtki, K (1973a). Physical Oceanography of the Indian Ocean in Ecological Studies. Analysis and Synthesis, Vol.3. Ed.B. Zeitzschel. Springer-Verlag Berlin, New York, p. 19-36.

Wyrtki, K (1973b). An Equatorial Jet in the Indian Ocean. Science, 181, 262-264.

Yoshida, K (1955). An example of variations in oceanic circulation in response to the variations in the wind field. J. Oceanogr. Soc. Japan, 11, 103-108.

Yoshida, K. and M.L.Mao (1957). A theory of upwelling of large horizontal extent. J. Mar. Res., 16, 40-54.

Yoshida, K. and T.Kidokoro (1967a). A Subtropical Countercurrent in the North Pacific - An eastward flow near the subtropical convergence. J. Oceanogr. Soc. Japan, 23, 89-91.

Yoshida, K. and T.Kodokoro (1967b). A Subtropical Countercurrent (II) - A prediction of eastward flows at lower subtropical latitudes. J. Oceanogr. Soc. Japan, 23, 231-246.

Yoshida, K (1970). The Kuroshio - A symposium on the Japan Current. East West Center Press, Honolulu, 197 pp.

---

*Not referred original